Plutonium and Its Alloys

From atoms to microstructure

Siegfried S. Hecker

Plutonium is an element at odds with itself—with little provocation, it can change its density by as much as 25 percent; it can be as brittle as glass or as malleable as aluminum; it expands when it solidifies; and its freshly-machined silvery surface will tarnish in minutes, producing nearly every color in the rainbow. To make matters even more complex, plutonium ages from the outside in and from the inside out. It reacts vigorously with its environment—particularly with oxygen, hydrogen, and water—thereby, degrading its properties from the surface to the interior over time. In addition, plutonium's continuous radioactive decay causes self-irradiation damage that can fundamentally change its properties over time. Only physicists would think of using such a material.

In the periodic table, plutonium is element 94, and it fits near the middle of the actinide series (ranging from thorium to lawrencium, atomic numbers 90 to 103). Plutonium is of practical interest principally because the 239 isotope has attractive nuclear properties for energy production and nuclear explosives. Manhattan Project physicists managed to extract the more than millionfold advantage of plutonium over conventional explosives. It was the chemists and metallurgists who learned how to extract plutonium, fabricate it, and keep it sound until the time of detonation. The Manhattan Project history of plutonium metallurgy recently published by Edward Hammel (1998) is a remarkable tale of scientific and engineering achievement. These pioneers were working with a metal whose electronic structure and consequent engineering properties were even more puzzling than its nuclear properties. In a remarkably short period, they learned enough to accomplish their goal and left the rest for us to decipher.

The end of the Cold War has signaled a dramatic change in the nuclear weapons programs of the nuclear powers. The challenge now is to help reduce the size of the nuclear arsenals while ensuring that the nuclear weapons are safe and reliable into the indefinite future—without nuclear testing and without a continuous cycle of new nuclear weapons development and deployment. Therefore, extending the lifetimes of plutonium components is more important now than in the past. Similarly, remanufacturing plutonium components for existing weapons systems has become a greater challenge because no new plutonium components have been fabricated for almost 12 years. Moreover, the manufacturing facilities no longer exist, and most of the technical experts have now retired. The long-term behavior of plutonium is also important at the back end of the nuclear weapons cycle—the dismantlement and disposition phases. Because many thousands of nuclear weapons are being withdrawn from the nuclear arsenals of Russia and the United States, we must deal with excess plutonium recovered from these warheads. But the reactive and continuously changing nature of plutonium makes this task a serious challenge. Compounding this challenge is the fact that excess weapons plutonium must be carefully secured against diversion or theft. Burning as fuel in nuclear reactors and geologic disposition are the most likely methods for its eventual disposal. In either case, plutonium must be stored for decades or longer. It has therefore become imperative that we understand the aging of plutonium and of its alloys or compounds. And if we are to accomplish this goal, the next generation of scientists and engineers must become deeply involved in deciphering the complexities of plutonium.

Both this article and "Mechanical Behavior of Plutonium and Its Alloys" (page 336) describe the fascinating mysteries of plutonium metallurgy in a forum open to the research community with the hope of attracting those young men and women into plutonium research. At Los Alamos, we are trying to move from an empirical approach to one based on fundamental principles. At the moment, however, our knowledge rests with the practitioners—and most of our experienced plutonium practitioners have retired or are nearing retirement. To develop a solid fundamental understanding of plutonium, we need the most modern ideas and tools from the international scientific research community. We can then apply this understanding to our practical problems, many of which must naturally remain secret to the public.

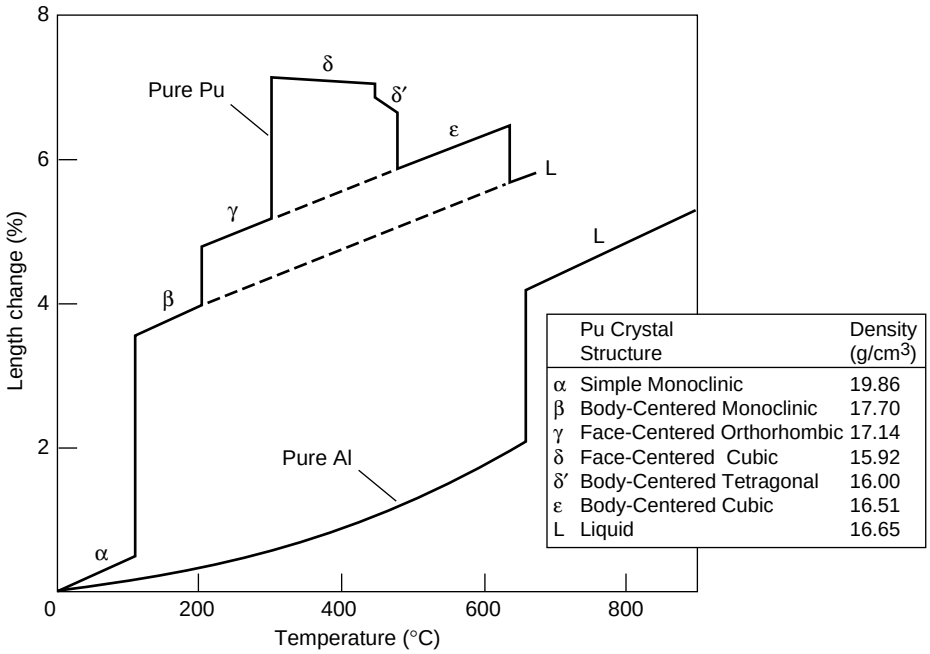

Figure 1. Anomalous Length Changes in Plutonium

Plutonium is a unique element in exhibiting six different crystallographic phases at ambient pressure (it has a seventh phase under pressure). In addition, unlike most metals, plutonium contracts on melting. Transformations to different crystal structures occur readily and are accompanied by very large volume changes. By comparison, aluminum's behavior is predictable and uneventful. It expands monotonically on heating in the solid phase, and it also expands on melting. The dashed lines show that thermal contraction on cooling the liquid (L) phase of plutonium extrapolates to that of the β-phase; the thermal contraction on cooling the ε-phase extrapolates to that of the γ-phase.

The Unusual Properties of Plutonium

Here, I will describe how plutonium is unusual before tackling the question of why it is so.

Manhattan Project pioneers were puzzled by plutonium's unusual behavior right from the beginning. As soon as they received sufficient amounts of the new element to measure its density, they found unexplained variations ranging from 8 to 24 grams per cubic centimeter (g/cm^3)—see the article "The Taming of '49'" on page 48. Also, some tiny samples were as malleable as aluminum, whereas others were as brittle as glass. The list of remarkable properties is quite long (see the box "The Unusual Properties of Plutonium" on page 294), but it was only after the war that those properties were studied systematically.

The most exasperating property from an engineering standpoint is the extraordinary thermal instability of plutonium—that is, the large length (or volume) changes during heating or cooling shown in Figure 1. These volume (or phase) changes are accompanied by significant changes in other properties (see Table I). In particular, the δ-phase, which is stable at high temperatures, is desirable because its highly symmetric face-centered-cubic (fcc) structure makes it very malleable (ductile) and easily formed into desired shapes. In contrast, the room temperature α-phase is an engineering nightmare—its simple monoclinic, low-symmetry structure makes it very brittle. (It has been the metallurgists' tradition to designate polymorphic phases of elements and alloys with symbols from the Greek alphabet, beginning with α for the lowest-temperature phase.)

The Manhattan Project pioneers soon discovered that they could prevent transformation to the three low-temperature phases by intentionally adding chemical elements such as aluminum or gallium. The benefits of adding gallium, and thereby retaining plutonium in the δ-phase, are easily derived from Figure 2.

All alloying elements are "impurities" in a nuclear chain reaction because they reduce the number of plutonium-239 atoms per unit volume, but metallurgical considerations strongly favor using the δ-phase alloys for weapons applications. The amount of alloying elements, however, must be kept to a minimum, so plutonium-rich alloys are of greatest interest. Because requirements for a controlled chain reaction in a nuclear reactor are very different, reactor alloys or compounds span a much broader range of plutonium concentrations.

The mysteries of plutonium metallurgy have been studied over the

years within the metallurgical and condensed-matter physics communities—unfortunately, with rather little collaboration between the two. These communities do not even share a common language. For example, they cannot agree on what to call a phase change—whereas physicists prefer transition, metallurgists prefer transformation. Yet, the behavior of plutonium defies conventional metallurgical wisdom. Understanding plutonium involves a close collaboration between physicists, metallurgists, and chemists. Metallurgists must learn to appreciate the intricacies of electronic bonding, especially the role of 5f electrons. Physicists must develop an appreciation for the role of microstructure and crystal defects in determining the engineering properties of plutonium. My intention in writing this article and the companion one on mechanical properties was to bridge the gap between the two communities and complement the very informative articles on plutonium condensed-matter physics found in Volume I of this issue of *Los Alamos Science*.

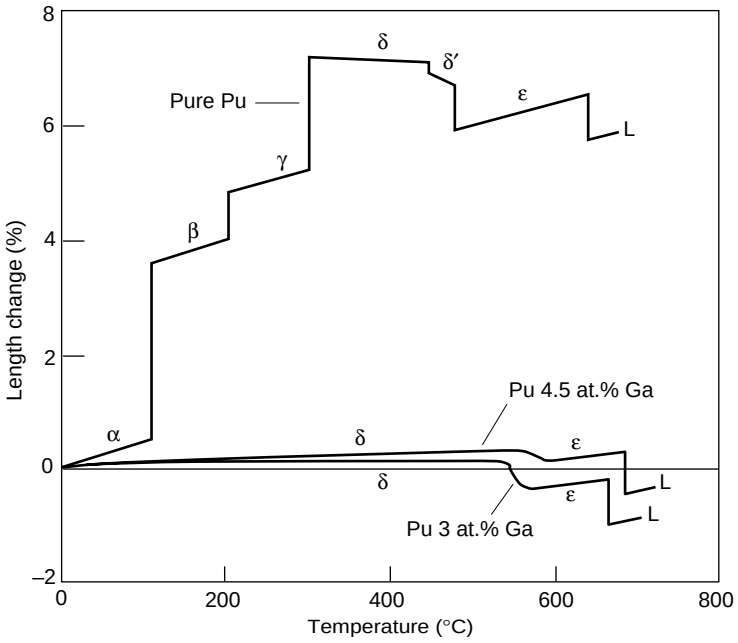

Figure 2. The Benefits of Alloying Plutonium

Both unalloyed plutonium and Pu-Ga alloys expand upon solidification to the bcc ε-phase, which expands when it transforms to the fcc δ-phase. Upon cooling, however, plutonium alloys do not exhibit the enormous shrinkage of unalloyed plutonium. They contract only slightly as they cool to room temperature because they remain in the δ-phase, avoiding the transformation to γ, β, and α. Increases in gallium concentration shift the melting temperature and the δ to ε transformation to slightly higher temperatures.

5f Electrons for Metallurgists

On a fundamental level, the properties of solids are determined by their electronic structure, and thanks to the painstaking work of the electronic-structure physics community, we have a fairly good picture of the simple alkali metals all the way through to the more-complex transition metals and rare earths (lanthanides). Today, the actinides are at the frontier of electronic-structure theory. The current status for actinide atoms and molecules is reviewed in the articles "The Complex Chemistry of Plutonium" (page 364) and "Computational Studies of Actinide Chemistry" (page 382); for metals, it is covered in the articles "Plutonium Condensed-Matter Physics" (page 90), "Actinide Ground-State Properties" (page 128), and "A Possible Model for δ-Plutonium" (page 154). In this section, I summarize those ideas—both old

Table I. Comparison of Some Properties of α- and δ-Phase Plutonium

Property	α-Plutonium (unalloyed)	δ-Plutonium (1.8 at. % Ga)
Crystal Structure	Simple monoclinic	fcc
Density (g/cm^3)	19.86	15.8
Thermal Expansion Coefficient (10^{-6} K^{-1})	53	3
Thermal Stability		
Upon heating	To β at 123°C	To δ + ε at ~500°C
Upon cooling	Stable	To α′ at –75°C
Pressure Stability		
Hydrostatic compression	Stable to >50 kbar	To α′ at 2.7 kbar
Hydrostatic tension	To δ at ~3.5 kbar	Stable
Young's Modulus (GPa)	100	~40
Poisson's Ratio	0.15	0.26
Compressibility (GPa^{-1})	0.020	0.033
Yield Strength (MPa)	–	68
Ultimate Tensile Strength (MPa)	425	100
Total Elongation	<0.1%	~35%
Electrical Resistivity (Ω cm × 10^{-6})	145	100
Thermal Conductivity [cal/(cm–s–K)]	0.010	~0.026 (3.4 at. % Ga)

The Unusual Properties of Plutonium

1. Plutonium has six allotropes—that is, six different crystal structures—and a seventh under pressure.
2. The energy levels of these allotropic phases are very close to each other, making plutonium extremely sensitive to changes in temperature, pressure, or chemistry.
3. The densities of the allotropes vary significantly, resulting in dramatic volume changes accompanying phase transitions.
4. The crystal structure of the allotropes closest to room temperature are of low symmetry, more typical of minerals than metals.
5. Among the six allotropes, the face-center-cubic phase (a close-packed atomic (arrangement) is the least dense.
6. Plutonium expands when it solidifies from the melt—like ice freezing from water.
7. Its melting point is low.
8. Liquid plutonium has a very large surface tension and the highest viscosity known near the melting point.
9. Diffusion in the highest-temperature solid phase, body-centered-cubic ε-phase is anomalously high.
10. The plutonium lattice is very soft vibrationally and very nonlinear.

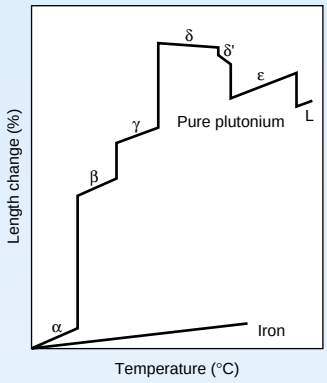

Thermal expansion of plutonium

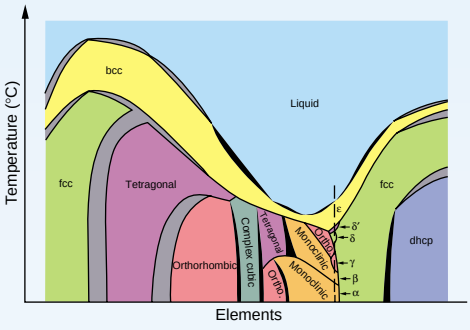

Low melting temperature

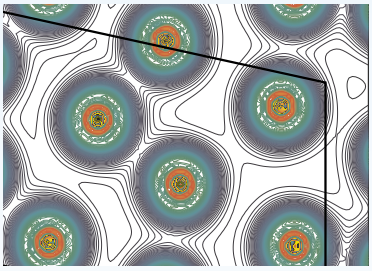

Charge-density contours in α-plutonium

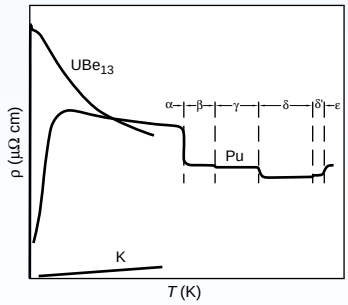

Resistivity

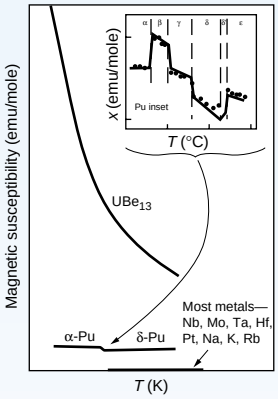

High magnetic susceptibility

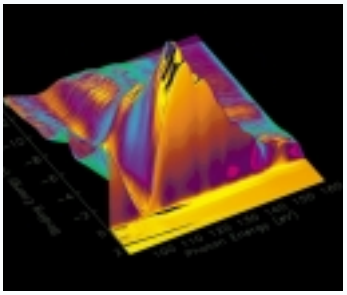

Photoelectron spectroscopy data

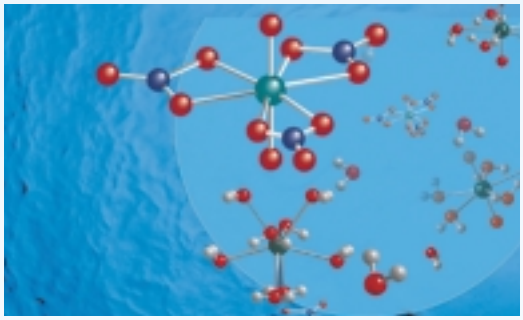

Complex chemistry of plutonium

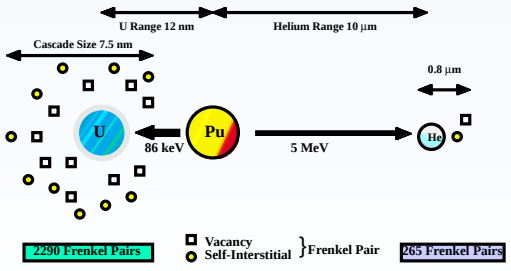

Self-irradiation

11. The low-symmetry allotropes have very high, positive thermal-expansion coefficients.
12. The fcc and tetragonal allotropes exhibit negative thermal-expansion coefficients—that is, they shrink when heated.
13. There are numerous anomalies in the low-temperature properties of plutonium—such as an increase in electrical resistivity down to 100 kelvins.
14. Plutonium allotropes exhibit dramatic variation in mechanical properties—they range from completely brittle to extremely ductile (malleable).
15. The fcc phase displays the greatest directionality in elastic properties known in fcc metals.
16. Plutonium undergoes self-irradiation because of the radioactive decay of its nucleus—resulting in both lattice damage and transmutation products, including other actinides and helium.
17. Plutonium has great affinity for oxygen and hydrogen.
18. Plutonium exhibits enormous, reversible reaction rates with pure hydrogen.
19. At elevated temperatures, plutonium is pyrophoric in certain atmospheres.
20. In solution, plutonium can appear in five different valence states—four of them have very similar reduction potentials.

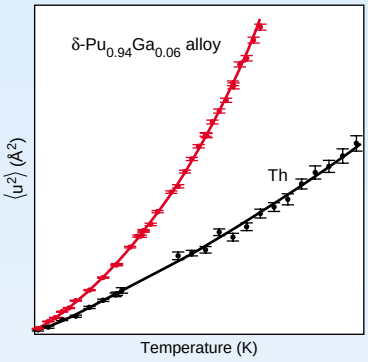

Lattice softening


Polycrystalline δ-phase plutonium alloy

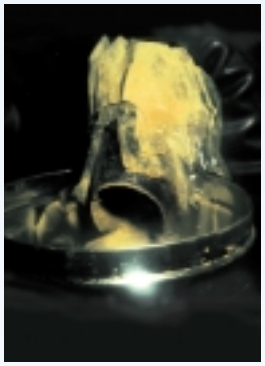
Plutonium corrosion product

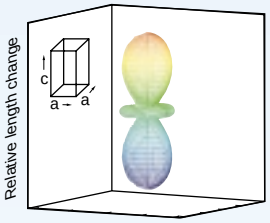

Anisotropic microstrain for δ′-plutonium

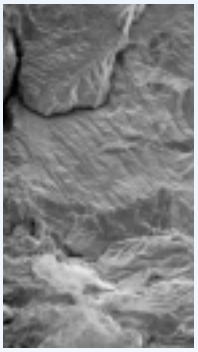
Brittle fracture

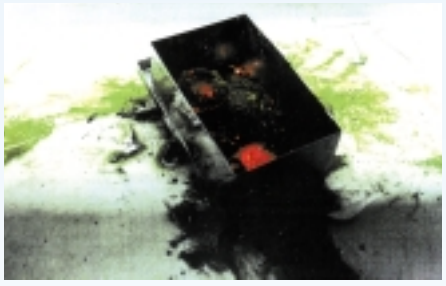
Pyrophoricity

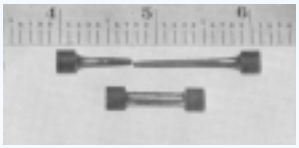
Ductile fracture

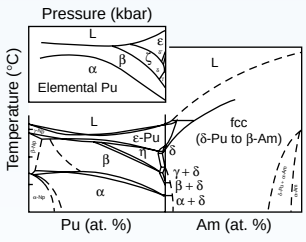

Pressure-temperature diagram and Np-Pu-Am phase diagram


Half sphere of as-cast δ-plutonium alloy

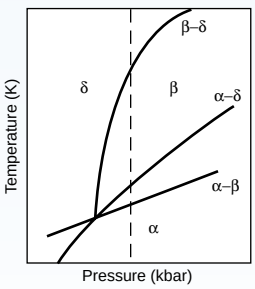

Phase change under hydrostatic tension

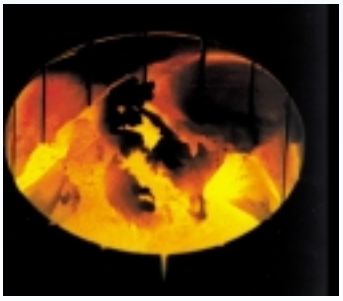
Molten plutonium metal

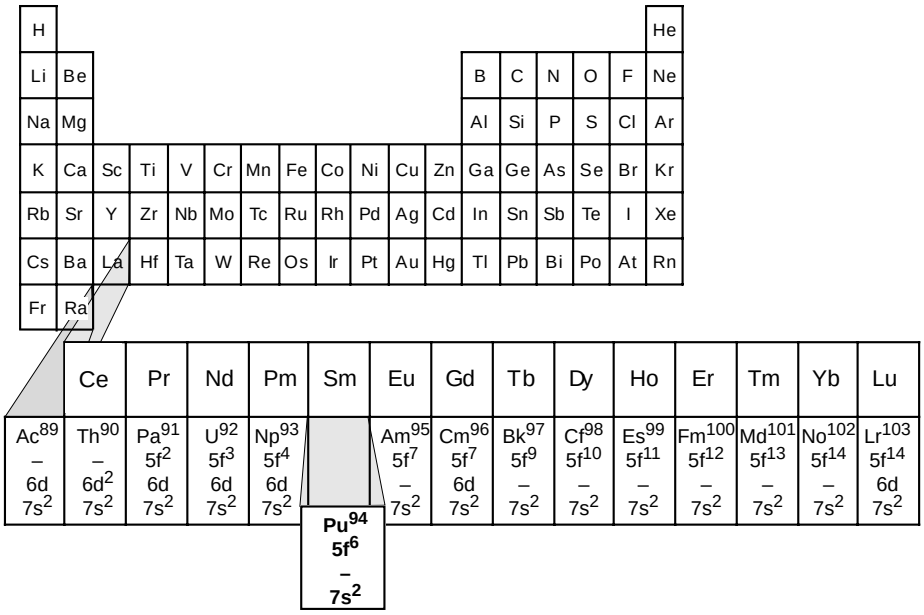

Figure 3. The Actinides and Their Outermost Configuration of Electrons
The actinides are the 14 elements (thorium through lawrencium) following actinium in the periodic table. With a few exceptions, an additional 5f electron is added to the outermost (valence) electron shell of each successive element. Early in the series, the 6d electrons are lower in energy than the 5f electrons. All the ground-state configurations of the first four actinides have a 6d electron in their valence shell. (Having two 6d electrons, thorium is irregular.) The energy of the 5f electrons decreases with atomic number, however, and starting with plutonium, all the actinides have only 5f electrons in the valence shell (with the exception of curium and lawrencium).

and new—that are crucial for metallurgists to understand as they ponder over the unusual behavior of plutonium and its alloys.

The actinide series marks the emergence of the 5f electrons in the valence shells of the elements. The actinide valence-shell configurations (beyond the filled atomic shells of the inert gas radon-86) are highlighted in Figure 3 because it is only valence electrons that form chemical bonds in molecules. This good fortune relieves us of the burden of accounting rigorously for all the other electrons, and it is, of course, the basis for the systematic correlations among chemical properties found in the periodic table. In metals, those valence electrons that overlap electrons from neighboring sites become conduction electrons and form the chemical bonds holding the solid together. The bonding between the conduction electrons and the ion cores is responsible in whole or in part for such properties as crystal structure, elasticity, phase stability, and melting temperature. It turns out that much of plutonium metal's extreme sensitivity and variability of properties can be traced to the unique behavior of plutonium's 5f valence electrons.

I will explain how the following three specific features of plutonium's electronic structure combine to set this metal apart from other metals in the periodic table: (1) the spatial extent of its 5f electrons is just enough to allow them to bond, (2) multiple low-energy electronic configurations have nearly equal energy levels, and (3) the 5f electrons sit on the knife-edge between bonding and localized behavior.

Spatial Extent of 5f Electron—Just Enough for Bonding. The atomic orbitals in Figure 4 provide the foundation for understanding bonding in molecules and metals. Isolated plutonium atoms have eight valence electrons with a configuration of $7s^2 5f^6$. The difference in energy between the 6d and 5f orbitals is very small and results in competing $5f^n 7s^2$ and $5f^{n-1} 7s^2 6d^1$ configurations in molecular bonding. That competition accounts for some of the complex chemistry of the actinides as related in the article "The Chemical Complexities of Plutonium" (page 364). The highly directional nature of the f electron orbitals (with three units of angular momentum) promotes very directional, covalent bonding in certain actinide molecules and molecular complexes.

In the metallic state, plutonium has the electronic configuration $7s^2 6d^1 5f^5$, and the most-important new result from modern electronic-structure calculations is that, in its α-phase, all eight valence electrons are in the conduction band, which means that the 5f electrons in α-plutonium behave like the 5d electrons of the transition metals: participating in bonding and holding the metal together.

Figure 5 illustrates what is meant by a conduction electron and how a conduction energy band forms in a simple metal. The figure first shows that, in order for two sodium atoms to bind as a diatomic molecule, the 3s valence electron orbitals from the two atoms must be close enough to overlap. In that configuration, the 3s energy level of a single sodium atom splits into two levels—one bonding, the other antibonding. Similarly, when 10^{23} sodium atoms condense so that the electron orbitals of neighboring atoms overlap, the atoms bind together in a crystalline array, and the 3s valence level splits into a band of approximately 10^{23} very closely spaced levels. The figure also shows that, as the atoms condense to form a crystal lattice, the electrostatic potential well seen by an electron in an isolated atom becomes a periodic array of potential wells. The core-level electrons (1s, 2s, and 2p) remain bound in individual potential wells at lattice sites, but the energies of the 3s valence electrons are above the wells. They feel the pull of many atoms in the periodic array and become itinerant, traveling

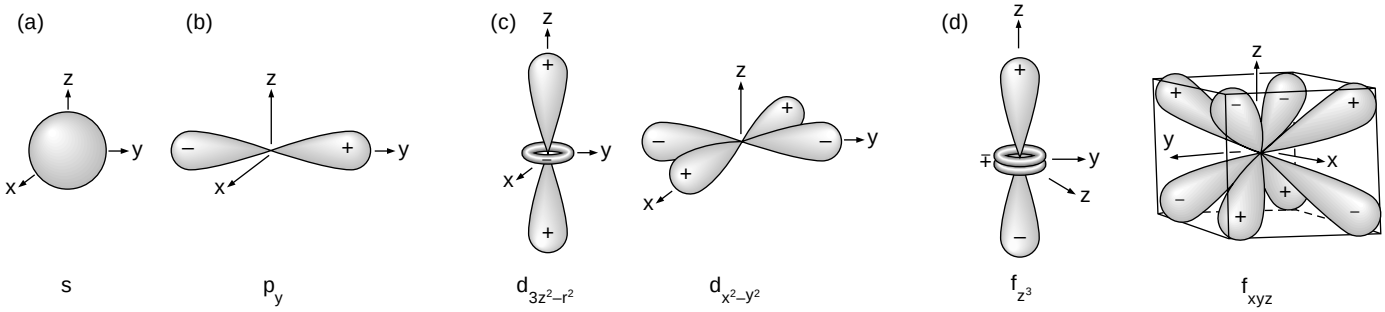

Figure 4. Angular Properties of s, p, d, and f Orbitals and Radial Extent for Samarium and Plutonium Atoms

The shape and orientation of an atomic orbital are characterized by a pair of quantum numbers (ℓ, m_ℓ). The azimuthal number ℓ is a positive integer that also has letter designations (s for $\ell = 0$, p for $\ell = 1$, d for $\ell = 2$, and f for $\ell = 3$). An electron in an orbital specified by ℓ has $\sqrt{\ell(\ell+1)}\,\hbar$ units of orbital-angular momentum. The magnetic number, m_ℓ is an integer that ranges from $-\ell$ to ℓ. Thus, for every ℓ value, there is a set of $2(\ell + 1)$ orbitals. (a) This is the spherically symmetric s orbital. (b) One of the three p orbitals is illustrated here. The other two are found by rotating the orbital by 90° about the *x*- and *y*-axis, respectively. (c) Shown here are two of the five d orbitals. Another orbital is found by rotating $d_{x^2-y^2}$ by 45° about the *z*-axis, and the remaining two by rotating $d_{x^2-y^2}$ by 90° about the *x*- and *y*-axis, respectively. (d) There is no unique polynomial description of the f orbitals. Two orbitals are shown in the cubic representation with simplified polynomial designations. Two more orbitals are found by rotating f_{z^3} by 90° about the *x*- or *y*-axis, and three more by rotating f_{xyz} by 45° about the *x*-, *y*-, or *z*-axis—for a total of seven orbitals.

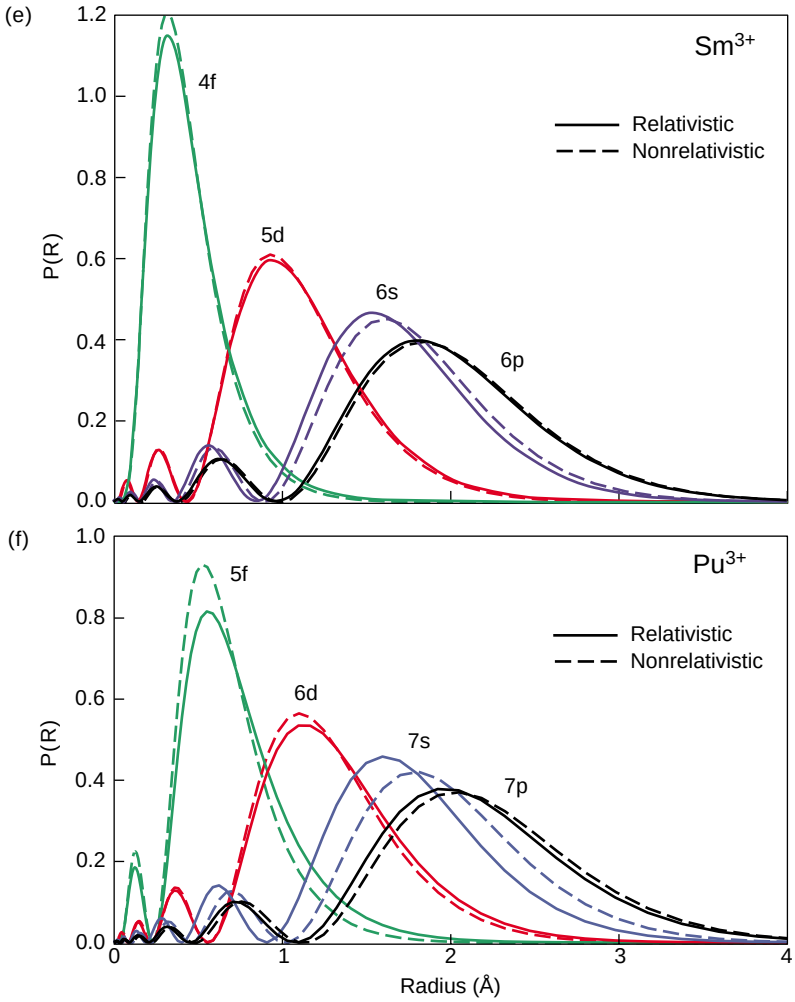

The probability density of finding an electron at a certain distance from the nucleus is shown for the valence electrons of isolated samarium and plutonium ions. (The peak in the distribution indicates only the most likely distance from the nucleus of that electron.) Using density functional theory, Jeffrey Hay and Richard Martin of Los Alamos calculated these results from first principles. (e) The 4f electrons in Sm^{3+} are localized close to the nucleus and have only a marginal influence on molecular bonding. They do not bond in the solid. (f) The 5f electrons in Pu^{3+} extend relatively far from the nucleus compared to the 4f electrons of Sm^{3+}. (Compare, for example, the probability at 1 Å). For this reason, the 5f electrons participate in the chemical bonding of molecules and also contribute to the chemical bonding of the solid. Also noteworthy is the much-greater radial extent of the probability densities for the 7s and 7p valence states in Pu^{3+} compared with those of the 5f valence states. The fully relativistic calculations show that the 5f and 6d radial distributions extend farther than shown by nonrelativistic calculations and the 7s and 7p distributions are pulled closer to the ionic cores.

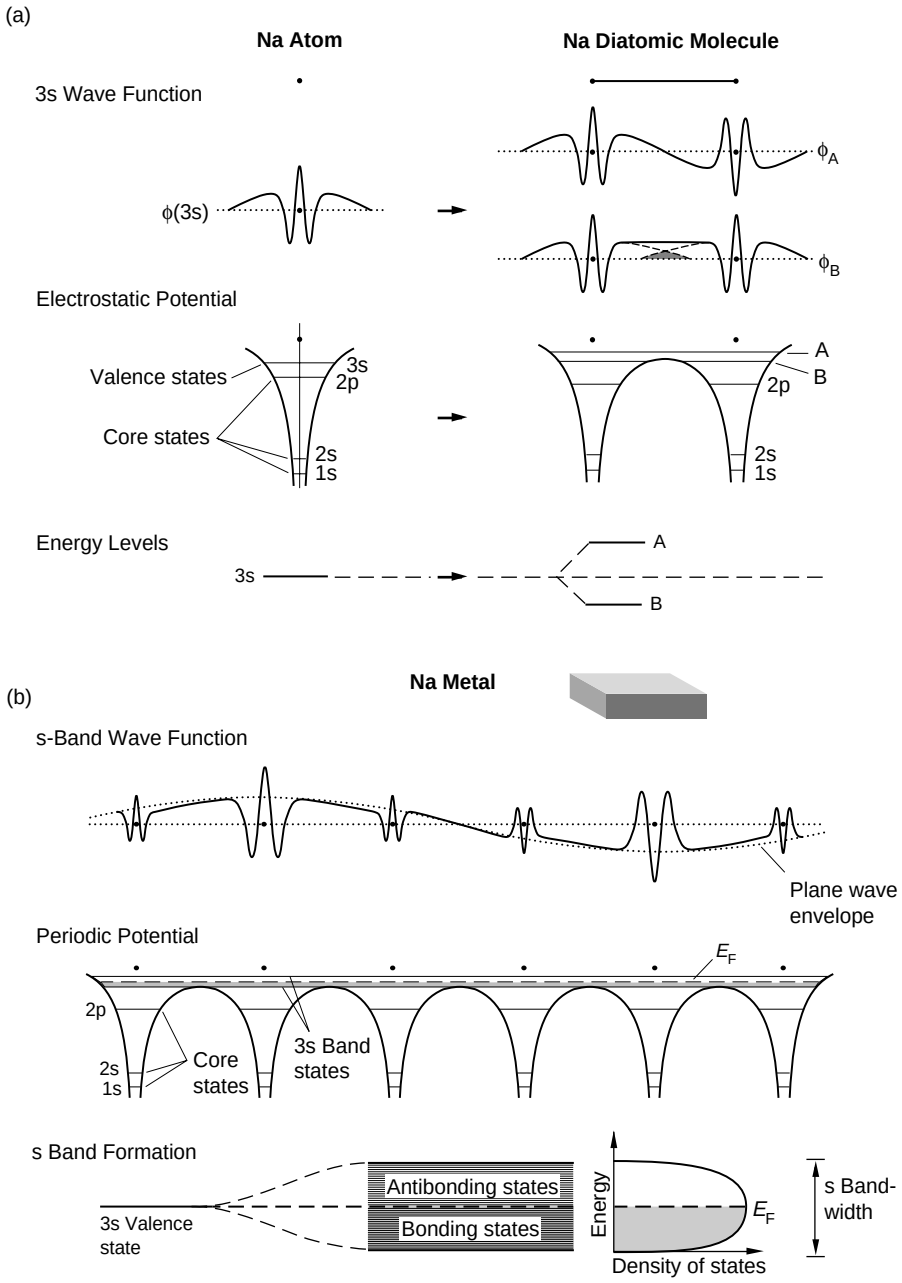

Figure 5. Band Formation, Bloch States, and the Density of States for the Simple Metal Sodium

(a) Two sodium atoms bond to form a diatomic molecule. (b) This bonding process is generalized to the metallic state. For the two sodium atoms, the sum and difference of the 3s valence wave functions of each atom form the bonding (B) and antibonding (A) molecular orbitals of the diatomic molecule, and the 3s atomic-energy level splits into energy levels A and B. Note the double well of the diatomic molecule and the bonding level, just below the top of the well. When many atoms are brought together, they crystallize in a periodic potential array of ion cores and conduction electrons that are shared among the atoms. The core-level electrons (1s, 2s, and 2p) remain localized at lattice sites. The 3s valence electrons form Bloch states consisting of a 3s wave function at each atomic site modulated by a plane wave. The original 3s levels of ~10^{23} atoms becomes a band of very closely spaced energy levels with a width related to the amount of overlap between atomic wave functions from neighboring sites. In sodium metal, the 3s conduction band is only half filled, and the highest occupied state at absolute zero temperature is denoted by E_F, the Fermi energy. The number of states at different energy levels is shown as the density-of-states curve.

through the entire crystal. Looking at it another way, we can say that the atoms in the solid are so close together that the individual 3s electron orbitals overlap those of neighboring atoms. As a result, a single electron has the probability of hopping from neighbor to neighbor throughout the crystal lattice.

Figure 5 also shows that for two atoms, the sum and difference of two overlapping 3s atomic orbitals form the bonding and antibonding molecular orbitals, respectively, of the diatomic molecule. In the solid, a 3s orbital from each lattice site combines with all the others in all possible linear combinations to form a set of Bloch states, the solid-state equivalent of molecular orbitals. Each Bloch state extends over the entire crystal, and just like a molecular orbital, it can be occupied by two electrons at the most—one with spin up, the other with spin down. Figure 5 shows a one-dimensional version of a Bloch state. It is made up of the 3s wave functions at each atomic site modulated by a plane wave. Because an electron in a Bloch state has a probability to be anywhere in the crystal, it has the potential to conduct electricity when an electric field is applied and is called a conduction electron.

Although each of the 10^{23} Bloch states has a slightly different energy (thus satisfying the exclusion principle for fermions), the levels are so close to each other that we treat them as a continuum and talk about the number of energy levels per unit energy, or

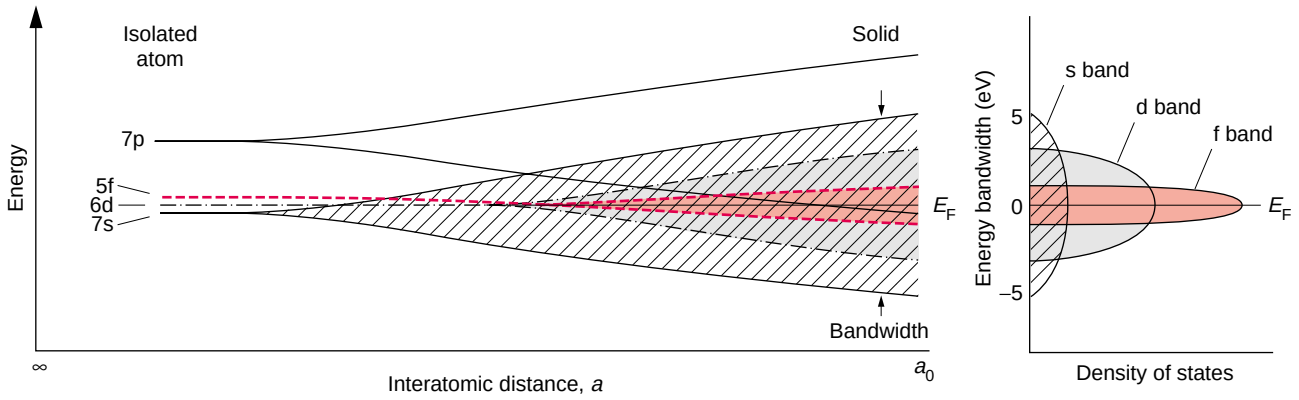

Figure 6. Overlapping Energy Bands in the Actinides

The 7s, 6d, 5f, and 7p valence levels of isolated actinide atoms are relatively close in energy and form overlapping energy bands when the atoms condense into solids. The width of each band is proportional to the overlap between the wave functions of neighboring atoms. The overlap goes in decreasing order from the s and p orbitals to the d and then to the f orbitals, and therefore the sp band is wider than the d band, which is wider than the f band. The f band compresses the energy levels for all the f-electron Bloch states into a very narrow energy range of about 2 to 4 eV, yielding a high density of states. For uranium, neptunium, and plutonium, there are enough 5f electrons per atom that the f band dominates the bonding. Bloch states of the same wave vector but different orbital character can hybridize, or mix, forming states of mixed orbital character.

the density of states, in the conduction band. The Fermi energy E_F is the energy of the highest occupied level for a given element at absolute zero temperature. In a metal, the Fermi level is toward the middle of the energy band—so, there are many empty states available at energies close to those of the occupied levels.

One of the important properties of an energy band is its width. Figure 5 shows that this bandwidth is approximately equal to the difference between the bonding and antibonding energy levels of the diatomic molecule, which is proportional to the amount of orbital overlap between neighboring atoms. Thus, the energy band becomes broader as the atoms get closer together. The fact that the bottom and top boundaries (defining the bandwidth) of each band represent the most-bonding and least-bonding Bloch states is not obvious from the figure but can be determined from the radial extents of the Bloch wave functions. These radial extents are greatest for states at the bottom of the band and least for those at the top.

The energy band structure becomes more complicated in the light actinides (see Figure 6). The sharp 7s, 6d, and 5f valence levels of the isolated actinide atom are so close in energy that they broaden into overlapping conduction bands in the metal. (At the same time, the Bloch states of the same energy but different orbital origin can combine or hybridize to yield states of mixed orbital character.) Figure 6 indicates that the bandwidth narrows with increasing orbital angular momentum (from s, p, d to f electrons). That narrowing reflects the decreasing radial extent of orbitals with higher angular momentum, or equivalently, the decrease in overlap between neighboring atoms.

Figure 4(b), which was calculated from first principles by Hay and Martin of Los Alamos, shows very clearly that the radial extents are much less for 6d and 5f valence electrons than for 7s and 7p valence electrons. Figure 7 demonstrates that the 7s orbitals of neighboring plutonium atoms overlap substantially. This overlap leads to a broad energy band, whereas the 5f orbitals barely overlap and produce a relatively narrow band. It is also significant that the 5f orbitals are very steep in the overlap region, so a small increase in interatomic distance leads to a rapid decrease in overlap and a narrowing of the band. Wills and Eriksson obtained the same qualitative results for energy bands in actinide solids.[1]

Large overlap, or broad bandwidth, of s and p electrons results in those electrons having a large probability of hopping from site to site, spending little time orbiting around a single ion core, and traveling quite freely throughout the crystal. In contrast, 6d and 5f electrons, with their smaller spatial extent and progressively narrow bandwidths, spend more time circling around the ion cores and interacting with other elec-

[1]Note that this confinement of states of higher angular momentum is familiar from classical mechanics. Conservation of angular momentum in an attractive central potential leads to an effective force (or potential barrier) that keeps a bound particle in a well-defined range of radial distances. As angular momentum increases but energy remains constant, the range of allowed radial distances decreases, and the potential barrier at the largest radius gets steeper. In quantum mechanics, electrons can tunnel through the barrier, but because the barrier is higher for particles of higher angular momentum, the probability of tunneling decreases, and the probability density outside the barrier is much smaller than that for states of lower angular momentum.

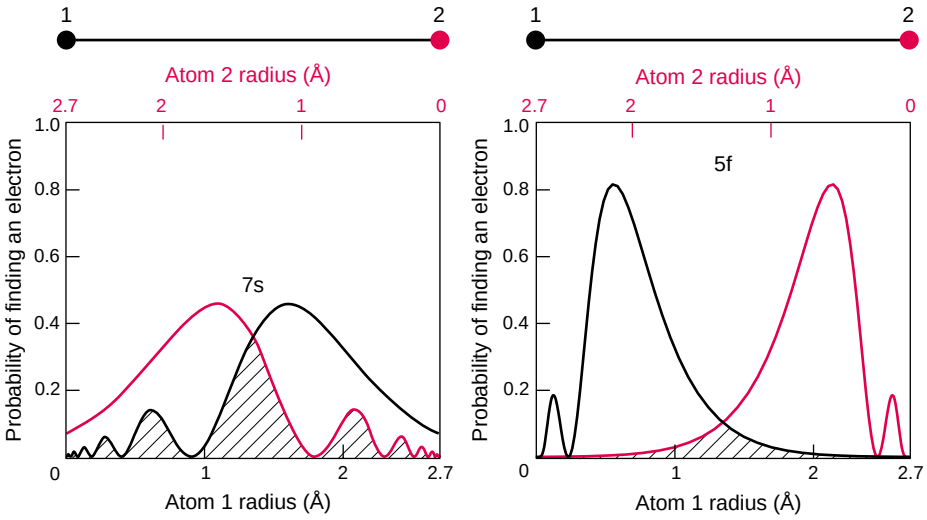

Figure 7. Schematic of Overlapping Wave Functions

The atomic orbitals for plutonium illustrated in Figure 4 are redrawn to show the overlap that occurs when two plutonium atoms are placed at a distance of 2.7 Å (which is the average distance of the short bonds in α-plutonium). The 7s wave functions overlap substantially; the 5f wave functions, only slightly. In plutonium metal, the orbitals become modified, but the 5f overlap is still sufficient for bonding. In the rare earths and heavy actinides starting with americium, the overlap is insufficient for bonding. As a result, 5f electrons remain localized, or bound, in the potential wells at each lattice site.

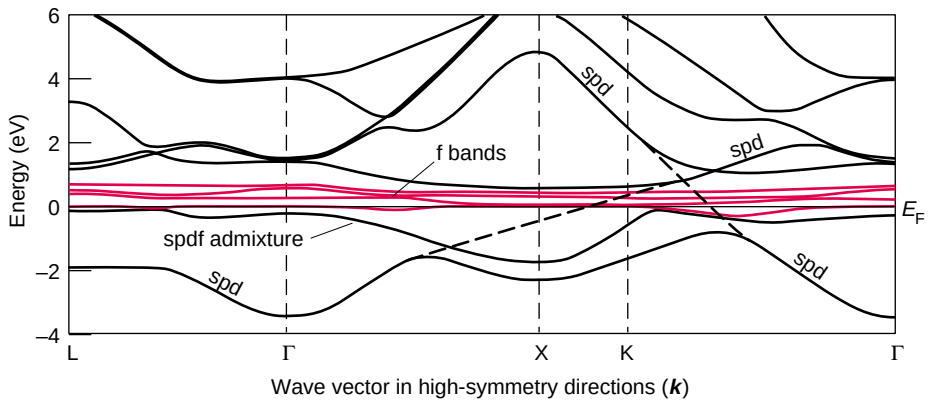

Figure 8. Narrow f Band in Cerium

Here, the one-electron energies in α-cerium are plotted as a function of the electron wave vector, or crystal momentum. Notice that the bands with substantial f character (red) are very flat—that is, the energy range (bandwidth) is very narrow. For a material with many f electrons, a crystal distortion will lower the energy of many of the occupied levels and create a structure that is more stable.

trons at lattice sites. They are thus more likely to depart from the free or nearly free electron behavior seen in the s and p bands of simple metals. In the language of physicists, the narrow-band d and f electrons are highly correlated and are responsible for the unusual behavior of so-called correlated-electron materials. The exact nature of those correlations in plutonium and other narrow-band materials is now under intense study in the condensed-matter physics community.

One last feature in Figure 6 is the very high density of states for f electrons—that is, a large number of Bloch states are confined to a very narrow band—on the order of 2 to 4 electron-volts (eV). Because in a band there are always approximately 10^{23} states (one per atom), narrow bandwidths automatically yield a high density of states. Figure 8 shows a plot of the narrow conduction band (energy vs crystal momentum ***k***) for the 4f electrons in α-cerium. The narrow bandwidth means the plot is very flat—that is, as the crystal momentum of the Bloch state varies, the energy of the state remains very close to the Fermi energy.

Narrow f Bands and Low-Symmetry Structures in the Light Actinides. Having glibly stated that the 5f electrons in α-plutonium occupy a narrow conduction band (2–4 eV in width), I need to point out that the nature of the 5f electrons and their role in determining properties have been a source of speculation for nearly half a century. Only recently has there been a breakthrough: Electronic-structure calculations yielded believable predictions for α-plutonium (see the article "Actinide Ground-State Properties" on page 128) and photoemission experiments confirmed them (see the article "Photoelectron Spectroscopy of α- and δ-Plutonium" on page 168).

In general, electronic-structure calculations predict the energy bands and the total binding energy from an assumed crystal structure and atomic density (or volume) of a metal. Today, these calculations are so fast and accurate that one can try out various crystal structures and atomic volumes as inputs and solve for the energy bands and total energy for many different combinations. Invariably, the lowest energy solutions have the right crystal structures and atomic volumes. But this approach has been very difficult to apply to the actinides, and to plutonium in particular, because the differences in total binding energy between different crystal structures are very small and relativistic effects are a significant factor in determining which structure and atomic volume yield the lowest energy. In the past decade, however, the elegant work by Söderlind et al. (1995), which

incorporates most of the physics that is difficult to calculate (for example, low-symmetry structures and the relativistic motion of core electrons), demonstrates convincingly that the 5f electrons are bonding in α-plutonium.

It is still true, however, that early pioneers such as Willie Zachariasen and Jacques Friedel led the way, predicting that the 5f electrons in the light actinides are bonding. They based their conjecture on a comparison of the atomic radii (or volumes) of the light actinides with those of the d-electron transition metals. Atomic volumes provide one of the best guides to what the electrons are doing.

As shown in Figure 9, the nearly parabolic decrease in atomic radii of the light actinides is very similar to that of the 5d transition metals, providing convincing evidence that, as 5f valence electrons are added across the early part of the actinide series, they increase cohesion and thus cause the atomic volume to decrease. This decrease in atomic volume due to 5f bonding was not anticipated for the 5f series. The 5f electrons were supposed to behave like the 4f valence electrons in the rare earths, which are localized in the ionic cores and are therefore chemically inert, or nonbonding. For that reason, the atomic volume remains relatively constant across the rare-earth series.

Another sign of electron localization vs itinerancy is the presence or absence, respectively, of local magnetic moments. The 4f electrons in the rare earths produce local moments (except for those elements with half-filled or filled 4f shells), whereas the 5f electrons in the light actinides, up to α-plutonium, do not.

Why do 5f electrons bond in the light actinides? Why do 4f electrons not bond in the rare earths? In other words, why are the 5f electrons spatially more extended than the 4f electrons? The Pauli exclusion principle requires that the 5f wave functions be orthogonal to the 4f core-level wave functions in the actinides. This requirement pushes the 5f wave functions somewhat farther from the ion cores. In addition, the greater nuclear charge of the actinides compared with that of the rare earths causes larger relativistic effects, increasing the radial extent of the 5f wave functions somewhat, while drawing the 7s and 7p orbitals closer to the cores, as shown in Figure 3. One implication is that the relative radial separation of the 5f, 6d, and 7s orbitals in the actinides is less than the corresponding radial separation of the 4f, 5d, and 6s orbitals in the rare earths. So, in the rare earths, the 5d and 6s orbitals of neighboring atoms overlap, whereas the 4f electrons remain nonbonding. In the actinides, on the other hand, as the 6d and 7s orbitals of neighboring atoms overlap and become bonding, so do the 5f orbitals.

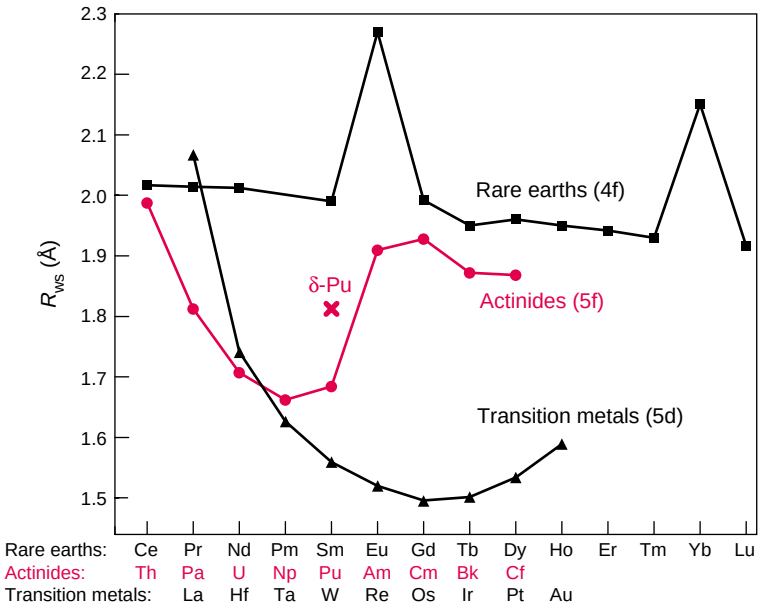

Figure 9. Experimental Atomic Radii of the Actinides, Rare Earths, and 5d Transition Metals

The atomic radius displayed is the Wigner-Seitz radius, defined as $4\pi/3\ R_{WS} = V$, where V is the equilibrium volume per atom of the primitive unit cell. The rare-earth elements show only a slight lattice contraction, indicating that the 4f electrons are added to the core (that is, they are localized) as the nuclear charge is increased across the series. The exceptions are europium and ytterbium for which one electron is removed from the conduction band to fill up half of the f shell and the entire f shell, respectively. Fewer conduction electrons (or lower valence) result in weaker bonding and an expanded volume. The actinides follow the transition-metal trend up to plutonium. Past americium, they behave more like the rare earths.

Boring and Smith emphasize (see the article on page 90) that the 5f conduction band determines the bonding properties and crystal structure of α-plutonium, which has five 5f electrons and only one d and two s electrons. They also emphasize the interplay of the different bands in determining the equilibrium crystal volume. Their simplified band calculations (for fcc structures with spherical potentials) show that occupation of the s states in plutonium provides a repulsive force, expanding the equilibrium crystal volume and making the f bands narrower than they would be otherwise. This general picture is borne out by the more-sophisticated full-potential band structure calculations performed by Wills and Eriksson. Those calculations demonstrate clearly that the 5f electrons

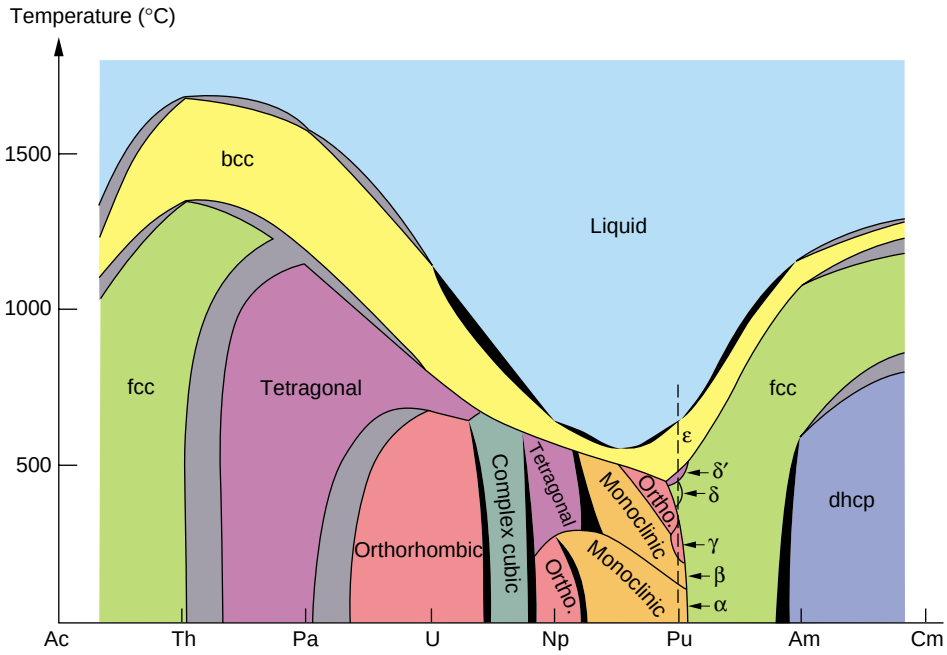

Figure 10. Connected Binary-Phase Diagram of the Actinides

The binary-phase diagrams (temperature vs composition) for adjacent actinide elements are connected across the entire series to demonstrate the transition from typical metallic behavior at thorium to the enormous complexity at plutonium and back to typical metallic behavior past americium. Two-phase regions are in black; uncertain regions are in gray.

in the light actinides extend just far enough to overlap and form narrow conduction bands, whereas the 4f electrons in the rare earths do not.

The calculations of Söderlind et al. (1995) also demonstrate how those narrow 5f bands stabilize low-symmetry structures. Until recently, the low-symmetry ground-state crystal structures and many other peculiar properties in the light actinides up to α-plutonium were attributed to the highly directional nature of the f-electron orbitals (see Figure 3). That orbital directionality was believed to cause covalent-like directional bonding (that is, electron charge buildup between the ion cores) in the solid. But band structure calculations show no charge buildup between the ion cores, refuting the original assumption.

Instead, Söderlind et al. show that it is the narrowness of the 5f conduction band that favors the stability of low-symmetry structures. As shown in Figure 8, a narrow energy band has a very large number of occupied states (high density of states) right below the Fermi energy. If the crystal structure is highly symmetric, the conduction bands are degenerate in high-symmetry directions—that is, there are two (or more) states of equal energy for each value of the crystal momentum. However, a distortion to a tetragonal, orthorhombic, or monoclinic lattice will split the degenerate portion of the band into two (or more) bands—one lower and the other higher in energy. If the band is narrow, the distortion will lower the energy of billions of occupied states (there are about a billion states within 10^{-14} eV of the Fermi energy), thereby tending to lower the total binding energy of the sample. This effect is demonstrated in Figure 11 on page 143 of the article "Actinide Ground-State Properties."

A competing influence is the electrostatic, or Madelung, energy (the result of conduction electrons not completely shielding the ion cores on the lattice sites). The Madelung energy is lowest for high-symmetry crystal structures, and it increases if the lattice is distorted. Thus, for moderate and wide bands (moderate to low density of states near the Fermi level), the Madelung energy, which favors high symmetry, wins out, and no distortion occurs. In narrow-band materials, the opposite is true.

Peierls (1955) was the first to suggest that lowering the symmetry of a one-dimensional lattice could lower the energy and increase stability, and Heine (1969) made a similar suggestion for s-p electron metals such as mercury, gallium, and indium, which also exhibit lattice distortions that favor low-symmetry structures. Söderlind et al. (1995) showed that, by forcing transition metals or p-bonded metals to have narrow bands (that is, by assuming an unnaturally large separation between atoms), the low-symmetry structure becomes the lowest-energy structure although no f electrons are involved.

One might argue that cerium provides a counter example to the rule that narrow bands favor low-symmetry structures. Cerium transforms from the fcc γ-phase to the much denser fcc α-phase when the temperature is lowered or the pressure is increased. Johansson (1974) suggested that this transition occurs because localized f states in the fcc γ-phase become itinerant (Bloch) states in the fcc α-phase, forming a narrow f band and increasing the bonding. (This transition is similar to the Mott insulator-to-metal transition, except only the f electrons are involved.) Thus, the existence of a narrow f band in the highly symmetric fcc α-phase of cerium seems to contradict the rule that narrow bands produce low-symmetry structures. However, in cerium, there is less than one full f electron per atom that can bond, compared with two s electrons and one d electron per atom. Hence, the s and d electrons, which favor high-symmetry structures, play a dominant role in determining crystal structure.

We can now begin to interpret the systematic changes in crystal structure that occur across the actinide series. Smith and Kmetko (1983) devised a clever graphic way to view these trends, a "connected" phase diagram (see Figure 10). Calculations show that f electron bonding begins at thorium with a

fraction of an f electron per atom in the conduction band. That contribution to bonding is insufficient to swing the energy balance toward a low-symmetry distortion, and cubic crystal structures are observed. From left to right across the actinide series down to plutonium, the number of f electrons in the conduction band increases, the f electrons play a larger role in bonding, and the ground-state crystal structures have increasingly lower-symmetry—plutonium is the least symmetric with a monoclinic structure. Beyond plutonium, the f electrons become localized (as in the rare earths), the s and d bands determine the crystal structure, and high-symmetry ground-state structures become prevalent.

Multiple Electronic Configurations of Nearly Equal Energy. The second fundamental feature leading to the unusual properties of plutonium was already mentioned in connection with Figure 5: The energy levels of the 7s, 6d, and 5f electrons in the isolated atom are very close to each other, resulting in overlapping energy bands and hybridized Bloch states. Wills and Eriksson have shown (in the article on page 128) that, under high pressure, the 6p core states may overlap and form Bloch states, producing an energy band that overlaps the s, d, and f bands.

Because the energy levels are so close, very little change in temperature, pressure, or chemical additions is required to prompt a change in crystal structure. Increasing temperature, for example, introduces entropy effects through lattice vibrations. The higher the temperature, the more important the entropy term becomes in determining the free energy of the system. So, it is easy to see why the crystal structures in plutonium are so unstable with respect to temperature. Unfortunately, it is very difficult to add the effects of vibrating (thermally excited) atoms to electronic-structure calculations because density functional theory, the basis for all modern calculations, only applies to the ground state ($T = 0$).

By varying the atomic volume, we can, however, model pressure. Increasing the pressure (assuming smaller atomic volumes) shifts the relative stability of the bands and broadens the bands. As I discuss later, we know empirically that increased pressure quickly squeezes out the high-volume, high-symmetry phases of the light actinides in favor of the low-symmetry structures. However, as the pressure is increased further, the bands will eventually broaden sufficiently for crystal distortions not to be energetically favorable, and high-symmetry structures are predicted to return. For the heavy actinides, increased pressure will cause a delocalization similar to that in cerium, yielding low-symmetry structures initially. Such calculations can be done at absolute zero for ground-state predictions. The predictions of Wills and Eriksson for pressure-induced phase transformations are highly accurate.

Changing chemistry by alloying can affect electronic structure. Moreover, alloying can affect vibrational and configurational entropy contributions. So, one would expect phase stability in the actinides to be very sensitive to chemical additions. Band structure calculations cannot yet deal with alloying effects to the level of required accuracy.

Brewer (1983) adopts the chemist's viewpoint to predict the effect of multiple, closely spaced energy levels in plutonium on crystal stability. On the basis of spectroscopic evidence, he claims that at least four different atomic configurations are of nearly equal energy in plutonium metal. Different atomic configurations result in atoms of different sizes, and those atoms account for increased liquid stability. Stability is increased when compared with that for cubic structures that have equivalent lattice sites. He also points out that atoms of different sizes can pack more efficiently in a complex structure. Whereas close-packed structures are most efficient at filling space when the atoms are of equal size, mixing atoms of different sizes can result in higher densities and larger coordination numbers.

For example, the Laves phases, the most-common intermetallic compounds, can be packed to a coordination number of 13.3 by A and B atoms with a radius ratio of 1.225 being arranged in either the cubic structure of $MgCu_2$ or the hexagonal structure of $MgZn_2$ or $MgNi_2$ (Haasen 1992). The α-phase monoclinic structure of plutonium is a slightly distorted hexagonal structure. Lawson et al. (1996) point out that its nature can be viewed as "self-intermetallic" because it contains 16 atoms per unit cell and 8 distinct positions for those atoms. They compare the α-plutonium structure with the very complex structure of α-manganese, which has 58 atoms per unit cell and 4 distinct atomic positions. In addition, short bonds are prevalent on one side of the α-plutonium atom, and long bonds are prevalent on the other side, suggesting that the atoms are also nonspherical, a feature that further complicates the crystal packing. Therefore, it seems intuitively correct to say that α-plutonium packs more closely than do single-sized hard spheres.

Sitting on the Knife-Edge between Bonding and Localized Behavior. Plutonium has one more feature that sets it apart from uranium, neptunium, and americium, its neighboring elements. That feature derives from its position in the actinide series. Plutonium sits right at the transition point at which the 5f electrons change from being bonding to being localized (chemically inert). As the nuclear charge increases across the actinides, the increase causes the atomic volume to contract slightly because the electron wave functions are pulled slightly closer to the ion cores (in the rare earths this same phenomenon is called the lanthanide contraction). The much larger effect is that, much like each additional d electron in transition metals, each additional 5f electron produces a relatively large decrease in atomic volume because the 5f electrons go into the conduction band and add to the bonding (see Figure 9).

The atomic volume of the transition

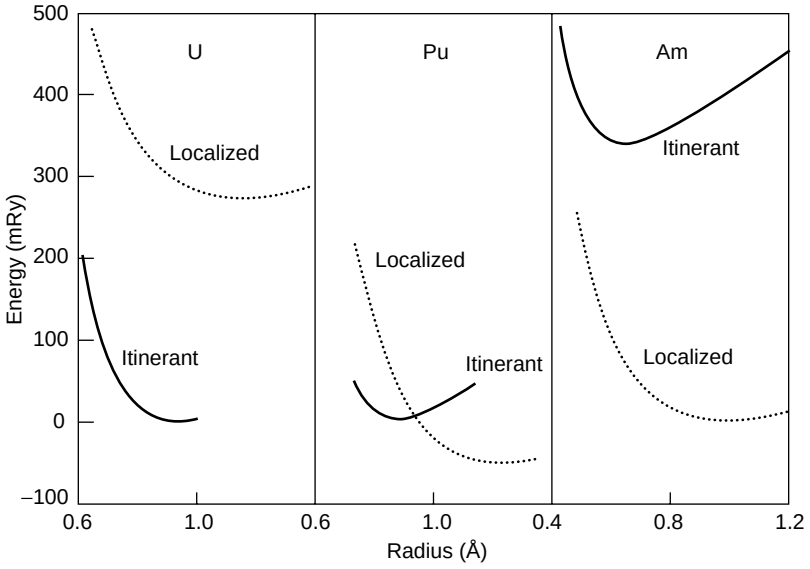

Figure 11. Bonding of 5f Electrons in Plutonium vs Adjacent Elements
These plots of total energy vs normalized lattice based on Eriksson et al. (1999) demonstrate the effects of shifting the 5f electrons from bonding states (solid line) to localized states (dotted line). At uranium, there is little question that 5f bonding produces the lowest energy state, and at americium, 5f localization produces the lowest energy state. At plutonium, the balance clearly shifts from bonding to localization. Experimental error in the estimated energy gain on localization—about 50 mRy—precludes a clear prediction of the nature of the plutonium ground state from these calculations. (This figure was adapted with permission from Elsevier Science.)

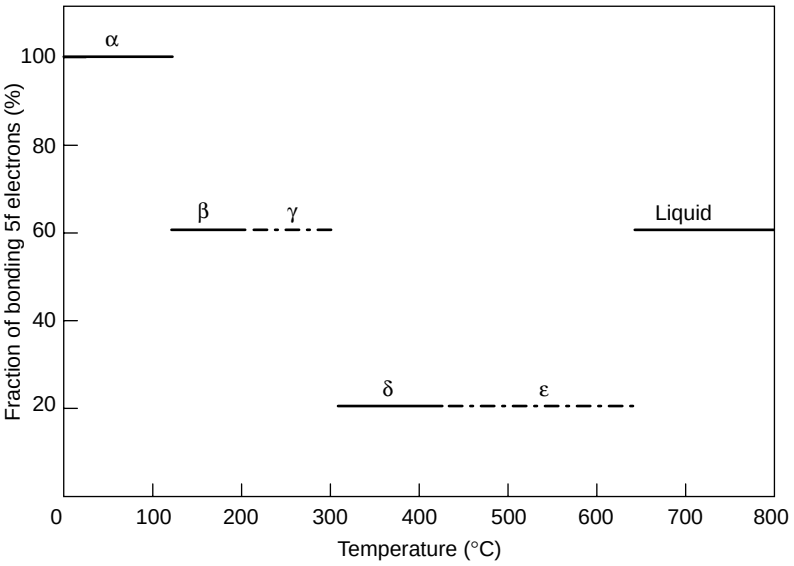

Figure 12. Notional Diagram for 5f Electron Bonding in Plutonium Phases
Söderlind et al. (1997) have shown that all five 5f electrons bond in the α-phase. To get the correct volume for the δ-phase, Eriksson et al. (1999) must allow four 5f electrons to localize and only one to bond. In the β-phase, γ-phase, ε-phase, and the liquid phase, the number of bonding 5f electrons is expected to be between five and one. In this diagram, the estimates for the β-, γ-, and ε-phase are based on the atomic volumes. The estimate for the liquid phase is based on the fact that, from these calculations, the thermal-expansion curve for the β-phase extrapolates to that of the liquid state.

metals reaches a minimum when the d shell, which holds 10 electrons, is half full. Past that point, cohesion begins to decrease and atomic volume begins to increase because the antibonding states of the d band start to be filled. The 5f shell holds 14 electrons, and one might expect the atomic volumes of the actinides to decrease in moving toward curium whose f shell is half full. Instead, the atomic volume of plutonium is slightly greater than that of neptunium. Total energy calculations of Eriksson et al. reproduce this upturn when the low-symmetry monoclinic structure of plutonium's α-phase serves as input. These scientists attribute the upturn to the openness of that structure. In any case, the increase in nuclear charge finally causes the 5f electrons to localize at americium, and the atomic volume expands dramatically because now none of the 5f electrons bond.

The transition from bonding (itinerant) 5f electrons in uranium to localized 5f electrons in americium is graphically illustrated by the plots of total energy vs relative lattice constant in Figure 11. Perhaps even more intriguing, the transition appears to occur right at plutonium, not between plutonium and americium. Eriksson et al. have tried to match the atomic volume of the fcc δ-phase in plutonium. They find that they have to let four of the 5f electrons localize but keep one of them bonding. (I will return to the puzzle of the δ-phase later). On the basis of discussions with Wills, I show a notional sketch of how localization may proceed in the plutonium allotropes (Figure 12). The value for the liquid is only a guess guided by comments made by Hill and Kmetko (1976) that the liquid accommodates 5f bonding better than the cubic solid phases. Based on the extensive work on liquid plutonium by Wittenberg et al. (1970) that showed that the molar volume of the liquid is the same as that of the β-phase, Hill and Kmetko called the β-phase the "solid-state" analogue of the liquid. Hence, I estimated the degree of 5f electron localization to be the same for the liquid as for the β-phase.

Having to describe different allotropes of the same element at room temperature and above by such different electronic states (mixtures of Bloch states and localized states) is unprecedented. Plutonium is truly unique among the elements in the periodic table. And more important for the metallurgists who must work with this material, the transition from Bloch states to localized states causes both the atomic volume and the crystal structure to change dramatically.

What Basic Properties Really Matter to Metallurgists?

The electronic structure at absolute zero is a starting point for understanding plutonium, but it is far removed from typical interests in the practical world of metallurgy. Metallurgists must relate the basic properties of metals and alloys to their microstructures and then tailor those microstructures to produce desired engineering properties for specific applications. As Peter Haasen pointed out (1992), microstructure begins where condensed matter physics typically leaves off. Crystal structure—the perfect periodic array of atoms in a single crystal—forms the foundation of condensed matter physics. Metallurgy is directly affected by those perfect crystalline arrays (see the box "Atomic Packing and Slip Systems in Metals" on page 308), but it also takes into account that they are mostly confined to very small, microscopic regions. In other words, between the macroscopic scale of continuum mechanics and the atomic scale of perfect crystal lattices, there is another scale, that of microstructure, which is governed by the properties of individual grains, their crystalline defects, and the interactions among them all. Examples of microstructures and their defect substructures are shown in Figure 13.

For most technologically important materials, especially structural materials, microstructure determines engineering properties. Therefore, the basic properties that really matter to the

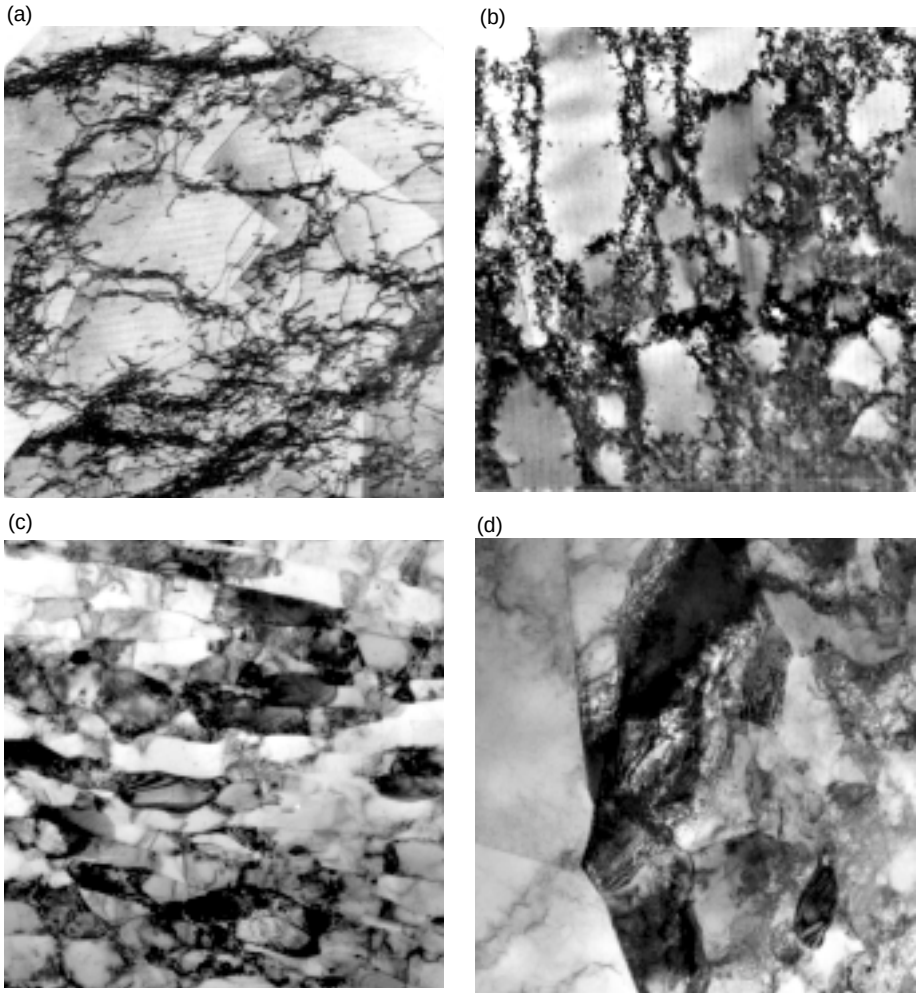

Figure 13. Dislocation Microstructures in fcc Metals

Dislocations are key microstructural features in solids. These line defects typically range in concentration from 10^6 to 10^{12} dislocations/cm^2. Readily formed during solidification or deformation, they easily arrange themselves to lower the overall energy of the system, leaving a substructure within a crystal or within the grains of a polycrystal. The examples here show that dislocations form and rearrange during cold-working and subsequent annealing. Dislocations are best imaged by their contrast in an electron beam. They can be observed as dark lines in a transmission-electron-microscope image. (a) Individual dislocations and dislocation tangles in the form of "braids" appear in copper deformed at 77 K. (b) Dislocations organize into cell walls during heavier deformation of copper at room temperature. (c) Commercially pure aluminum undergoes even greater organization of dislocations during heavy deformation at room temperature, forming clean cell walls (sample was cold-rolled 83% at room temperature—cells are stretched out in the direction of principal elongation). (d) During annealing at 440°C, commercially pure aluminum recrystallizes, or forms new, nearly-strain-free grains as indicated by the high-angle grain boundaries. Some of the dislocation cells, or subgrains, are still visible in the right-hand grain.

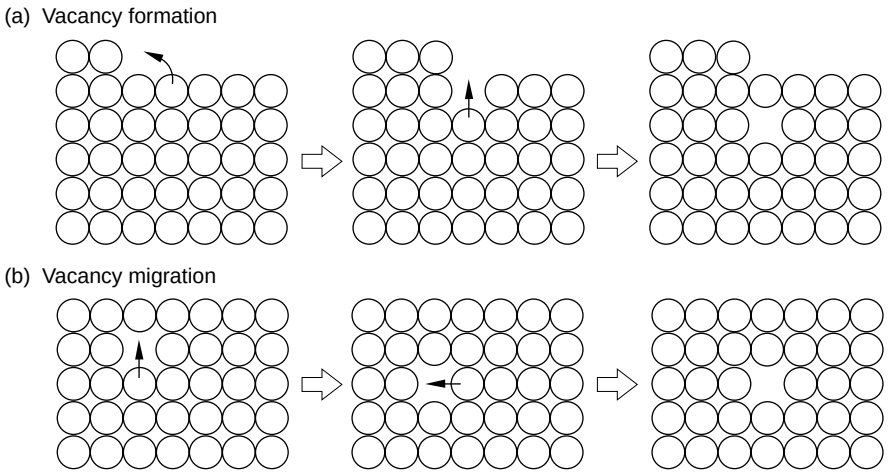

Figure 14. Vacancy Mechanism for Diffusion and the Strong Dependence of Metallurgical Properties on Homologous Temperature

(a) A lattice vacancy is created when an atom at an interior lattice site jumps to a site on the surface. The equilibrium ratio of vacancies to atoms is $n_v/n_0 = \exp(-Q_F/k_BT)$, where Q_F is the activation energy for vacancy formation. (b) Vacancies migrate in a crystal as atoms jump to vacant lattice sites. The number of jumps per atom is $r_a = n_v/n_0 A \exp(-Q_m/k_BT)$, where Q_m is the activation energy for vacancy migration. Note that both vacancy formation and migration are highly dependent on the homologous temperature rather than the absolute temperature. For example, in copper at 1350 K (6 K below the melting point of copper, or T/T_m = ~1.0), the equilibrium vacancy concentration is 10^{-3}, the jump rate is 10^9/s, and the vacancies are ~10 atoms apart on average, whereas at room temperature ($T/T_m < 0.25$), the vacancy concentration decreases to 4.5×10^{-15}, the jump rate decreases to 10^{-6}/s, and the vacancies are ~10^5 atoms apart. At room temperature (T/T_m = ~0.5), the jump rate in lead is 22/s, and the vacancies are ~100 atoms apart.

plutonium metallurgists are those that have the greatest influence on microstructure: crystal structure, melting point, and phase stability.

Crystal Structure. The internal energy of metals depends primarily on their atomic volumes. Energy differences resulting from different structural arrangements are typically very small. For example, in sodium the heat of transformation from a body-centered-cubic (bcc) to hexagonal close-packed (hcp) structure at 36 kelvins is only one-thousandths of the total binding energy. Yet, crystal structure has a dominant effect on metallic properties.

Metallic bonding exhibits little directionality because the conduction electrons that hold the atoms together are shared throughout the crystal lattice. Therefore, atoms in metals tend to pack uniformly, leaving the minimum amount of void space. Indeed, metals solidify preferentially into close-packed fcc and hcp structures and into the nearly close-packed bcc structure (see the box "Atomic Packing and Slip Systems in Metals" on page 308). In fact, in their ground states, 53 of the elements up to plutonium (element 94) have fcc or hcp structures and 23 have bcc structures. If the tetragonal structure is also considered nearly close-packed, all but four of the metals in the periodic table exist in one of these four simple crystal structures.

The host crystal structure determines macroscopic structural properties of metals in many ways. For example, as shown on pages 308 and 309, crystal structure determines the operative slip planes, as well as the nature of crystalline defects, and those defects control the strength of the material and most other structural properties. For example, plastic deformation by slip does not occur homogeneously when entire lattice planes are slipped over each other. Instead, it is made significantly easier by the motion of line defects known as dislocations (see Figure 4 in "Mechanical Behavior of Plutonium and Its Alloys" on page 341).

The formation and motion of point defects such as lattice vacancies are also influenced by crystal structure. We will show later that migration of vacancies is the primary mechanism for bulk diffusion in metals. Interestingly, because relaxation of atoms surrounding a vacancy is controlled by atomic coordination and the strength of the bonding, vacancy migration is easier in the bcc structure than in close-packed structures, and therefore diffusion is significantly faster in the bcc structure. On the other hand, vacancies are formed more easily in the close-packed structures.

Crystal structure also has a direct effect on the nature of thermal lattice vibrations and, therefore, on the vibrational entropy of crystals. At high temperatures, the entropy contribution to the free energy can become very large and therefore have a dominating influence on phase stability. For example, because it has fewer nearest neighbors than close-packed metals, the bcc lattice exhibits lower vibrational frequencies and therefore higher vibrational entropy (or a high uncertainty of position in the lattice) than other crystal structures. Indeed, the bcc lattice is the structure with the lowest free energy at high temperatures. Consequently, most metals melt from the bcc structure.

It should now be apparent that the phase changes in plutonium are more than an annoyance because the accompanying changes in crystal structure have a dramatic influence on structural properties. In particular, at low and slightly elevated temperatures, the low-symmetry α-, β-, and γ-phase become stable as opposed to the high-symmetry, ductile structures found in most metals.

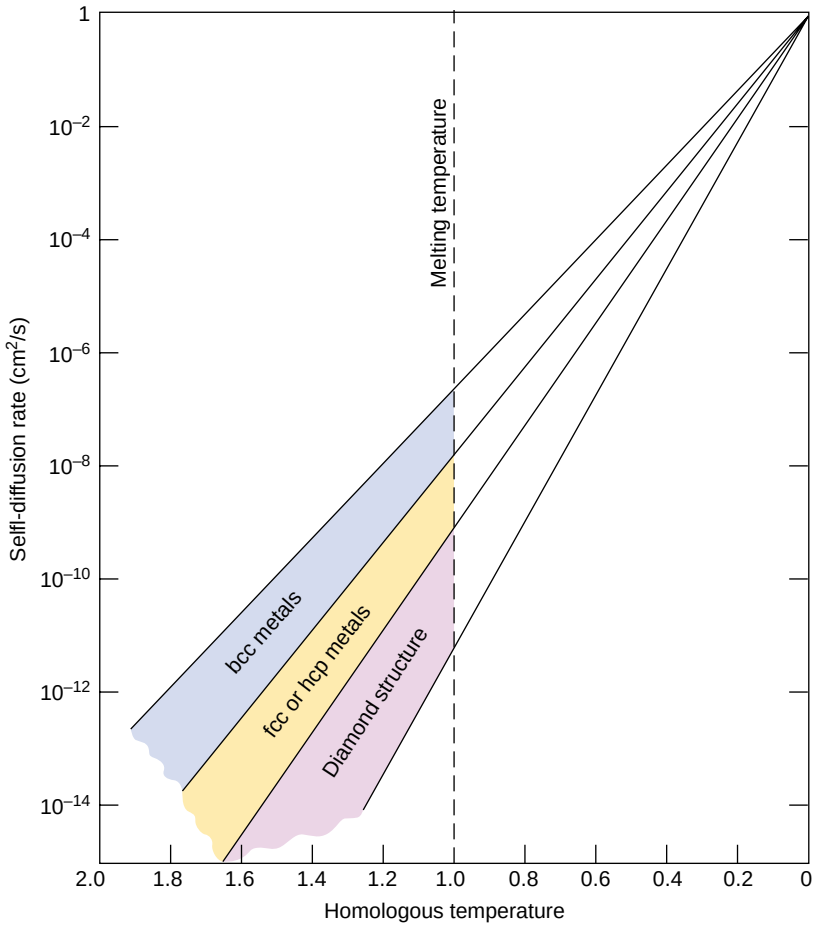

Figure 15. Self-Diffusion Rate, Melting Point, and Crystal Structure

Sherby and Simnad (1961) demonstrated that rates of self-diffusion in metals fit a common form, $D = D_0\exp(-KI(T/T_m)$, scaling with the homologous temperature T/T_m. There is also a crystal-structure dependence with the open bcc structure exhibiting faster diffusion than the close-packed and diamond-cubic structures. Only the trends are indicated here. You can refer to the above-mentioned reference for specific data on the following: bcc metals—γ-uranium, sodium, α-iron, lithium, niobium, β-titanium, chromium, tantalum, and β-zirconium; hcp metals—magnesium, zinc, cadmium, α-titanium, α-zirconium, complex hexagonal β-uranium, and graphite; fcc metals—platinum, gold, silver, copper, β-cobalt, γ-iron, nickel, lead, and face-centered-tetragonal (fct) indium; and diamond structures—germanium, complex bct β-tin. At high temperatures, several bcc elements, such as β-zirconium and ε-plutonium, have anomalously high self-diffusion rates that do not fit the trends.

Melting Point. The melting point marks the end of solid-phase stability—the temperature at which the free energy of the liquid drops below that of the solid phase (or solid allotropes). Although liquid metals have a finite bulk modulus and many other properties common to metals, they have no shear strength. (They do, however, have internal friction, otherwise known as viscosity). Some theories of melting, such as that of Lindemann (Lawson et al. 1996), predict that melting occurs when the amplitude of atomic vibration reaches a critical fraction of the separation between atoms. That critical fraction is typically found to be approximately one-tenth. Other theories relate melting to a critical density of mobile vacancies.

The melting point is of interest to metallurgists not only because it marks the end of solid stability, but also because it indirectly affects most processes of engineering interest. For example, most processes that affect formation and evolution of microstructures depend on temperature through an Arrhenius-type rate equation, $R = R_0\exp(-Q/k_BT)$, where Q is the activation energy for the process and R_0 is a constant. At moderate temperatures, those processes tend to be thermally activated, meaning that thermal vibrations help to overcome activation barriers, but as the temperature is increased (typically to nearly half of the melting point), diffusional processes begin to dominate microstructural evolution.

The most prevalent mechanism for bulk diffusion is the vacancy mechanism shown schematically in Figure 14. As suggested above, formation and migration of vacancies obey an Arrhenius relationship. As metals approach their melting points, vacancies form and move easily because thermal lattice vibrations become large enough to overcome activation barriers. Consequently, diffusion rates in solids increase rapidly near the melting point. It seems reasonable then that atomic mobility should depend not on the absolute temperature, but on the homologous temperature (T/T_m); that is, on how close the temperature is to the melting point of the material.

Sherby and Simnad (1961) demonstrated the importance of homologous temperature on the rate of diffusion in solids (Figure 15). They found that the Arrhenius-like rate equation for self-diffusion, $D = D_0\exp(-Q/k_BT)$, where D_0 is a constant and Q is the activation energy for self-diffusion (vacancy formation and migration), provided a good fit to most of the measured diffusion data in solids when it was rewritten as a function of homologous temperature: $D = D_0\exp(-K/(T/T_m)$. In addition to the dependence on homologous temperature, they also found that the diffusion rate—in particular, the activation para-

Atomic Packing and Slip Systems in Metals

The details of atomic packing (space filling, coordination number, and symmetry) govern most physical and mechanical properties of metals. In particular, the slip planes and slip directions of each structure determine the response to shear stresses. Here we focus on the atomic packing and slip systems of the most-common crystal structures of metals: face-centered cubic (fcc), hexagonal close-packed (hcp), and body-centered cubic (bcc). These three have direct relevance to plutonium: the fcc δ-phase Pu-Ga alloys are the most important from an engineering standpoint, monoclinic α-plutonium can be thought of as a slightly distorted hcp structure, and plutonium and its alloys melt out of the bcc ε-phase—see Figures (a)–(c) below.

The fcc and hcp crystal lattices (with a *c*/*a* ratio of 1.633) are close-packed, filling space most efficiently. If one assumes spherical atoms, 74 percent of the volume is filled, and each atom has 12 nearest neighbors (or a coordination number of 12). By comparison, simple cubic packing of atoms at the cube corners fills only 52 percent of the volume. The nearest neighbors in the close-packed lattices are very close at $0.707a_0$, where a_0 is the lattice parameter and the 6 next-nearest neighbors are at a_0. Higher coordination numbers are possible if the atoms have different sizes.

The bcc structure (c) has only 8 nearest neighbors at a distance of $0.866a_0$, but it has 6 next-nearest neighbors at a_0. The more open bcc structure results in significantly different properties as well. The directionality (or anisotropy) of properties depends on the symmetry of the crystal lattice.

Stacking of Close-Packed Planes. The fcc and hcp lattices have identical close-packed planes (shaded), but as shown in the figure, the relative placement of those planes differs as they are stacked on top of each other—ABCABC for fcc and ABABAB for hcp. In other words, the placement repeats every third layer for fcc and every second layer for hcp. Note that the close-packed planes in the fcc structure are perpendicular to the fcc body diagonal, or [111] direction. The difference in stacking between hcp and fcc, although seemingly small, has profound effects on metallic properties because the fcc structure has many more equivalent slip systems than the hcp.

The figure also shows the close-packed directions in each close-packed plane. For example, the face diagonals of the fcc structure are close-packed. The atoms can be considered as touching in this direction, and it is easy to imagine that the elastic response (the reversible stretching of the atomic bonds) in a close-packed direction may be much stiffer than in other directions in which the atoms do not touch. The number of close-packed directions depends on crystal symmetry.

Slip Planes and Slip Directions. Plastic deformation leading to a permanent shape change (at constant volume) occurs by shear.

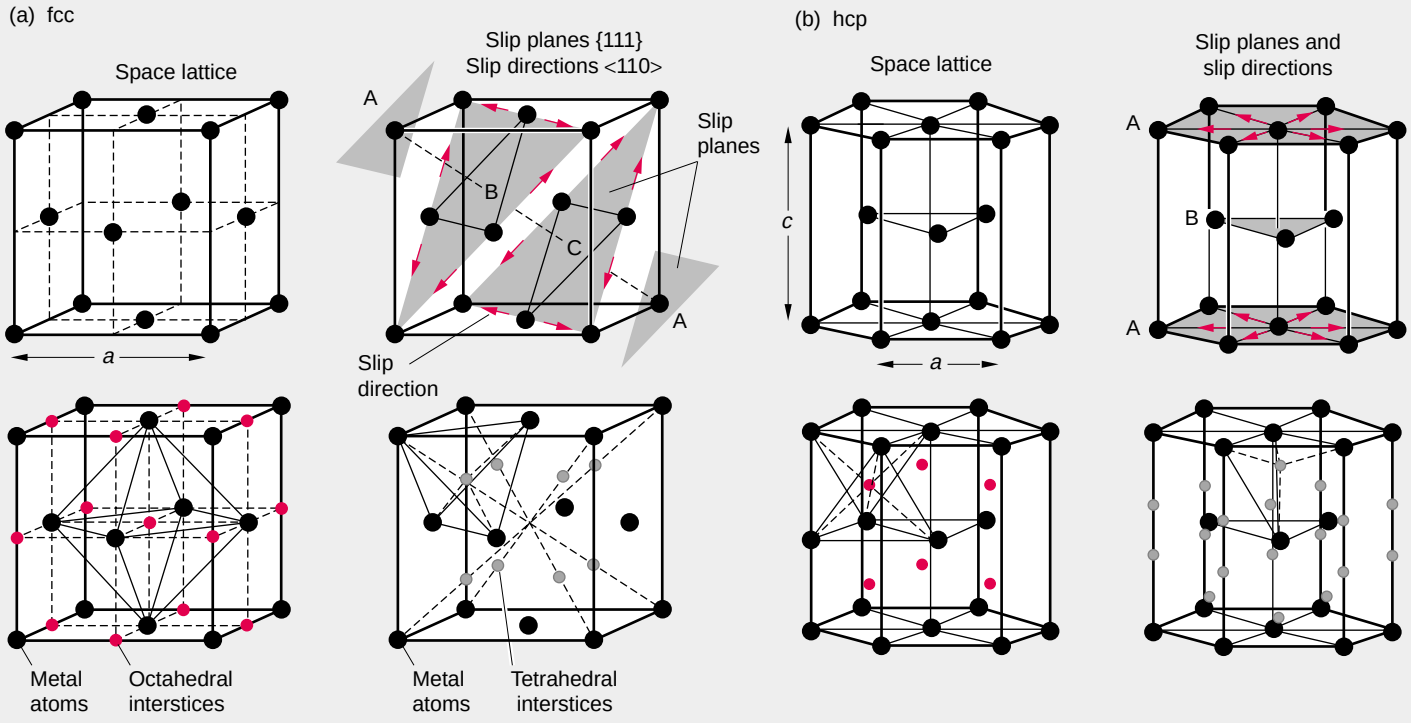

From a simple hard-sphere model, it is apparent that it is easiest to shear (or slip) rows of atoms over close-packed planes and along close-packed directions because close-packed planes have the largest separation and sliding them along close-packed directions offers the least geometrical resistance to shear.

Slip occurs when the critical resolved shear stress (shear stress in a slip plane at which dislocations begin to move, and plastic flow is initiated) is reached on one of the close-packed slip systems (combination of slip plane and slip direction). The greater the number of crystallographically equivalent slip systems that exist, the easier it will be to reach the critical resolved shear stress on one of the slip systems. The fcc structure has 4 equivalent close-packed planes—the octahedral or {111} Miller indices planes—and each of these planes has 3 equivalent close-packed directions (the face-diagonals or <110> directions) for a total of 12 equivalent slip systems. This redundancy of slip systems makes fcc metals typically very malleable (or ductile).

In the hcp structure, on the other hand, the basal plane is the only close-packed plane. It has three equivalent close-packed directions (same as the fcc lattice) and, hence, only three equivalent slip systems. However, some properly oriented hcp single crystals (for example, of magnesium) can still exhibit large amounts of slip. In addition, at higher stresses or elevated temperatures, other slip systems can be activated. Also, an entirely different deformation mode, twinning, is readily activated in hcp metals in which slip does not occur readily. An additional serious complication in hcp metals is that the structure is close packed only if the *c*/*a* ratio is 1.633, the ideal ratio for spherical atoms. Most hcp metals deviate from this ratio, indicating that the atoms are not ideally spherical. The ductility of most polycrystalline hcp metals is limited because of their inability to operate a sufficient number of multiple slip systems simultaneously.

The bcc structure has no close-packed planes similar to the {111} planes in the fcc structure. The most-closely-packed planes are the six {110} planes, which contain two close-packed <111> directions along which hard spheres would be in contact. Many bcc crystals slip along almost any plane that contains a close-packed direction. The {112} slip planes are the most common ones for bcc crystals at ambient temperature. At low temperatures, the {110} planes are more prevalent. In fact, one generally finds that, in any of the structures, the rule that slip occurs in close-packed directions is almost never violated, whereas the close-packed plane rule is less stringent. The multiplane slip character of bcc crystals is decidedly different from slip in fcc and hcp crystals. Another peculiarity of bcc crystals is that they are essentially unstable when subjected to a shear on the {110} planes in the <110> direction. This instability plays an important role in the collapse of most bcc lattices to close-packed lattices by martensitic phase transformations.

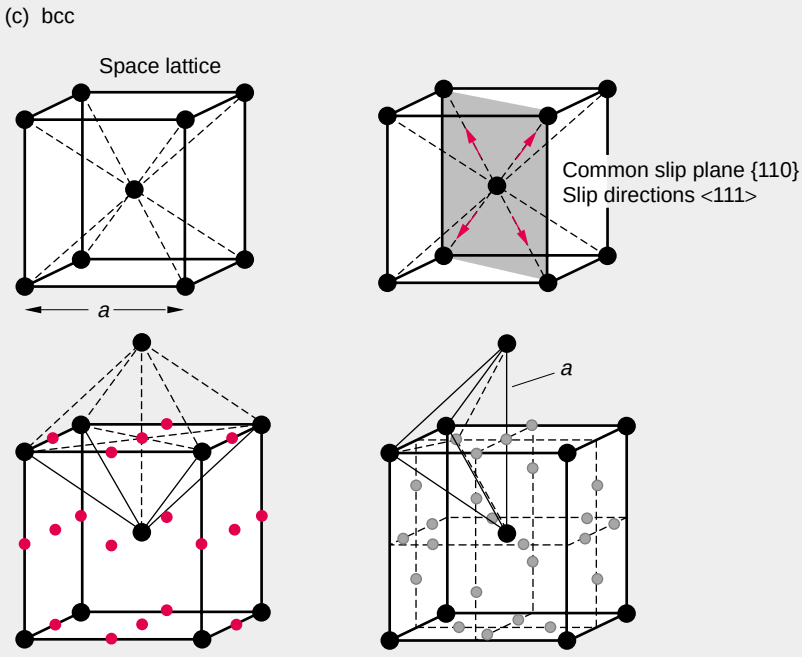

Interstitial Lattice Sites. The size, shape, and coordination of interstices (or holes) in the different lattices control how easily foreign atoms can be accommodated in interstitial positions. The close-packed structures (a) and (b) have two types of interstices—octahedral and tetrahedral (the interstices are arranged differently in the two lattices). The octahedral holes will accommodate a sphere of maximum radius equal to 0.41r (where r is the spherical radius of the close-packed atoms) and the tetrahedral holes will accommodate spheres of 0.225r. In the bcc structure (c), the interstices are smaller in spite of the fact that it is considered the more-open structure. The tetrahedral holes will accommodate spheres of 0.291r and the octahedral holes, 0.154r. However, the shape of the interstices is also important. For example, a carbon atom (r = 0.8 angstrom) in bcc iron prefers the smaller octahedral sites (0.19 angstrom) to the tetrahedral sites of 0.36 angstrom because the different shape and coordination of the interstices require the carbon atom squeeze in between four iron atoms in the tetrahedral sites and only in between two atoms in the octahedral sites.

Table II. Dependence of Several Metallurgical Processes on Temperature

Process	Temperature Range
Thermal recovery of nonequilibrium point defects	
Interstitials	~0.02 T_m
Limited vacancy migration	~0.2 T_m
Bulk vacancy migration	>0.45 T_m
Thermal recovery of dislocation structures[a]	~0.3 T_m
Recrystallization of highly strained microstructure	0.3–0.5 T_m
Homogenization of segregated microstructures	>0.5 T_m
Grain growth	>0.5 T_m

[a]Metals with high stacking fault energies, such as aluminum, show significant recovery of dislocation structures below 0.33 T_m, whereas metals such as copper with lower stacking fault energies show little recovery before recrystallization.

meter *K*—depended on crystal structure. It is intuitively reasonable that the activation energies for the formation and migration of vacancies should depend on both homologous temperature and atomic packing (crystal structure). They also claimed a correlation with valence, but this idea was less convincing.

Many metallurgical processes that control microstructure depend strongly on the homologous temperature as summarized in Table II. For metals and alloys with multiple allotropes, Ardell (1963) pointed out that the homologous temperature depends on the effective or hypothetical melting point of the lower-temperature allotropes, not the melting point for the highest-temperature allotrope. The effective melting point is determined by constructing metastable free-energy diagrams that extend the free-energy curve of the low-temperature allotrope to higher temperatures and that of the liquid downward to lower temperatures. The effective melting point of the allotrope is the temperature at which the free energies are equal. This correction is especially important for metals that have low-temperature allotropes, far removed in temperature from the actual melting point. For example, for α-uranium, α-titanium, and α-zirconium, this correction lowers the effective melting point by ~200 kelvins. Nelson, Bierlein, and Bowman (1965) used Ardell's method to show that the effective melting point for δ-plutonium is lowered only by 52 kelvins, whereas that for α-plutonium is lowered by 360 kelvins. Hence, whereas room temperature is 0.33 of the absolute melting point of plutonium calculated by conventional methods, it is effectively 0.35 for δ-plutonium and 0.53 for α-plutonium. I will examine the ramifications of these corrections later.

Phase Stability. The most immediate impact of a phase change is the change in crystal structure and the accompanying volume change. In metals such as pure aluminum, this is not a problem since aluminum cannot be coaxed, either by changing pressure or temperature, to crystallize in any other structure but the fcc. Iron, on the other hand, exhibits both fcc and bcc lattices at ambient pressure, and a hexagonal version under increased pressure. For thousands of years, metallurgists and artisans have taken advantage of transformations in iron to craft iron and steels to exhibit useful properties. However, for both aluminum and iron, several phases can be retained at room temperature by alloying—that is, intentional chemical additions. Additions of copper, magnesium, silicon, zinc, lithium, and other elements to aluminum can help stabilize phases with different crystal structures. If these phases are created as microscopic precipitates, they can effectively strengthen pure aluminum. Strengthening metals and alloys by controlling the fraction, size, and shape of second-phase constituents lies at the heart of metallurgy. The aircraft, auto, and sporting goods industries depend on such treatments. Similarly, iron has been alloyed with carbon and other elements to process steels with desirable structural properties.

Having reviewed the most important material properties of direct metallurgical interest, I will now discuss what we know about those properties in plutonium and its alloys. I will focus on the high phase instability in plutonium as well as the unusual phase transformations and their effect on microstructure. The article "Mechanical Behavior of Plutonium and Its Alloys" on page 336 reviews the effect of those strange properties on mechanical behavior, including the unusual interaction between stress (or deformation) and phase transformation in plutonium.

Phase Instability in Plutonium and Its Alloys

For plutonium and its alloys, understanding phase stability is most important. Plutonium is notoriously unstable to almost any external disturbance. In this section, I will outline how small changes in temperature, pressure, or chemistry transform plutonium easily from one crystal structure to another, and I will also summarize our level of understanding in each case.

Temperature Instability. As it is heated, plutonium transforms from its ground-state monoclinic structure, indicating that the relative levels of the total free energies (*F*) of the different phases are shifting with temperature. As discussed previously, several electronic configurations in plutonium have nearly identical potential energy. Therefore, small changes in any of the four terms that compose F (see the box on the facing page) can give rise to a phase change. The static lattice potential ϕ_0 typically changes very little with

Predicting Temperature Effects

Electronic-structure calculations are performed at absolute zero, at which temperature the only contribution to the total free energy of a solid is the internal energy due to the electrostatic interaction among the ions and electrons of the crystal lattice. However, to predict the stability of crystalline phases and their bonding properties at finite temperatures, it is necessary to compute all contributions to the total free energy of a solid. Wallace (1998) developed a rigorous lattice-dynamics treatment that requires four terms to describe the crystal Helmholtz free energy:

$$F = \phi_0 + F_H + F_A + F_E \quad ,$$

where ϕ_0 is the static lattice potential (the energy of the crystal with ions located at the lattice sites and the electrons in their ground state—that is, the energy calculated in electronic-structure calculations); F_H, the quasiharmonic free energy due to lattice vibrations, or phonons; F_A, the anharmonic free energy due to phonon-phonon interactions; and F_E, the thermal excitation of electrons, which includes electron-phonon interactions.

In general, the temperature dependence of F is dominated by lattice vibrations (F_H), except at very low temperatures, where the T^2 internal electronic-energy term dominates the T^4 internal-energy term of lattice vibrations. Each temperature-dependent term of the free energy (F_H, F_A, and F_E) is composed of both an internal energy term and an entropy term. The differential form of the Helmholtz free energy shows that the preferred independent variables for F are T and V:

$$dF = -SdT - PdV \quad ,$$

where S is the entropy, T is the absolute temperature, P is the pressure, and V is the volume. In most applications involving condensed phases, the convenient control parameters are the temperature and the pressure. While changing the temperature, it is easier to keep a solid at constant pressure and more difficult to keep it at constant volume. For systems controlled by T and P, the Gibbs free energy, $G = F + PV$, is the appropriate thermodynamic function to describe equilibrium and phase transformations. The differential is now $dG = -SdT + VdP$. In transformations between condensed phases, the PV term is negligible compared with F. Then, the difference between the Gibbs and Helmholtz free energies becomes insignificant. In metallurgy and chemistry, it is customary to express the Gibbs free energy as $G = H - TS$, where H is the enthalpy, and accept the change in the Gibbs free energy, $\Delta G = \Delta H - T\Delta S$, as the driving force for a phase change.

First-principles calculations of total free energy at finite temperatures are still beyond our reach. However, one can determine the quasiharmonic phonon density of states and dispersion curves by calculating potential energies of configurations in which the nuclei are displaced from crystal lattice sites. Successful calculations based on electronic-structure theories have been greatly aided by inelastic-neutron-scattering measurements of phonon dispersion curves. The power of inelastic neutron scattering is demonstrated in the article "Vibrational Softening in α-Uranium" (page 202). Unfortunately, information for plutonium is scarce because appropriate samples of plutonium-242 are unavailable (the large neutron-absorption cross section of the more-abundant plutonium-239 isotope makes the latter unsuitable for neutron-scattering experiments). Another approach to estimating the various contributions to the free energy is to determine the vibrational entropy terms semi-empirically. For a more detailed discussion, see the article "Elasticity, Entropy, and the Phase Stability of Plutonium" on page 208.

temperature. However, we suspect that the degree of 5f-electron localization in plutonium varies considerably from one phase to another (Figure 12), so we cannot rule out that significant changes in the static lattice potential occur with temperature.

In addition, as the temperature is increased, the other three terms of the total free energy can easily change crystal structure stability. Although plutonium is considered to be very anharmonic—that is, its lattice vibrations increase abnormally with increased temperature (indicating that the bonding, or spring stiffness, between atoms decreases substantially with temperature because of the thermal expansion of the lattice)—Wallace (1998) concluded that the temperature-dependent contribution to the free energy is dominated by the lattice vibration (quasiharmonic) contribution rather than the anharmonic effects. He also concluded that the dominant source of entropy in plutonium, as in other crystals, is represented by the phonons, or thermally induced lattice vibrations. However, lack of thermodynamic data and incomplete theoretical understanding do not allow us to pin down which terms in F are mainly responsible for the temperature instability of plutonium. In other words, we do not know whether the instability is caused by electron localization or just by entropy.

Low Melting Point. Another puzzling aspect of temperature instability in plutonium is its low melting point. Plutonium melts at a temperature much lower than one would expect from the trends observed in the transition metals. In fact, at first glance, one would expect the volume contraction of the light actinides (Figure 9) to signal increasing cohesive energies as the atomic number increases and, therefore, also higher melting points. This trend is generally observed in the transition metals. In the light actinides, as shown in Figure 10, the melting point decreases rapidly with increasing

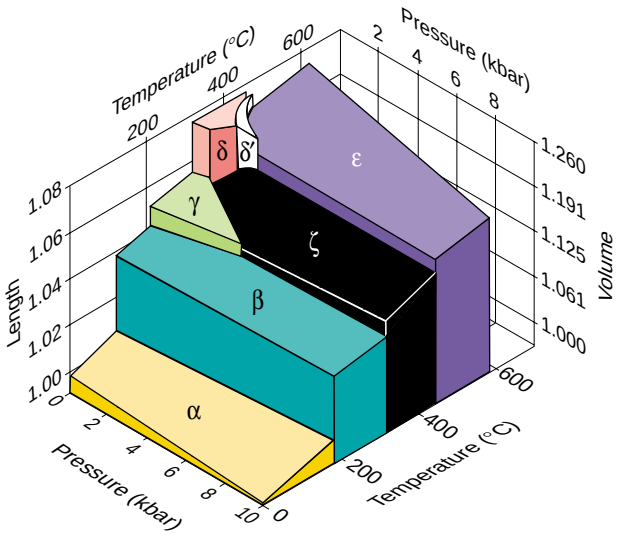

Figure 16. Plutonium Instability with Temperature and Pressure

Plutonium is notoriously unstable under almost any external disturbance. Over a span of only 600°, it exhibits six different allotropic phases with large accompanying volume changes before it melts. Pressures on the order of kilobar (100 megapascals) are sufficient to squeeze out the high-volume allotropes (Morgan 1970). Small chemical additions can stabilize these high-volume phases.

(Reproduced with permission from The Metallurgical Society.)

atomic number. The cohesive energies, however, decrease only slightly across the light actinides. In addition, the liquid phase is denser than three of the high-temperature solid phases of plutonium, it has a very large viscosity, and the highest known surface tension of any liquid metal. What makes the liquid so stable?

Lawson et al. (2000) relate the low melting point to the large thermal atomic vibrations associated with the strongly reduced elastic constants at high temperature. They incorporated a temperature-dependent Debye temperature into Lindemann's rule for melting. Lawson et al. demonstrated reasonable agreement with the melting points of the actinides by making the temperature-dependence correction for the Debye temperatures of the light actinides.

Hill and Kmetko (1976) made the intuitive argument that 5f electrons bond quite readily in the liquid phase because the atoms have greater spatial and rotational freedom. Brewer (1983) offers a very appealing explanation from a chemist's point of view. Since several electronic configurations of comparable stability exist in plutonium (he has used thermodynamic data to show that four or more electronic configurations exist in elements such as uranium, neptunium, and plutonium), there is a natural tendency for plutonium atoms to exist in different sizes (to match the different electronic configurations). When there are size differences, structures with equivalent lattice sites such as bcc, fcc, and hcp are destabilized by the resulting strain energy of accommodating such atoms. The liquid state, on the other hand, is actually stabilized by a mixture of sizes because it can use space better. Hence, the stability of the liquid is enhanced as one cools the melt, and metals such as uranium, neptunium, and plutonium exhibit a low melting point compared with what is expected based on their cohesive energies. Similarly, manganese and cerium favor multiple electronic configurations, and they also exhibit abnormally low melting points. It is also interesting to note that the thermal contraction upon cooling in liquid plutonium extrapolates to the β-phase contraction curve. As shown earlier, I set the degree of 5f bonding in the liquid to the same level as that in the β-phase in the notional diagram of Figure 12.

Pressure Instability. The electronic structure calculations of Wills and Eriksson demonstrate that pressure increases the 5f-electron orbital overlap, thereby initially stabilizing the high-density α- and β-phase in plutonium. The experimentally determined pressure-temperature-volume phase diagram in Figure 16 and the diagram shown in Figure 17 (Liptai and Friddle 1967) confirm the increased stability of these phases and the rapid "squeezing out" of the high atomic volume of the δ- and ε-phase. The γ-phase also gives way to a seventh plutonium allotrope, ζ, whose precise crystal structure has yet to be determined. The melting point of plutonium is initially lowered as pressure is applied, which is consistent with the fact that the liquid favors 5f bonding and is denser than the high-temperature solid phases. With continued pressure, however, the solid phases compress to a greater density than the liquid, and the melting point rises.

The calculations of Wills and Eriksson show that continued increased pressure broadens the f band, making it energetically unfavorable to lower the crystal energy through a Peierls-like distortion—thereby, eventually stabilizing the high-symmetry cubic or hcp structures. Pressure also increases 5f overlap in americium and the heavier actinides, leading to low-symmetry crystal structures followed by high-symmetry structures as pressure is increased. One can also conjecture that applying a negative pressure (hydrostatic tension) to the monoclinic α-phase should decrease the 5f electron overlap, thereby increasing

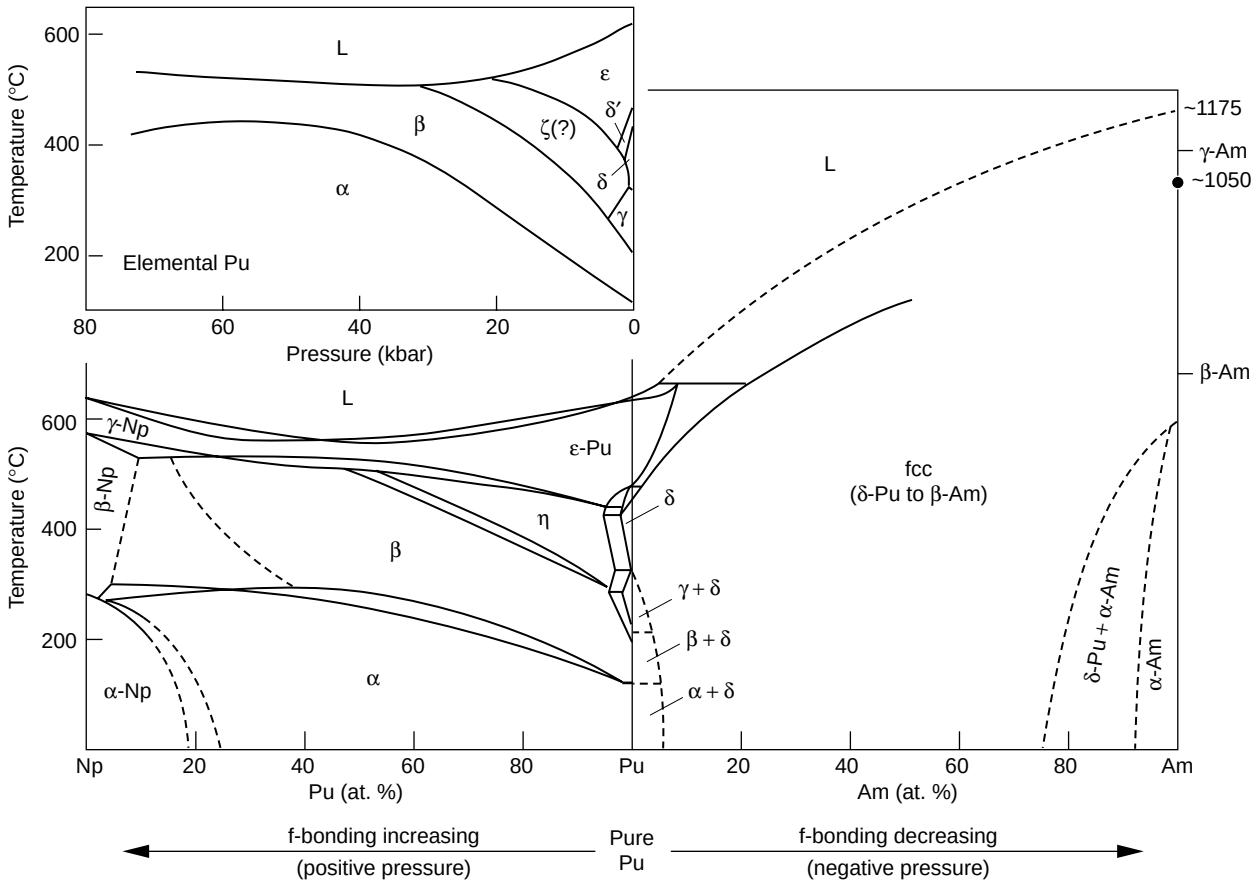

Figure 17. Pressure-Temperature Diagram of Pure Plutonium vs Np-Pu-Am Phase Diagram

The pressure-temperature phase diagram for unalloyed plutonium (Liptai and Friddle 1967) is drawn above the Np-Pu phase diagram (Ellinger et al. 1968) to show the striking similarities. It appears that adding neptunium to plutonium acts like increasing pressure. In both cases, the melting point drops initially, the α- and β-field expand, and a new phase (designated as either ζ of η) appears. By analogy, the addition of americium may mimic the application of hydrostatic tension (that is, negative pressure). As shown, americium additions cause the retention of the fcc δ-phase across the entire phase diagram.

the volume and favoring the high-temperature δ- or ε-phase cubic structures. Of course, applying negative pressure is not an easy feat.

A very informative way of looking at potential pressure effects was devised by Reed Elliott at Los Alamos in the 1980s (unpublished work). He compared the pressure-temperature phase diagram of plutonium to the phase diagrams of Pu-Np and Pu-Am as shown in Figure 17. Elliott pointed out that adding neptunium to plutonium acts just like increasing pressure in unalloyed plutonium. The melting point decreases initially; the low-temperature, dense phases are stabilized; and the high-temperature, high-volume phases become less stable. A new phase appears, which looks very much like the new high-pressure ζ-phase in unalloyed plutonium. In fact, the plutonium-rich side of the diagram looks almost identical to the pressure-temperature diagram for unalloyed plutonium. On the other side, adding americium simulates applying negative pressure (hydrostatic tension). The high-volume phases are stabilized; the low-symmetry, high-density phases disappear rapidly; and the melting point increases. This view is consistent with the fact that, as one moves from plutonium to neptunium, the f bonding increases whereas from plutonium to americium, f bonding decreases.

Alloying and Current Efforts to Understand the δ-Phase. Adding other elements to plutonium leads to dramatic changes in its phase stability, as demonstrated in Figure 17 (neptunium and americium additions) and Figure 18 (gallium additions). These effects are even more difficult to predict than temperature effects (see the box "Predicting Alloying Effects" on page 315).

Because the δ-phase alloys of plutonium are of particular interest, I will review our current understanding of the fcc δ-phase in unalloyed plutonium (between 583 and 725 kelvins). The δ-phase most closely resembles the structure of typical metals such as aluminum. However, both the δ-phase

Figure 18. Alloying Effects on Plutonium Stability

Small chemical additions can stabilize the high-volume phases of plutonium. The Pu-Ga phase diagram shows how gallium additions of a few atomic percent form a solid solution (gallium atoms are incorporated into the plutonium fcc δ-phase) that is retained to room temperature. The rest of the diagram shows the enormous complexity and richness of alloying behavior. The Pu-Ga system exhibits 11 different intermetallic compounds and several new phases that are different from those of elemental plutonium or gallium (Peterson and Kassner 1988).

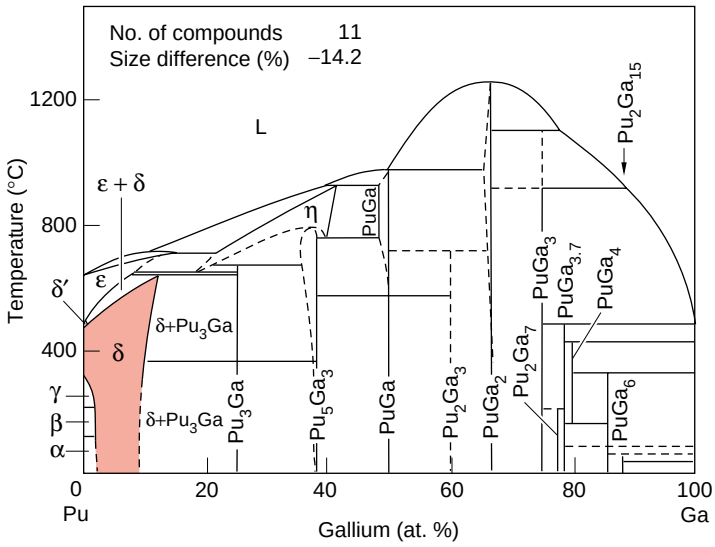

and the δ′-phase appear to be aberrations in the lineup of plutonium phases (the ε-phase thermal expansion line extrapolates almost exactly to that of the γ-phase in Figure 1). Of all plutonium phases, the δ-phase has the largest atomic volume in spite of its close-packed structure. Its volume falls between that of α-plutonium and americium (Figure 9). These properties are yet to be explained, and δ-phase stability and electronic structure remain the topics of hot debates.

Although the electronic-band-structure calculations of Wills and Eriksson based on local-density approximation (LDA) do a very impressive job of predicting pressure effects in the actinides, they cannot predict the existence of the high-temperature phases. They do, however, predict the correct atomic volume of the δ-phase (calculated at 0 kelvins) by constraining four of the five 5f electrons to localize (collapse into the ionic core). These constrained calculations capture the essential features of the electronic structure of the δ-phase as measured for the first time on gallium-stabilized δ-phase polycrystals. However, their unconstrained band calculations (all five 5f electrons are bonding) do not agree with either the α- or δ-plutonium photoelectron spectroscopy (PES) results of Arko and his colleagues. (See the article "Photoelectron Spectroscopy of α- and δ-Plutonium" on page 168.) Boring and Smith (see page 90) point out that there is no obvious mechanism that allows for partial localization of the 5f electrons. They also show, however, that if only one of five 5f electrons bonds in the δ-phase, the repulsive sp band contributions will expand the lattice and the symmetry of the crystal structure will be determined by the three spd electrons—that is, cubic structures will be favored.

Instead of partially localizing 5f electrons, Arko and Albers of Los Alamos (unpublished work) now suggest that all 5f electrons participate in bonding, but at reduced bond strengths. They link reduced bond strengths to strong electron-electron correlations. Such correlations effectively narrow the 5f band and enhance the density of states at the Fermi energy. Arko and Albers argue that reducing the bandwidth weakens the bonding because the average bond strength is directly proportional to the bandwidth. They also suggest that correlation effects may be at work even in α-plutonium, causing the 5f electrons to be more localized than LDA calculations predict. According to them, understanding α- and δ-plutonium requires that calculations use a perturbation theory extension to the first-principles LDA band-structure calculations.

In the article "A Possible Model for δ-Plutonium" (page 154), Cooper also goes beyond the LDA band-structure models to a two-electron, impurity-like model to explain the δ-phase. He proposes that the δ-phase is the result of a self-induced Anderson localization of the 5f electrons. According to Cooper, in Anderson localization, the electrons are driven from coherent-wave bonding in the α-phase to localized behavior by strong impurity scattering. To create an "impurity" in unalloyed plutonium, Cooper envisions two types of plutonium atoms—one in which the 5f electrons are localized and the other in which they oscillate between being localized and bonding. The fcc δ-phase becomes the lowest free-energy phase over a certain temperature interval because of the gain in configurational entropy (an additional contribution to entropy when more than one type of atom is incorporated into a crystalline array) of a solid solution of the two types of plutonium atoms occupying crystallographically equivalent sites in a disordered array. Unfortunately, the calculations necessary to deal with two-electron models for such complex systems are several years from fruition.

The bottom line is that we do not have a satisfactory explanation of the δ-phase in unalloyed plutonium today. It remains as one of the unsolved challenges in condensed-matter physics.

Predicting Alloying Effects

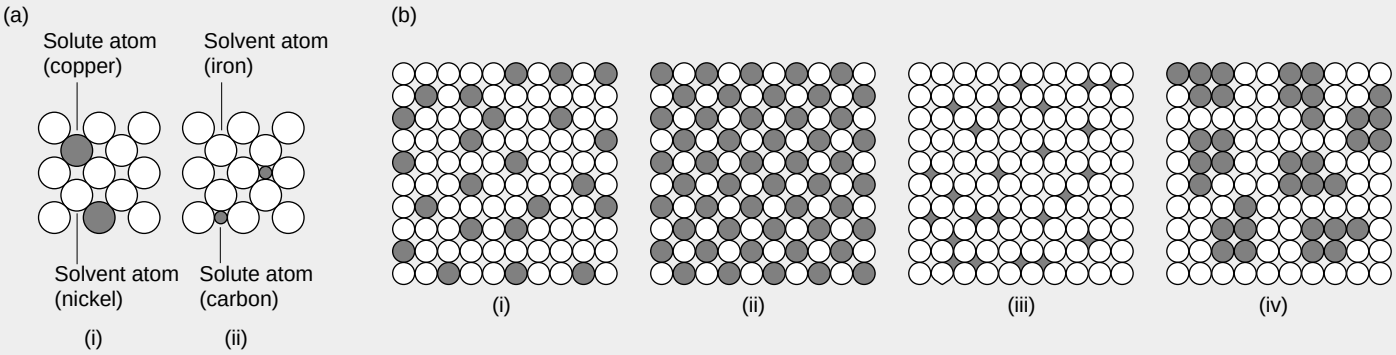

Substitutional and Interstitial Solid Solutions

(a) There are two types of solid solutions: (i) solute atom substitutes for the parent (solvent) atom, and (ii) solute atom fits into the interstices of the solvent atom lattice. (b) Four schematic models of solid solutions are illustrated: (i) substitutional random; (ii) substitutional ordered; (iii) interstitial random; and (iv) solute clusters in solid solution.

Alloying effects are even more difficult to predict from first principles than temperature effects. Alloying changes both the internal energy and the entropy—the latter, by changing both the vibrational spectrum and the configurational entropy. Metallurgists are keenly interested in the elusive goal of predicting what structures form when solute element B is added to solvent element A. The alloy is called a solid solution if the solute atoms are incorporated into the lattice of A without changing its basic structure. Solutes can substitute for solvent atoms or fit into the interstices of the solvent lattice as shown in the accompanying figure. The maximum amount that can be accommodated varies significantly from one alloy system to another. In addition, if there is limited solubility, the amount of A that can be dissolved in B is typically not the same as the amount of B that can be dissolved in A. For metals with multiple allotropes (such as plutonium), it is important to know how little solute it takes to expand a high-temperature phase regime to low temperatures. Alloying can also produce new compounds or new phases. Intermetallic compounds with specific ratios of A to B are very common in metallic systems. Such compounds typically form if there is a strong chemical affinity of element A for B. Another possibility is for A and B to be immiscible—that is, solvent A rejects element B altogether.

Whereas first-principles treatments have not been very helpful in predicting alloying behavior, the Hume-Rothery rules, developed in the 1920s, reformulated 30 years ago, and reviewed recently by Massalski (1996), are still used by metallurgical practitioners today. These rules relate the limits of solid solubility as well as the stability and extent of intermediate phases to three factors: (1) If the atomic size difference between A and B is greater than 15 percent, solid solubility will be restricted. Significant experimental data support this essentially “negative” rule, which makes intuitive sense because large size differences produce very large elastic-strain energies and should therefore be unfavorable. Within favorable size ranges, the exact size differences have only secondary importance and the following two factors become important. (2) High chemical affinity of A for B (usually denoted by large differences in electronegativity) helps promote the formation of intermetallic compounds and therefore limits solid solubility. (3) The relative valence rule stresses the importance of electron concentrations, or e/a ratios, in determining alloying behavior. (Typically, e/a is the number of valence electrons per atom, or equivalently, the group number in the periodic table.) Meaningful and useful correlations exist between crystal structure types and the e/a ratios of alloys. However, the physics behind those correlations remains elusive. Moreover, the success of the relative valence rules in metals with d or f electrons is limited because the values of the valence and the e/a ratio are by no means straightforward to assign.

It is now time to extend the very successful first-principles electronic-structure predictions of Wills and Eriksson for the actinide elements (including their excellent predictions of pressure effects) to alloys. It would also be very useful to extend to plutonium alloys the semi-empirical methods developed by Kaufman and Bernstein (1970) to predict phase diagrams (binary and higher order) based on thermodynamic measurements (heat capacities and enthalpies of transformation) and predictions that involve the construction of free-energy curves as a function of concentration and temperature. Such methods would provide near-term guidance on what to expect if more than one element is alloyed with plutonium or to predict the effects of multiple impurity elements.

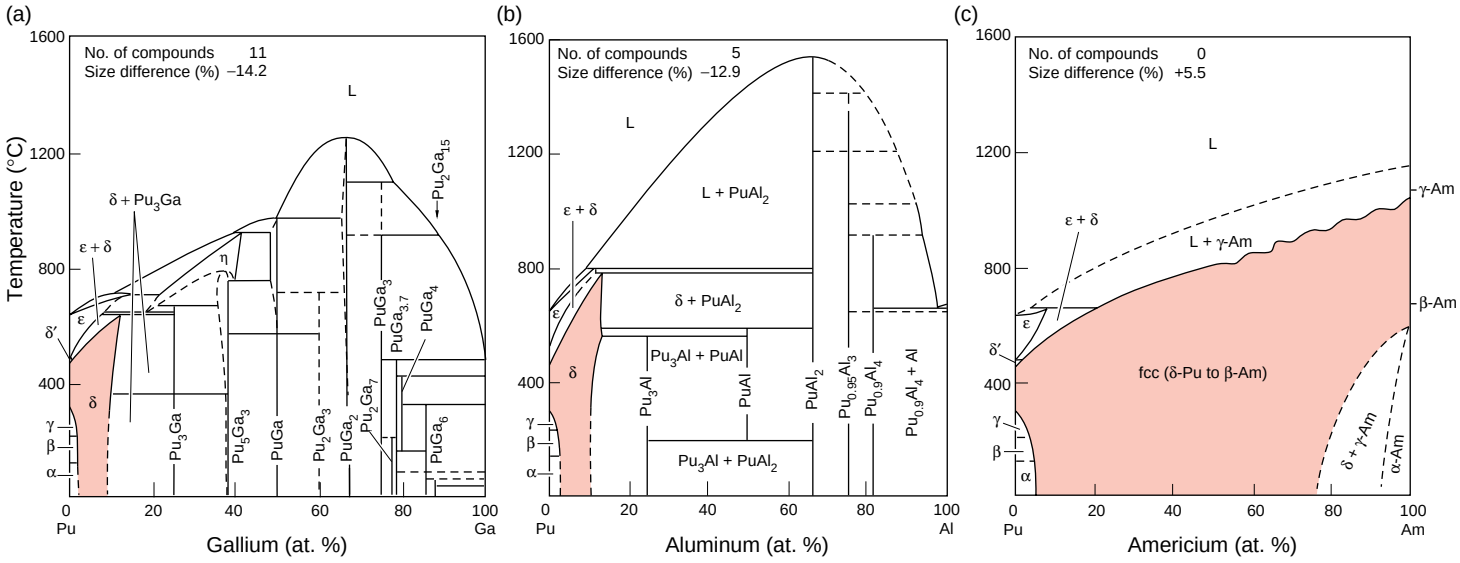

Figure 19. Binary-Phase Diagrams and Their Significance for Plutonium Metallurgy

The binary diagrams (a)–(c) are of δ-phase stabilizers. Gallium, aluminum, americium, scandium, and cerium retain the fcc δ-phase to room temperature, and all, except cerium, increase plutonium's melting point. For Pu-Ga alloys (a), gallium concentrations from approximately 2 to 9 at. % stabilize the δ-phase to room temperature. This phase is a solid solution of gallium atoms in an fcc plutonium lattice. Gallium atoms are 14.2% smaller than plutonium atoms, their electronegativity is greater, and they crystallize into a face-centered orthorhombic crystal structure. According to most empirical alloying rules, gallium barely fits the class of δ-phase stabilizers for plutonium. The Pu-Al (b) and Pu-Ga phase diagrams are controversial with Russian researchers who claim that the δ-phase is metastable at room temperature and will decompose, albeit over a period of thousands of years, to the monoclinic α-phase plus the intermetallic compound Pu_3Ga (see the article "A Tale of Two Diagrams" on page 244). (c) In the Pu-Am diagram, the δ-phase solid solution extends across the entire concentration range.

A second group of elements (silicon, indium, zinc, and zirconium) retains the δ-phase in a metastable state under rapid cooling from high temperatures (in either the ε- or δ-phase fields), but those elements do not stabilize the δ-phase at room temperature as shown in (d) for Pu-Si. In addition, alloying with substantial amounts of hafnium, holmium, and thallium will also retain some of the δ-phase to room temperature. (Interestingly, Pu-Zr, Pu-Al, and Pu-Ga alloys were once considered as potential metallic fuel elements for fast reactors).

Neptunium is an α-phase stabilizer, and it does an exceptional job (see Figure 18). No other element has been shown to have any equilibrium solubility in the very dense, monoclinic α-phase. Neptunium is also the only element that significantly expands the β-phase region. However, uranium, hafnium, and zirconium have limited solubility in the β-phase. Titanium, hafnium, and zirconium retain the β-phase to room temperature and below by rapid quenching. Neptunium and uranium lower the melting point of plutonium slightly; hafnium, zirconium, and titanium raise it significantly, even when added in small amounts.

Although based on the thermal expansion curve of Figure 1, the δ-phase appears to be an aberration, it is clearly the harbinger of what is to come as the atomic number is increased, as shown in the connected phase diagram of Figure 10. As Boring and Smith (page 90) point out, the δ-phase in plutonium is only the "tip of the iceberg." It is the transitional phase from the unusual properties of the light actinides to the rather well-behaved properties of the heavy actinides. Alloying plutonium with gallium or americium (as shown in Figures 17 and 18) helps retain the δ-phase to room temperature, thereby making it an alloy of great engineering significance.

Unfortunately, electronic-band-structure calculations cannot yet predict the effects of alloying in such complex systems. Clearly, electronic and stress effects arise when atoms of different electronic structure and size are added to the parent plutonium lattice. We would like to explain how and why some elements extend the stability of the fcc δ-phase to room temperature as plutonium solidifies and cools from the melt. But the key experimental data (such as phonon dispersion curves) that could help guide theorists are very scarce. No realistic interatomic potentials are available to allow approximate treatments of temperature and alloying effects. It will be important to understand entropy contributions because alloying may affect entropy both configurationally and through a change

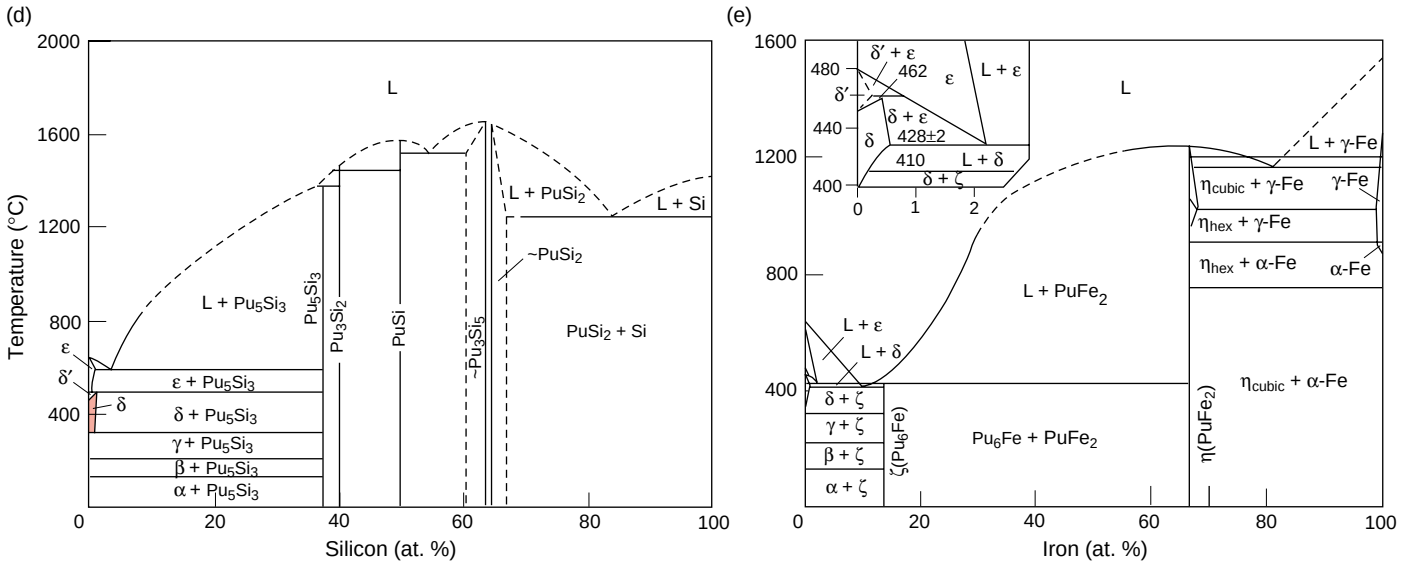

Iron, nickel, or cobalt lowers the melting point of plutonium dramatically, forming a low-melting eutectic, much as the addition of lead to tin makes solder. (e) The eutectic point for the Pu-Fe alloy (~10 at. % iron) is at 410°C. (This eutectic alloy was used in the first metallic plutonium fuel elements of the Los Alamos Molten Plutonium Reactor in the late 1940s). Silicon, magnesium, osmium, ruthenium, rhodium, and thorium form eutectics at somewhat higher temperatures. Eutectic-forming elements limit the useful temperature range of plutonium and its alloys. For example, plutonium metal heated above 410°C in steel will melt through the steel by forming the eutectic. Even when present in small amounts in plutonium, the alloying elements can segregate to grain boundaries, enriching the local alloying concentration and causing local melting or embrittlement at temperatures close to the eutectic temperature.

When nonmetallic elements with very small radii are alloyed with metals, they tend to form interstitial solid solutions. A general rule is that, if the radius of the nonmetallic element is <0.59 that of element A, an intermetallic compound with a simple structure (often fcc or hcp) forms. If the ratio is greater than that, then compounds with complex structures form. The important nonmetallic elements for plutonium are oxygen, carbon, nitrogen, and hydrogen. The first three form several high-melting (refractory) intermetallic compounds. For example, PuO_2 is a refractory oxide that melts at 2400°C and is used in radioisotopic heat sources and as reactor fuel (mixed with UO_2). Similarly, the carbides and nitrides of plutonium were once of considerable interest as reactor fuel for breeder reactors. Hydrogen also has a tendency to form compounds, but these decompose readily.

Almost all the rest of the elements in the periodic table show only limited solubility in the δ-phase. Many of them (for example, barium, strontium, and calcium) are immiscible. Most of these elements increase the melting point. Some have very shallow eutectics before the melting point increases. More than half of the elements in this group show solubility in the ε-phase (for example, thorium, neptunium, uranium, titanium, ruthenium, rhodium, platinum, osmium, and most rare earths).

in lattice vibrations. We pointed out earlier that the semi-empirical alloying theories have not been very successful in predicting alloying effects in plutonium. Cooper (page 154) suggests that gallium atoms located randomly in the plutonium lattice provide sufficiently strong scattering to lower the temperature for self-induced Anderson localization to below room temperature, thereby accounting for δ-phase retention. However, rigorous calculations to provide quantitative guidance appear to be a long way off.

Fortunately, metallurgists and chemists learned how to measure phase diagrams experimentally long before the advent of electronic-structure theory. Phase diagrams such as those shown in Figures 17 and 18 were measured painstakingly by thermal analysis, dilatometry (length-change measurements), calorimetry, x-ray diffraction, and metallography (optical microscopy of the grain and phase structures). For the actinides, Finley Ellinger and his colleagues at Los Alamos spent their professional careers determining the binary-phase diagrams of plutonium with many other elements in the periodic table. They also published a few ternary-phase diagrams (that is, two elements added to plutonium), but the number is limited because of the enormous effort required. We must develop better theories to help us understand alloying (and impurity) behavior.

Figure 20. Plutonium-Rich Pu-Ga Phase Diagram
(a) The phase diagram of Ellinger et al. (1968) as modified by Peterson and Kassner (1988) shows that the fcc δ-phase regime in plutonium is extended by alloying with gallium. Nearly 13 at. % gallium can be dissolved in the fcc δ-phase at high temperature. (Note that 1 wt % gallium is roughly 3.4 at. % because of the disparity in the atomic mass of the elements.) At ambient temperature, the limit is closer to 9 at. %. During solidification and cooling, alloys within this gallium range must cool through the liquid plus the ε-phase region and the ε- plus the δ-phase region. In a two-phase region, the composition of each phase is given by the phase boundaries at that temperature. Therefore, at point A, the first δ-phase to form has the gallium concentration shown at point B. As the temperature is lowered, the gallium concentration in the δ-phase moves along the BD line whereas the gallium concentration in the ε-phase moves along the AC line provided that diffusion is sufficiently rapid to allow migration of gallium consistent with the imposed cooling rate. (The average gallium concentration in the alloy, of course, has to be the initial concentration.) Because the gallium diffusion rate in the open bcc structure of the ε-phase is approximately 10^4 times faster than that in the δ-phase, gallium concentrations in the δ-phase remain above their equilibrium values for most cooling rates, whereas those in the ε-phase are pushed farther and farther below equilibrium values as cooling proceeds. The net result is increased gallium segregation, or coring, within a δ-phase grain over that expected from equilibrium conditions.

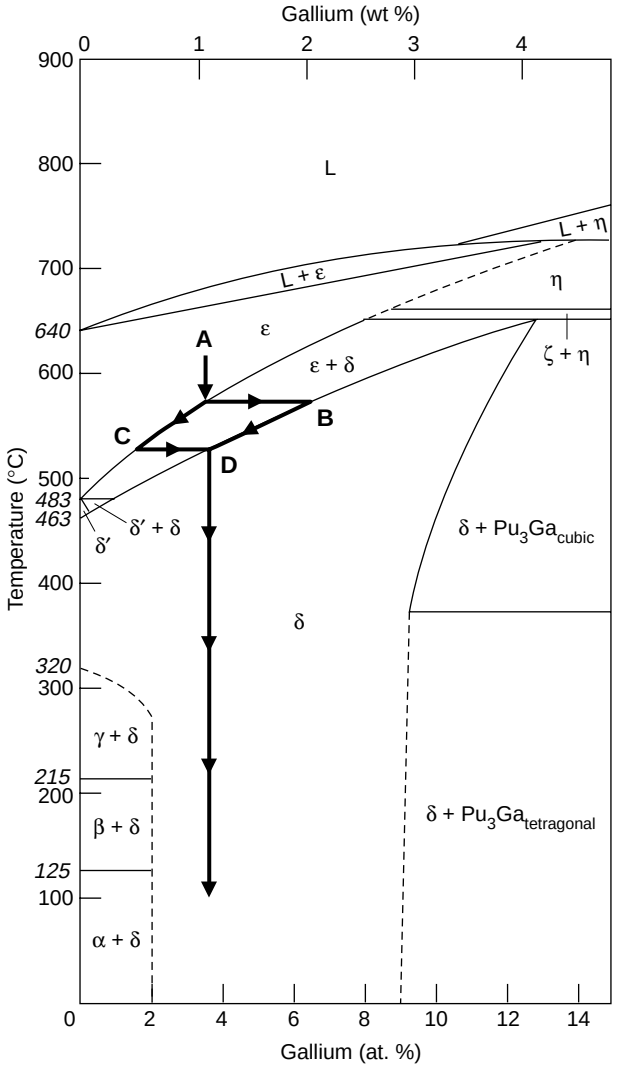

I have tried to capture the principal features of the phase diagram compendium of Ellinger et al. (1968) in Figure 19, hoping that this knowledge will provide guidance for theorists and experimentalists. This compendium has served as the most valuable document for plutonium metallurgists. Little has been added to it since the time it was published. It demonstrates that when alloyed with plutonium, the elements in the periodic table fall into the following groups: (1) δ-phase stabilizers and δ-phase retainers, (2) α-phase stabilizers, (3) eutectic-forming elements, (4) interstitial compounds, and (5) all the remaining elements, most of which either show little solubility in the δ-phase or form very shallow eutectics before raising the melting point.

Metallurgical Considerations for δ-Phase Pu-Ga Alloys

It should be quite apparent by now that more than chemical analysis is required to describe the properties of alloys. Microstructure is important, and it is determined by chemical composition and processing—namely, thermal and mechanical treatments. For example, thermal and mechanical treatments will affect the homogeneity of the chemical composition, the presence of second phases or inclusions (as well as their volume fraction, morphology, and distribution), and the types and distributions of defects. Typical mechanical processes include rolling and forging, which introduce stored energy into the system in the form of increased defect concentrations (mostly increased dislocation density). This stored energy, in turn, can be reduced or eliminated by subsequent thermal annealing treatments that lead to recovery (rearrangement and elimination of many dislocations) or recrystallization (formation of new, relatively strain-free grains) of the deformed structure. Moreover, there are other external conditions such as irradiation (or in the case of plutonium, self-irradiation) that create new defects and store energy. All these effects must be considered if one is to understand the properties of plutonium alloys.

I will begin a brief examination of thermal treatments by discussing the plutonium-rich portion of the Pu-Ga phase diagram shown in Figure 20. The minimum amount of gallium

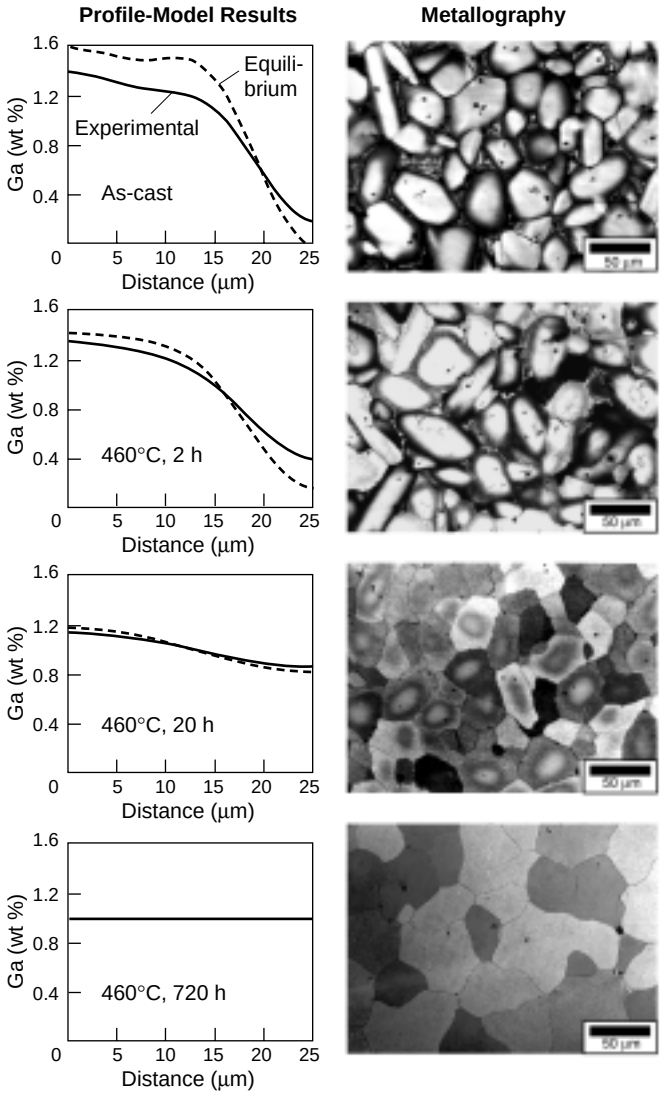

(b)The microstructure of a typical as-cast δ-phase alloy exhibits a range of gallium concentrations between points B and C in (a). The interior of the δ-phase grains reflects the gallium concentration at point B, and the grain boundaries may have very little gallium, reflecting the last ε-phase to transform with gallium at or below point C. As shown, the resulting microstructure appears heavily "cored" or segregated. It consists of a gallium-rich δ-phase in the center, a gallium-lean δ-phase shell (dark areas) at the core boundaries, and an intercore region very lean in gallium that transformed to the α-phase during cooling because of insufficient gallium content. The measured and calculated gallium-concentration profiles from the center to the edge of a grain (Mitchell et al. 2000) are also shown. This type of microsegregation typically occurs during cooling through the liquid plus solid region of most alloys because diffusion in the liquid is typically so much faster. The anomalously high diffusion rate in ε-plutonium avoids the problem in the liquid- plus ε-phase region, only to have it appear in the ε- plus δ-phase region. To equilibrate the gallium concentration, it is necessary to return to very high temperatures in the δ-phase region and hold those temperatures for long times. The progression of gallium homogenization and consequent change in microstructure are also shown for a temperature of 460°C.

required to stabilize the δ-phase at ambient temperature is 2 at. % according to Ellinger et al. (1968). In reality, this phase boundary is very uncertain (shown by a dashed line) because it is difficult to achieve equilibrium. Over 30 years ago, Elliott and others reported that as little as 1 at. % gallium or aluminum effectively retains the δ-phase to room temperature if samples are cooled rapidly enough from elevated temperature. It is quite remarkable that only one gallium atom in one hundred plutonium atoms causes such a dramatic change in crystal structure. On the other hand, as discussed by Hecker and Timofeeva (page 244), carefully performed Russian work showed that all δ-phase Pu-Ga alloys are metastable at room temperature.

One of the principal differences between δ-phase alloys and unalloyed plutonium is the solidification behavior important in casting. As shown in Figure 2, unalloyed plutonium exhibits a large expansion upon solidification, followed by very large contractions in the solid state. Cracking and distortion are the rule. Consequently, it is very difficult to make a full-density (19.86 g/cm^3), sound α-phase casting. The Pu-Ga alloys, on the other hand, show a smaller expansion upon solidification followed by a small, quite uniform contraction. However, for reasons demonstrated in Figure 20, it is quite common for alloy castings to exhibit two phases—the gallium-rich δ-phase and the gallium-lean monoclinic α-phase. The exact amount of each phase depends primarily on the average gallium concentration and on the cooling rate. To minimize gallium microsegregation and "homogenize" the gallium distribution, it is necessary to anneal at the highest possible temperature in the δ-phase region. The time required for homogenization decreases with decreasing grain size and increasing temperature (as long as the temperature remains in the δ-phase region).

Density and x-ray diffraction measurements have demonstrated conclusively that the crystal structure of the δ-phase alloy is the same as the high-temperature δ-phase of unalloyed plutonium except that gallium solute atoms substitute for plutonium atoms in the fcc lattice. Results of x-ray diffraction typically show well-defined Bragg peaks of the single fcc phase. The lattice parameters of the alloys shrink with the addition of gallium. The con-

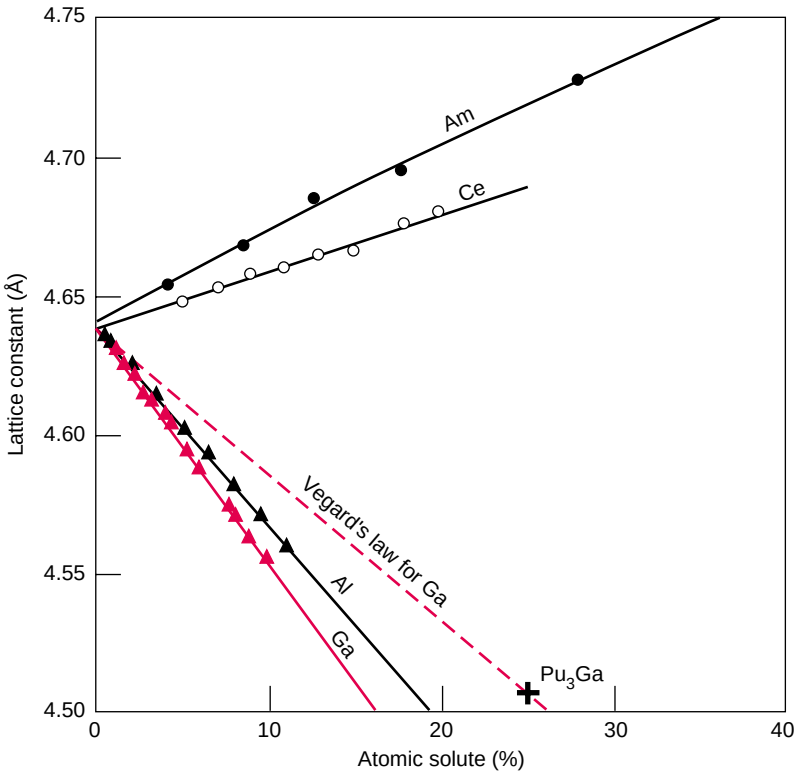

Figure 21. Lattice Parameters and Vegard's Law for fcc Plutonium Alloys
When gallium, aluminum, scandium, cerium, and americium are added to plutonium, they substitute for plutonium in the fcc δ-lattice, causing the retention of the δ-phase to room temperature. Additions of gallium, aluminum, and scandium contract the lattice, whereas those of cerium and americium expand it. The contractions for gallium and aluminum are greater than the contraction predicted by a rule of mixtures based on atomic radii (known as Vegard's law). The figure compares Vegard's law and experimental results for gallium additions.

traction is greater than expected from a rule of mixtures (called Vegard's law) as shown in Figure 21. The only two elements that increase the lattice parameter of the δ-phase are cerium and americium.

We do not know if gallium atoms are present at random in the fcc plutonium lattice or in an ordered array. In the past few years, Steve Conradson of Los Alamos and researchers in France have used x-ray absorption fine structure (XAFS) spectroscopy techniques at synchrotrons to probe the local environment around both plutonium and gallium atoms in the alloys. They confirmed the substitutional nature of the gallium atoms. The Pu-Pu atom spacing is considerably larger than the Pu-Ga spacing. For gallium-lean alloys, Conradson's data suggest a short-range, local order in addition to the long-range structure characterized by the usual fcc lattice parameters. We do not fully understand these finer details at this time. However, these features may be very important to the aging of plutonium alloys.

The role of impurities, or unintentional chemical additions, on phase stability in δ-phase fcc alloys is also not well understood. Impurities typically result from solidification or other processing operations, and the levels in plutonium metal are typically 1000 to 2000 parts per million (ppm) total by weight. Purification by electrorefining drops this level easily to <500 ppm, and levels of tens of parts per million have been achieved with great care (see the article "Preparing Single Crystals of Gallium-Stabilized Plutonium" on page 226). At the higher levels, impurities can influence phase stability, transformation behavior, mechanical properties, and a whole array of other physical properties. In recent work, Dan Thoma and coworkers at Los Alamos have convincingly demonstrated these effects for uranium. No theory or modeling is currently available to help us understand the role of impurities in plutonium.

From a practical standpoint, the effect of impurities on phase stability is best assessed if impurities are classified according to the scheme used for alloying elements in Figure 19. Hence, common impurities such as aluminum, silicon, and americium that retain the δ-phase are simply added to the gallium concentration (on an atomic percentage basis) to give an equivalent content for Pu-Ga alloys. Since these impurity elements are present on the plutonium lattice sites, they are not distinguishable by typical metallographic or x-ray diffraction techniques. XAFS offers some hope for distinguishing the impurity atoms if they are present in sufficiently large concentrations. However, even small amounts of impurities can cause serious degradation of properties because impurities typically concentrate in the melt during casting. Solute atoms are usually rejected during the early stages of solidification because atoms of different size are more easily accommodated in the liquid. This tendency to segregate impurity elements leads to inclusions (second-phase particles) in the microstructure of plutonium or its alloys. Typical eutectic-forming impurities and refractory-compound forming inclusions are shown in Figure 22. There is also the tendency for impurities to form complex compounds such as oxycarbides and carbo-nitrides, or for them to scavenge some of the intentional alloying elements or other impurities. We understand very little about these effects in plutonium.

To conclude this section, let me reiterate the importance of metallurgical processing in understanding the behavior

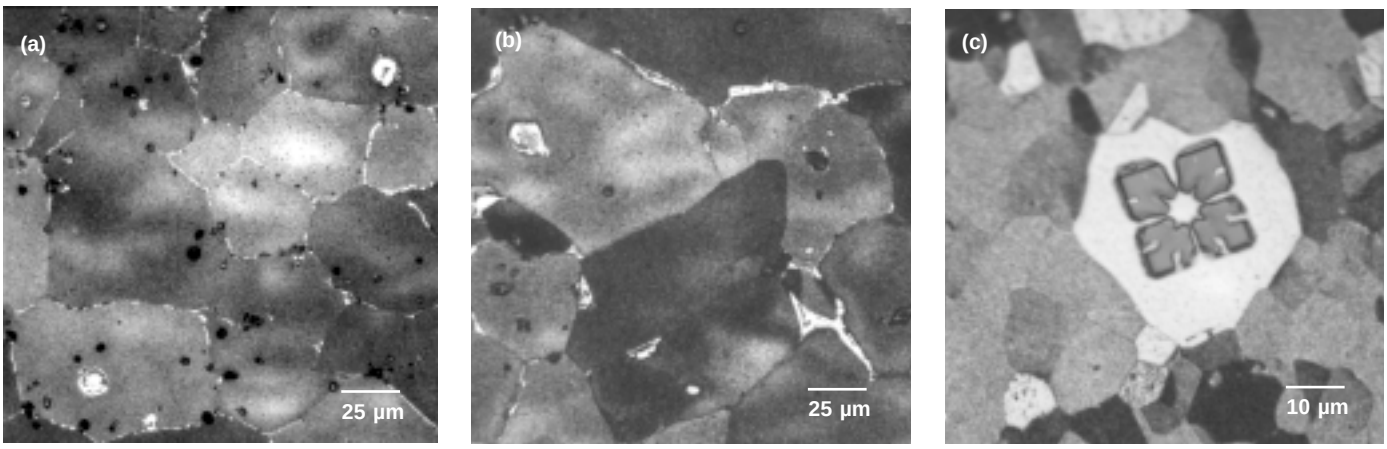

Figure 22. Iron and Nitrogen Impurities in Plutonium

Impurities typically segregate in the melt and form microscopic inclusions in the δ-phase structure. Even reasonably small concentrations of impurities, on the order of a few hundred parts per million by weight, can give rise to micrometer-size inclusions as shown in (a) and (b), which are representative of Pu-Ga alloys with 300 to 500 ppm iron concentrations. In (a), the processing conditions favored inclusions of the low-melting eutectic compound Pu_6Fe strung out along the grain boundaries, whereas in (b) processing conditions favored the conglomeration of Pu_6Fe at the grain-boundary triple points in particular. The reasons for the different morphology of inclusions for different processing conditions are not understood. In (c), an isolated plutonium nitride inclusion is shown in Pu-Ga alloy containing several hundred parts per million by weight nitrogen in the bulk alloy.

of plutonium alloys. An accurate chemical analysis is necessary, but not sufficient. Knowing the processing parameters is crucial to ascertain the level of segregation of the alloying element and the state of the impurity atoms. In addition, mechanical treatments will change the microstructure. These effects are discussed by Hecker and Stevens (page 336). So, even if a plutonium alloy is retained in the fcc δ-phase at room temperature, it is at best metastable and very sensitive to external conditions, such as temperature, pressure, or other applied stresses. The phase diagrams provide us with an overall guide to phase stability, but they do not tell us much about just how stable these alloys will be to all possible external changes.

We know from experience, for example, that plutonium alloys with <2 at. % gallium transform readily to the monoclinic α-phase just below room temperature. And I mentioned above that the δ-phase is squeezed out easily by the application of pressure at room temperature. In addition, under the stresses induced during cutting, machining, or polishing, the lean alloys readily transform to the α-phase on the surface (sometimes in combination with the γ-phase). As the gallium concentration is increased, stability with respect to these external forces increases steadily. Predictions of phase stability as a function of solute concentration and external stresses may be helped significantly by electronic-structure calculations, especially if these calculations were to include temperature effects. It would also be very helpful if theorists could develop other physics-based models that incorporate realistic interatomic potentials capable of calculating the influence of defects and microstructure on phase stability.

Phase Transformation in Plutonium and Its Alloy

The Ellinger compendium of plutonium alloy phase diagrams provides structural maps of possible phases and crystal structures at thermodynamic equilibrium (or, at least, the best one can do in a practical sense given kinetic limitations). Phase transformations provide the vehicle to get from one phase region to another. And, more important, the nature of the phase transformations governs resulting microstructures, which control the properties. In plutonium, phase transformations are triggered easily by changes in temperature, pressure, stress, or chemistry. Plutonium and its alloys exhibit virtually every phase transformation found in all other elements combined. To understand phase transformations, we must first understand the thermodynamic driving forces, the crystallographic mechanisms at the atomic level, and the kinetics of the transformation processes. (see the box "Phase Transformation Basics" on page 322). Direct observations of transformations in plutonium—either in situ or after they have occurred—are very difficult because of the metal's reactive and radioactive nature. Moreover, the large number of allotropes and large surface distortions also make such observations difficult. Consequently, most information about transformation mechanisms in plutonium and its alloys is based on

Continued on page 328

Phase Transformation Basics

All phase transformations are driven by a reduction in the Gibbs free energy from the original to the final structure. Although the driving force for a phase change may exist, thermal activation is typically necessary to overcome the existing activation barriers. As a result of the random thermal motion of atoms, the energy of any particular atom or small collection of atoms will be just sufficient to initiate the phase change. Kinetics will determine how fast the transformation proceeds, and the transformation mechanism will help shape the resulting microstructure.

Diffusional Transformations. Phase transformations can be divided into two predominant types—diffusional and diffusionless. Most transformations occur by diffusional processes—that is, they occur at sufficiently high homologous temperatures to allow diffusion to play a role in the nucleation and growth processes of the transformation itself. In single-component systems (such as the high-temperature allotropes of plutonium), the only atomic process that occurs is the random, short-range (on the order of an atomic spacing) thermally activated atom-by-atom jumps across the interface from the parent to the product crystal structure. In transformations in which the product and parent phases have different compositions, two successive processes occur: (1) long-range transport by diffusion of, say, the solute atoms over distances of many atomic spacings and (2) short-range atomic transport across the parent-product interface. The atoms make thermally activated random jumps across the interface to create a product nucleus, or a new small region that has a completely different composition and/or structure from the parent phase. The product nucleus is separated from the parent matrix by an interface with an interfacial energy. Most of the matrix remains untransformed until the product nucleus grows to consume it. Figure A shows an example of a diffusional transformation in steel, in which both structure and composition are changed.

Diffusional transformations can proceed isothermally to completion, being limited only by adequate diffusion rates. They may or may not display specific crystallographic orientation relationships, and the product-parent interface may be coherent, semicoherent, or incoherent (Figure B), involving the nucleation and growth of the product phase from the parent phase. In all of them, an activation barrier must be overcome to reach a critical nucleus size. Because of the diffusional nature of the atomic movements required, the activation energy and the critical embryo size vary exponentially with temperature and scale with the melting point. The kinetics is described by an Arrhenius rate equation. The rate is proportional to $\exp(-\Delta G/k_B T)$, where G is the Gibbs free energy.

The principal barriers that must be overcome to nucleate the product phase are the interfacial free energy of the product-parent phase and the misfit strain energy. For homogeneous (uniform) nucleation, the interfacial energy represents an almost insurmountable obstacle. So, most diffusional transformations in solids are nucleated heterogeneously at defects such as excess vacancies, dislocations, grain boundaries, stacking faults, inclusions, and free surfaces. Defects can greatly reduce the size of the activation barrier required to nucleate the new phase in response to the thermodynamic driving force to lower the Gibbs free energy. The optimal shape of the new product phase typically minimizes the total interfa-

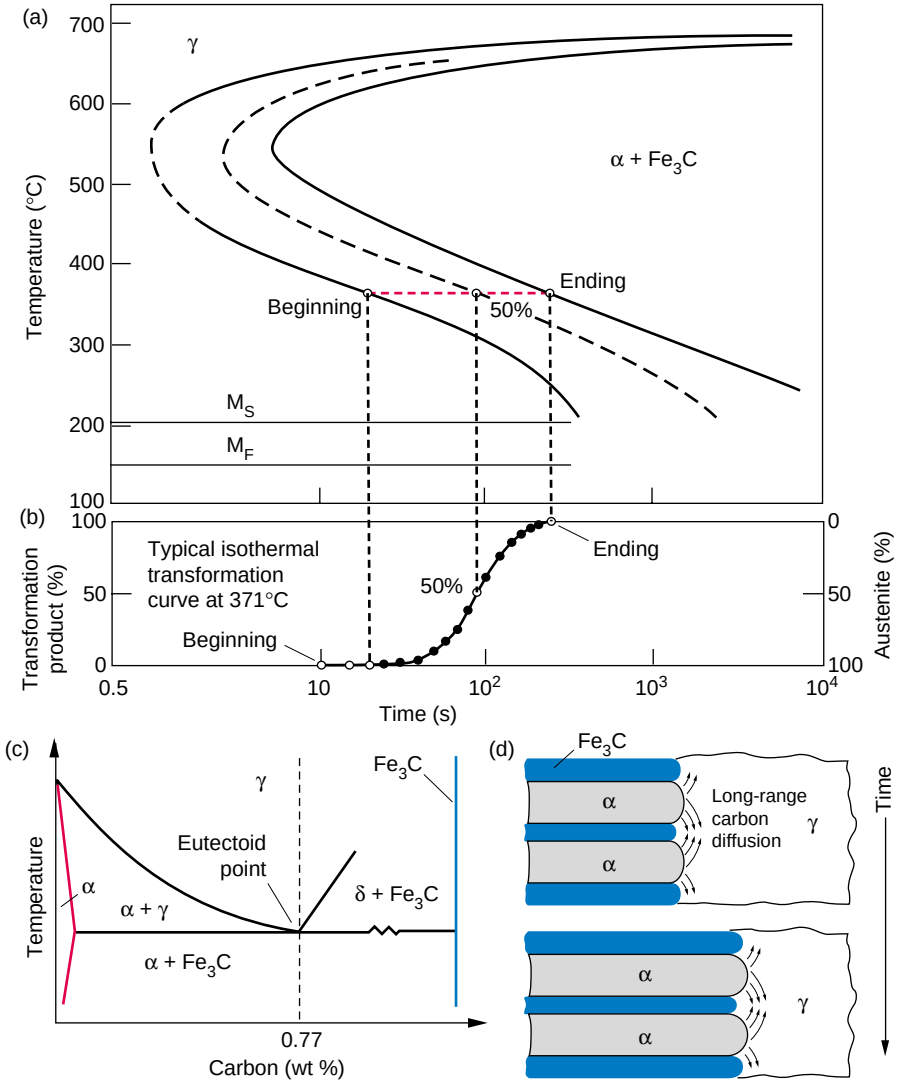

Figure A. Schematic Temperature-Time-Transformation (TTT) Diagram for Steel

The high-temperature γ-phase of steel (called austenite) is fcc. At lower temperatures, this phase transforms to a bcc ferrite (α-phase) and Fe_3C (an orthorhombic intermetallic compound). (a) The results of isothermal-transformation experiments are shown on a temperature vs time plot (TTT diagram), in which C-shape curves mark the start and finish of each isothermal experiment. That shape results from a tradeoff between the thermodynamic driving force and diffusion. At high temperature, diffusion is fast, but the driving force is too low to trigger the transformation. At low temperature, the driving force is high, but diffusion is too slow for the transformation to proceed. (b) The lower diagram shows how the transformation products increase with time if the γ-phase is quenched to miss the nose of the C-curve and then is held isothermally at 371°C (dashed red line). If the γ-phase is cooled quickly enough to avoid the C-curve altogether, then it will begin to transform martensitically (diffusionless and displacive) at the M_s temperature. Typically, the amount of transformation product depends on temperature only—not on the length of time the γ-phase is held at that temperature. The M_f temperature marks the point below which no additional martensite forms. (c) If the γ-phase has the eutectoid composition (0.77 wt % carbon), carbon must diffuse so as to create the α-phase with very little carbon (given by the red phase boundary of the α-region) and Fe_3C with 25 at. % carbon. (d) This schematic illustrates that long-range diffusion is required in austenite (γ-phase) to allow the transformation to α-phase plus Fe_3C to proceed.

cial free energy. Grain boundaries are very effective sites for transformations with incoherent interfaces. Grain edges or corners (called triple points in two-dimensional micrographs) are even more effective. Likewise, impurities and inclusions are very effective nucleation sites. Dislocations are not very effective at lowering the interfacial energy, but the lattice distortions in the vicinity of dislocations can reduce the total strain energy of the nucleus. Dislocations can also expedite diffusion of solute atoms as can grain boundaries and excess vacancies trapped during rapid cooling.

For the nucleus to grow, the interfaces—typically a combination of semicoherent and incoherent ones—must migrate. Incoherent interfaces typically move rapidly, whereas semicoherent interfaces do so with difficulty. Consequently, precipitates in many systems take on a disc- or plate-like shape. Growth of nuclei, like nucleation itself, requires diffusion; hence, it is also controlled by an Arrhenius-type rate equation. Transformation kinetics is typically displayed in TTT diagrams, named for showing the progression of the transformation with time and temperature (Figure A) and provide valuable engineering insight into the expected evolution of microstructures expected for various heat treatments.

Figure B. Parent-Product Interfaces
The interfaces between parent and product phases can be coherent, semicoherent, or incoherent. Many transformation products contain a combination of the interface types shown here. (a) Coherent interface between two phases with slight lattice mismatch leading to elastic coherency strains in both lattices. (b) Semicoherent interface with the misfit parallel to the interface being accommodated by a series of edge dislocations. (c) Incoherent interface with complete lack of atomic registry at the interface.

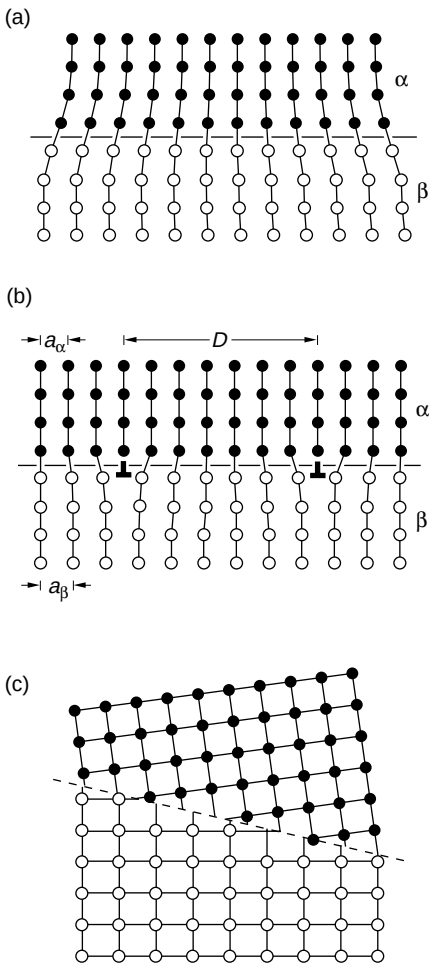

Martensitic Transformations. Diffusional transformations can be very sensitive to cooling rate. In many systems, these transformations can be avoided by a sufficiently fast quench to temperatures too low for diffusion to take place during the transformation (as shown in Figure A). In such cases, the transformations occur in a diffusionless manner. Martensitic transformations are the most important class of diffusionless transformations. They are displacive and dominated by the strain energy that arises from shear-like displacements. Diffusionless in this context means no random-walk mixing of atoms, or atom-by-atom jumping across the interface, during the structural change. Consequently, the product phase inherits the same composition, atomic order, and lattice defects that are present in the parent phase. Since solute or interstitial atoms are trapped in the martensite product, such products are always metastable—meaning that the system is not in its lowest free-energy state, and a driving force exists for decomposition to the equilibrium phases. Displacive signifies that atoms move in an organized manner by a coordinated shift of atoms—a combination of a homogeneous lattice shear and shuffle. (These are often called military transformations because they require a coordinated and regimented motion of atoms). In such transformations, the atoms move less than an interatomic spacing relative to a habit plane and a line in the product that remains undistorted and unrotated from its original form in the parent phase. In other words, it is an invariant plane relative to the parent phase. Such habit planes generally do not have simple crystallographic (Miller) indices.

During most martensitic transformations, the amount of transformation product depends on the temperature at transformation, but not the length of time at that temperature. The transformation is therefore called athermal. The overall kinetics of the martensitic transformation depends on both nucleation and growth processes, with the slower of the two largely dominating. For example, slow, thermally activated nucleation can dominate in some cases and lead to time-dependent martensitic transformations called isothermal.

A definite crystallographic relationship—lattice correspondence—exists between the product and the parent phases. The lattice correspondence for most martensitic transformations typically consists of the close-packed planes and close-packed directions in the product and parent phases being approximately parallel. The plate-like or lens-like product phase (called martensite) forms in only a limited number of orientations in the parent phase, and therefore the habit planes, which are approximately parallel to the large-area cross sections of the martensite, have those same orientations (Figure C). The martensite shape develops to minimize the sum of the strain and interfacial energies.

The lattice deformation required to produce the product phase involves (1) the coordinated shift or shear of atoms that homogeneously converts one crystallographic lattice to another—illustrated in Figure D and called the Bain strain because it was originally proposed by E. Bain (1924) to explain the face-centered-cubic (fcc) to body-centered-cubic (bcc)—actually, body-centered-tetragonal—martensitic transformation in ferrous alloys—and (2) any lattice rotation required to couple the transforming region and the adjacent parent matrix.

Many displacive transformations also involve a shuffle—that is, a coordinated shift of atoms within the unit cell that changes the structure but does not constitute a homogeneous lattice-distortive strain. In martensitic transformations, lattice deformations dominate, not shuffles. As mentioned above, the shear component of deformation must play the prominent role in the kinetics and morphology of the transformation. That is why, for example, the diffusionless fcc γ to α transformation in cerium at low temperatures is not classified as a martensitic transformation. Instead, it involves a large hydrostatic volume collapse but no shear component. On the other hand, the γ to γ^o to α'' transformation in U–6 wt % Nb is classified as martensitic although it involves an

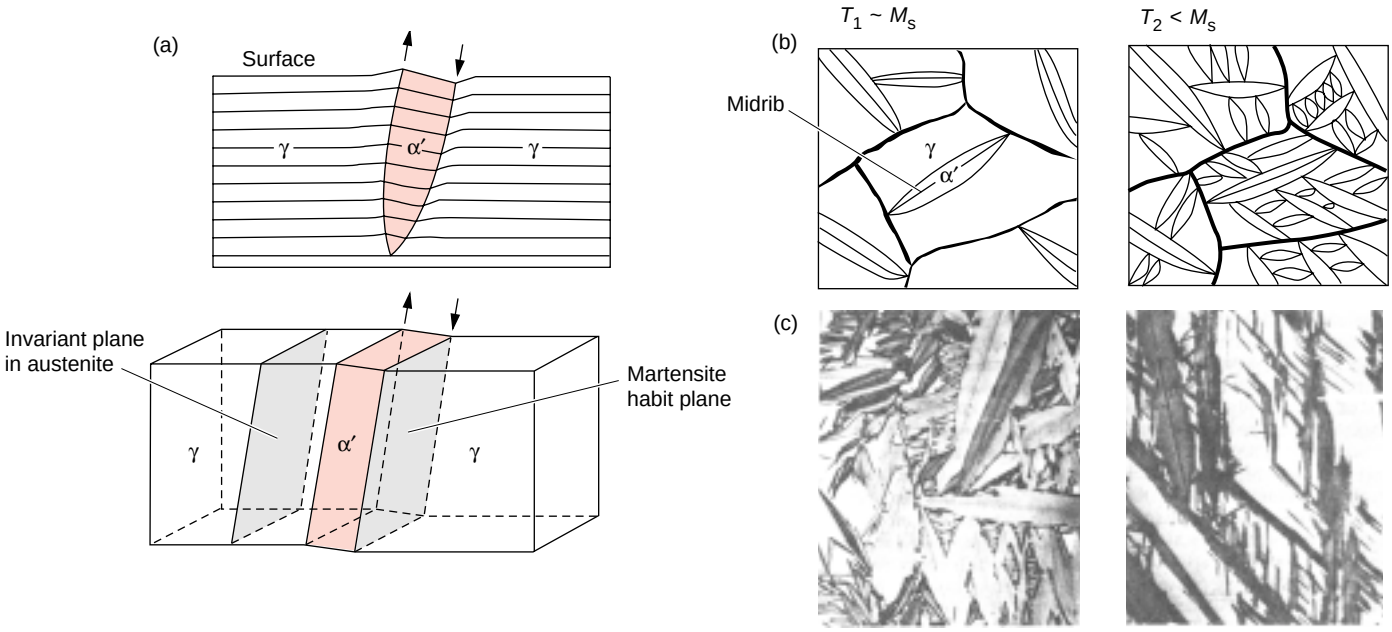

atomic shuffle because the overall transformation is dominated by shear.

The lattice-distortive nature of the martensitic transformation generates strain energy that must be relieved by additional displacements that may occur inhomogeneously as an integral part of the transformation. These displacements take place by slip or twinning in the product and are called lattice invariant because they do not change the crystal structure of the product phase—see Figure D(b–c). Hence, the lattice deformation produces a distortion of the transforming region, whereas the lattice-invariant deformation acts to reduce the magnitude of that distortion. The inhomogeneous lattice-invariant shear allows the habit plane to remain macroscopically undistorted.

The free energy required to nucleate martensite homogeneously by thermal fluctuations alone is prohibitively high, and therefore defects play a critical role in nucleation. However, unlike diffusional transformations, which tend to begin at grain boundaries and inclusions, martensitic transformations are nucleated predominantly by arrays of dislocations because their elastic strain fields help to lower the misfit strain energies of the product. Olson and Cohen (1981) demonstrated that pre-existing arrays of lattice dislocations provide the necessary embryos for nucleation. If properly arranged, and driven by the thermodynamic driving force for a phase change, these dislocations can dissociate to carry out the nucleation process. Alternatively, Clapp (1973) proposed that nucleation is triggered by a strain-induced elastic instability in special regions of the parent lattice, and that the inclusion of anharmonic terms in the elastic free energy will considerably reduce the nucleation barrier—meaning that thermal vibrations (phonons) in these anomalous regions play an important role in the nucleation process. Such nucleation processes should be accompanied by a "premartensitic" phonon softening of the lattice. Soft modes have been seen in several systems such as Ti-Ni, Au-Cd, and Au-Cu, but not in ferrous alloys. Mechanisms of martensite nucleation are not fully resolved and remain an active area of research today.

Once the activation barrier is overcome, martensite plates will grow rapidly until they hit a barrier such as a grain boundary or another martensite plate. Because martensites grow at low temperature and high velocities, the transformation interface must be very mobile. In steels, martensite plates have been measured to form in 10^{-7} second with speeds approaching the speed of sound. The marten-

Figure C. Martensitic Transformations

(a) In the 2-D schematic, the parent fcc γ-phase has transformed to a bcc α′–martensite platelet that has coherent interfaces with the parent phase and creates a distortion, or tilt, where it intersects the surface. The corresponding 3-D drawing shows the invariant plane in the parent phase that corresponds to (is parallel to) the habit plane in the α′–martensite platelet. (b) Schematic shows α′-platelets in the parent γ-grains at M_s, and the subsequent growth of new platelets between existing ones at a lower temperature. The black line in the α′-platelets is called a midrib and results from the martensite growth process. The α′-platelets are visible in a metallographic cross section polished before transformation because of their surface tilt, as shown in (a). They are also visible in a sample polished after transformation because the different crystal structures and orientations etch preferentially, thereby providing contrast. (c) Actual micrographs of martensite platelets in a medium-carbon steel and a Fe-Ni alloy. **(Figure adapted from D. A. Porter and K. E. Easterling. 1981. *Phase Transformations in Metals and Alloys*. New York: Van Nostrand Reinhold.)**

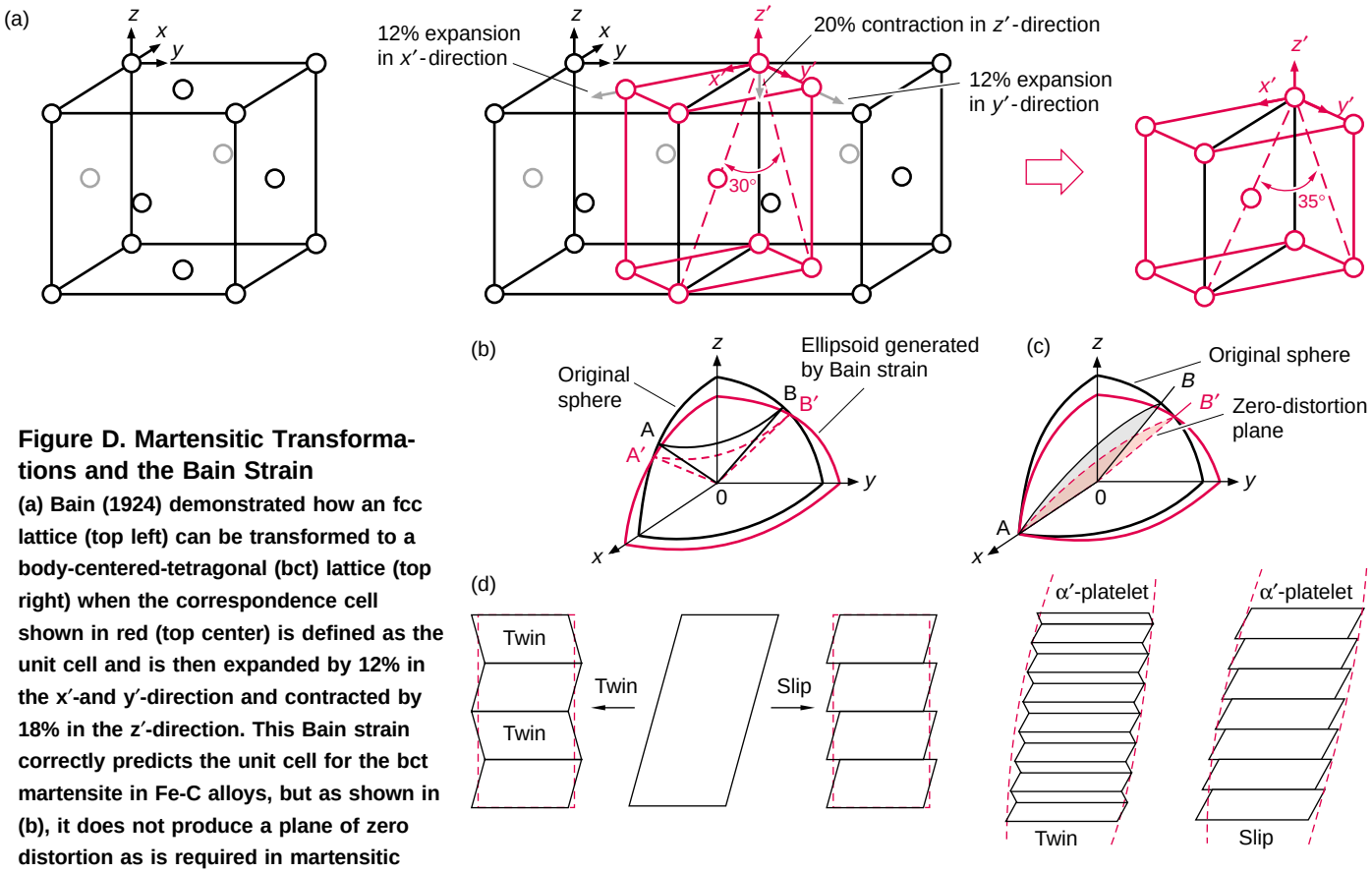

Figure D. Martensitic Transformations and the Bain Strain

(a) Bain (1924) demonstrated how an fcc lattice (top left) can be transformed to a body-centered-tetragonal (bct) lattice (top right) when the correspondence cell shown in red (top center) is defined as the unit cell and is then expanded by 12% in the x′-and y′-direction and contracted by 18% in the z′-direction. This Bain strain correctly predicts the unit cell for the bct martensite in Fe-C alloys, but as shown in (b), it does not produce a plane of zero distortion as is required in martensitic transformations. The Bain strain generates an ellipsoid from an original sphere present in the parent with no plane of zero distortion. To obtain a plane of zero distortion following the Bain strain, one must collapse the lattice back to its original position along one axis, for example, along the x-axis as in (c). Now a plane of zero distortion exists, but it has rotated in direction from OAB to OAB′. Hence, a martensitic transformation can be described by three formal operations: (1) Allow the Bain strain to generate the new lattice. (2) Introduce a shear to collapse the lattice back in one direction. (3) Rotate the martensite matrix so that the zero-distortion plane has its original position. (d) The shear introduced in (c) must be a lattice-invariant deformation so as not to change the bct structure produced by the Bain strain. The deformation can be accomplished by either slip or twinning in the martensite product. Hence, the martensite phase is required to have an internal substructure of twin stacks or to be severely slipped along parallel planes. Indeed, these substructures are found in martensite laths and plates.

site nuclei thicken by slip or twinning. Transformation dislocations are essential for the interface motion required during nucleation and growth (Olson and Cohen 1981). Specific models have been developed for some of the most studied martensites in ferrous alloys. Twinning is also critical in accommodating the overall shape and volume changes of the transformation—as shown in Figure D (c).

In most martensites, the transformation interface appears to become immobilized after a martensite plate has thickened. Since the interface is pinned by its damaged surroundings, it will be unable to reverse its motion during reverse transformation upon heating. Instead, the reverse transformation will have to be nucleated anew inside the martensite plates. Damage in the form of dislocations is typically introduced if the stress fields in the parent phase during the initial nucleation and growth of martensite plates cause the parent phase to yield plastically. On the other hand, if the martensite plates are accommodated elastically in the parent, the interface may remain mobile and the transformation can reverse itself by the shrinkage of the interface. Such transformations, called thermoelastic martensitic transformations, are fully reversible as in some Ti-Ni alloys.

As mentioned earlier, most martensitic transformations are athermal and depend principally on the temperature, not on the length of time at that temperature. The temperature for the start of the transformation is called the M_s temperature as shown in Figure 23. Although diffusion plays no direct role in the martensitic transformation itself, thermal activation is important during the nucleation stage in isothermal martensitic transformations, and diffusion is important in the post-transformation "tempering" stage. In isothermal martensitic transformations, the nucleation stage is thermally activated, followed by rapid propagation of the martensite plates or laths (morphology depends on many factors, especially the misfit strain energy). During the time-dependent nucleation stage thermally assisted motion of interfacial dislocations is necessary to reach the critical embryo

configuration and size. Since dislocations play such a prominent role in the nucleation and growth of martensites, it is easy to see that these transformations will be greatly influenced by the microstructure of the parent phase. For example, the presence of solute atoms may "pin" the dislocations necessary for nucleation. Likewise, since accommodation is necessary in the parent and product, the properties of both have a profound effect on the transformation.

In alloy systems, more solute (substitutional or interstitial) can typically be dissolved in the parent phase at high temperature than in the product at the transformation temperature. Since the composition in martensitic transformations is invariant (that is, it does not change because there is no diffusion), the product is then supersaturated (beyond its equilibrium solubility) and metastable. Depending on temperature and time (and the stresses associated with the supersaturated solute atoms), the solute atoms will begin to migrate and achieve a lower energy state. In steels, this process is called tempering and is used to beneficially control the properties of the martensite product.

Martensitic transformations can also be triggered by mechanical stresses. For most metallic systems, shear stresses are most effective in triggering martensitic transformations. Olson and Cohen (1981) have shown how one can divide such transformations into stress-assisted and strain-induced transformations. In the former, the applied stress adds to the thermodynamic driving force and has the effect of increasing the temperature for the start of the martensite transformation (the stress-assisted M_s temperature is now called M_d, where "d" designates 30 percent deformation). In strain-induced martensite transformations, plastic flow introduces new and more potent nucleation sites. Although martensitic transformations under dynamic loading have been studied little, it is well documented that they occur readily under shock-loading conditions.

Another interesting purely electronic effect that can trigger phase transformations is the charge density wave (CDW)—a static modulation of the conduction electrons typically associated with a periodic distortion of the lattice. As pointed out earlier, Peierls (1955) first suggested that periodic lattice distortions can lower the total energy of a system for a one-dimensional solid. One- or two-dimensional solids can form CDWs relatively easily because energy gaps can be created at the Fermi surfaces that will allow the system's energy to be lowered more than it is increased by the strain associated with the periodic lattice distortion. A phase (structural) change will occur when the CDW formation is accompanied by ion displacements that stabilize the charge perturbation. Often, a precursor phenomenon such as soft phonon modes occurs above the transition temperature to assist the CDW instability (Wayman and Bhadeshia 1996).

Although CDWs should be rare in solids because favorable Fermi-surface geometry is unlikely, they have been observed in conjunction with "premartenstic" effects in Ti-Ni martensites. For example, Ti-Ni alloys containing a few percent iron show a two-stage evolution of three-dimensional CDWs. First, there is a gradual, second-order transition to a structure with distorted cubic symmetry, then a first-order transformation to a lower-symmetry rhombohedral structure. Typically, phonon softening accompanies the first stage. Although these premartensitic effects are scientifically interesting and exhibit numerous nanoscale structures, it has not been demonstrated that they influence martensitic transformations in structural alloys in a substantial manner.

I present this extensive tutorial on phase transformation basics because these concepts are necessary for understanding phase transformations in plutonium discussed in the main text. For a more complete description of phase transformations, you can refer to the cited references. ■

Continued from page 321

indirect information from dilatometry (length changes), differential thermal analysis, and other methods to measure the reaction kinetics.

Much of the early work on phase transformations in plutonium focused on understanding the polymorphic transformations from one phase of pure plutonium to another. The β to α transformation during cooling and the reverse transformation during heating received the most attention. Under equilibrium conditions, these transformations take place at 123°C, a sufficiently low temperature for diffusional transformations to proceed with great difficulty. Indeed, various transformation behaviors and resulting microstructures have been observed (Goldberg and Massalski 1970). The β to α transformation temperature is depressed substantially by high cooling rates and by the presence of impurities. Goldberg and Massalski concluded that both the β to α and reverse transformations may proceed by diffusional or diffusionless mechanisms. The conditions that govern the operative mechanisms have never been fully understood, and very little work has been done in this area over the past three decades.

Interest in the α to β and reverse transformations has now been revived because of concerns over long-term storage of plutonium, especially plutonium that has been declared excess to the weapons programs of the United States and Russia. One potential concern is the stability of the α-phase and potential volume changes and distortions associated with changes in storage temperatures should they accidentally reach the α to β transformation temperature. In addition, the ε to δ transformation is of interest because it holds the key to the nucleation of the δ-phase. We know that this transformation is diffusional, but very little work has been done to understand it.

However, the most interesting transformations in plutonium are those in δ-phase alloys retained to room temperature by the addition of a few atomic percent aluminum or gallium. Cooling such alloys below room temperature triggers a diffusionless transformation to the α-phase. Similarly, the application of external stresses at room temperature can transform δ- to α-phase alloys. The transformation product in both cases is referred to as α′ because it has aluminum or gallium atoms trapped in the monoclinic α-lattice, which has no solubility for these solutes under equilibrium conditions. The other intermediate phases, β and γ, are often "skipped" in the δ to α′ or reverse transformations. I will highlight only some of the most interesting features and challenges of martensitic transformations in δ-phase plutonium alloys.

At first glance, we expect martensitic transformations in δ-phase plutonium alloys to resemble those studied extensively in steel and illustrated in Figure 23. The transformation from the fcc δ-phase to the monoclinic α′-phase is expected to be diffusionless during cooling because it takes place below room temperature, below which diffusion rates are too slow. Similarly, either pressure- or stress-induced transformations at room temperature are also expected to be diffusionless. However, we know that the δ to α′ transformation involves not only a change in crystal structure but also a significant change in electronic structure accompanied by a large volume decrease (on the order of 20 percent). Volume changes of this magnitude have been observed in only a few other metallic systems, such as cerium and tin, but they are much larger than the few percent typical of most martensitic transformations in steel. Only recently has it been established that the δ to α′ transformation can be classified as martensitic because it was believed unlikely that an undistorted habit plane (necessary for a martensitic mechanism) can be retained if such a large volume change has to be accommodated. A martensitic transformation must be displacive and dominated by the strain energy that arises from the shear-like displacements of the atoms (as explained in the box "Phase Transformation Basics" on page 322) rather than by volume changes.

I will present some experimental results. In Figure 23, both temperature-induced and stress-induced (by the application of hydrostatic pressure) transformations are illustrated for a Pu–2 at. % Al alloy (Hecker et al. 1982, Zukas et al. 1982). The samples were homogenized at 450°C for 200 hours. In this way, the fcc δ-phase was retained to room temperature. Both cooling and isostatic pressing resulted in a slight contraction followed by an abrupt length change (or volume collapse), marking the onset of the δ to α′ transformation. The transformation continued upon cooling or pressing but at decreased rates. Holding at liquid nitrogen temperature or at 1 gigapascal pressure yields very little additional transformation product. Only minor reversion of α′ to δ occurred during warming back to room temperature or during pressure release. However, a small amount of additional transformation occurs initially while warming up to room temperature (because transformation stresses are relieved in the δ-phase matrix). A significant fraction of the α′ transformation product is retained at room temperature or ambient pressure in the original δ-phase matrix (as confirmed by x-ray diffraction measurements) because the transformation is not fully reversed.

The α′ transformation product (the light-etching platelets in Figure 23 and at higher magnification in Figure 24) present at room temperature after a cooling cycle resembles conventional martensite platelets in steels. It is lenticular in shape, has specific crystallographic orientations, and terminates at grain boundaries or at intersections with other platelets (it even exhibits a midrib centerline seen in many steels as shown schematically in Figure C in the box "Phase Transformation Basics"). The transformation sequence for the isostatic pressure experiment was δ to β′ to α′, with α′and β′ coexisting over most of the transformation range. Results of

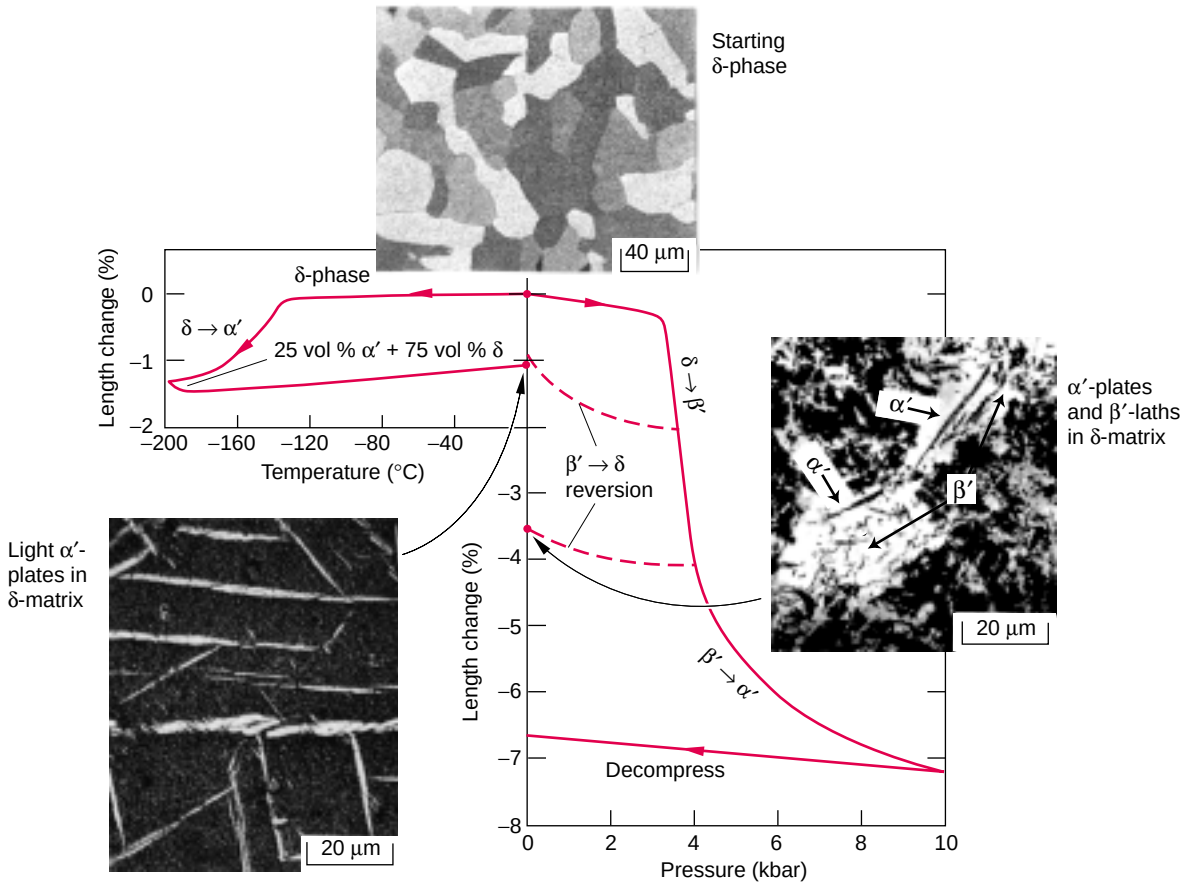

Figure 23. Temperature and Pressure Transformations in a δ-Phase Plutonium Alloy

A high-purity Pu–2 at. % Al alloy was homogenized for several hundred hours at 450°C to produce an all-fcc d-phase microstructure as shown in the top micrograph. The red curve on the left-hand side illustrates the transformation from d to a¢ during cooling at a relatively slow rate of 1.5°C/min. Approximately 25 vol % of a¢ is retained when the sample is returned to room temperature. The micrograph on the left shows the white a¢-platelets in the dark-etching d-phase parent grains. The curve on the right-hand side illustrates the transformation behavior under hydrostatic compression (isostatic pressing) conducted in a Bridgman press to allow length changes to be measured during pressing. A larger amount of a¢ is retained when the sample is returned to ambient pressure. The entire experiment takes about 2 hours. The a¢ transformation product is shown in the micrograph on the right. (More detailed descriptions are provided in Hecker et al. 1982, Zukas et al. 1982).

x-ray diffraction measurements of the sample returned to ambient pressure after isopressing to 1 gigapascal showed most of the δ-phase had transformed to a combination of 90 percent α′ plus 10 percent β′. The morphologies of the transformation products for the isostatically transformed products were lath-like martensite for β′ and lenticular martensite for α′. The lattice parameters of the α′-phase are expanded compared with those of unalloyed α-plutonium. Analysis of crystallographic relationships for the δ to α′ transformation is complicated by the low symmetry of the monoclinic α-structure and the large volume changes. The lattice parameters of β′ were indistinguishable from those of unalloyed β-plutonium. Crystallographic relationships between δ and β′ and β′ and α′ were not determined.

Lomer (1963) postulated specific crystallographic relationships for the δ to α′ transformation by viewing the α-monoclinic structure as a distorted hexagonal structure (Figure 25). Choudry and Crocker (1985) reported preliminary theoretical results, and then Adler et al. (1986) and Adler et al. (1992) made rigorous predictions of the likely crystallographic relationships and resulting lattice strains and demonstrated that these are consistent with a martensitic transformation. Adler et al. had to examine as many as three possible lattice correspondences and 53 possible lattice-invariant shear systems to determine the most likely crystallographic parameters because of the complex monoclinic lattice.

Experimental confirmation of their results proved difficult because the tools typically used for studying transformation crystallography, namely, transmission electron microscopy (TEM) and electron diffraction, proved elusive for plutonium. As described by Zocco in the article “Transmission Electron Microscopy of Plutonium Alloys” on page 286, plutonium is very

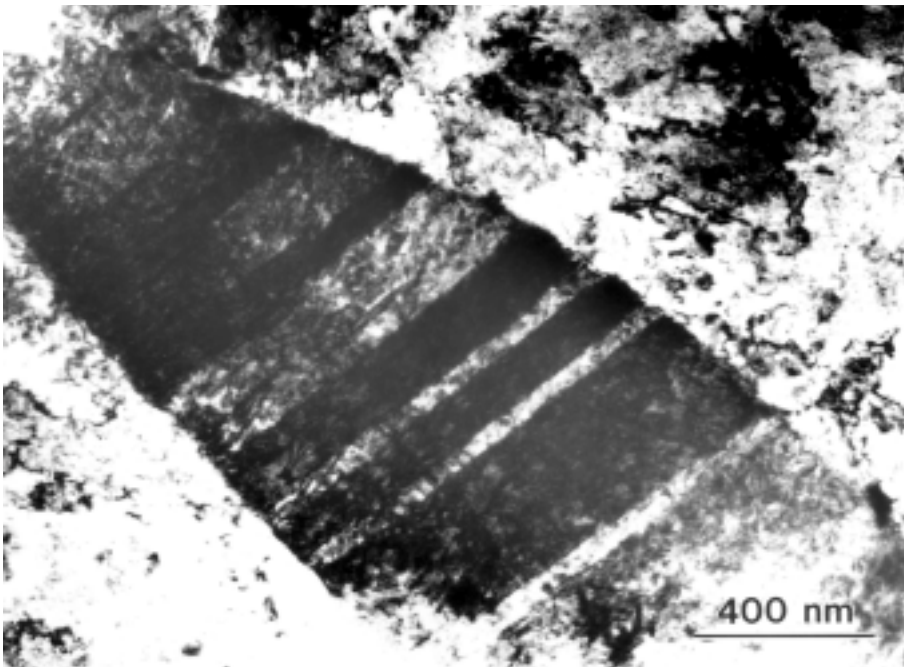

Figure 24. Transmission Electron Micrograph of α′-Martensite in δ-Phase Pu-Ga Alloy

This TEM photomicrograph is one of the few ever captured of an α′-platelet in a transformed Pu–1 wt % Ga alloy (Zocco et al. 1990). Note that the twins in the α′-platelet resemble the schematic shown in Figure D on page 326. The photomicrograph is for the [11- 0] α-zone. The orientation relationships for the twin and the matrix are $(001)_{matrix}$ parallel to $(2\text{-}\ 01\text{-}\ )_{twin}$ and $(225)_{matrix}$ parallel to $(2\text{-}\ 25\text{-}\ )_{twin}$.

difficult to prepare in sufficiently thin and clean sections for such an examination (the radioactive nature of plutonium is additionally complicated by its very reactive nature, making the preparation of clean surfaces difficult). However, Zocco et al. (1990) for the first time successfully examined and interpreted the transformed microstructure of plutonium by TEM (Figure 24).

Direct TEM examination of the transformed product revealed a lattice correspondence of nearly parallel close-packed planes and directions in the product α′-phase and parent δ-phase—$(111)_\delta$ and $(020)_\alpha$ planes and $[\bar{1}10]_\delta$ and $[100]_\alpha$ directions. The α′-phase habit plane was found to be near $(1\bar{3}\bar{2})_\alpha$. The lattice-invariant deformation mode in the product α-phase was determined to be $(205)_\alpha$ twinning. These experimental results are consistent with the theoretical predictions of Adler et al. (1986) and confirm that the δ to α′ transformations in Pu-Al and Pu-Ga alloys under these conditions are diffusionless and martensitic, in spite of the unusually large volume change. Unfortunately, TEM has not become a routine experimental tool for plutonium. The results shown in Figure 24 remain essentially the only examples of transformation studies using TEM in plutonium alloys. Hence, we have very little detailed understanding of temperature and stress-induced transformations in plutonium today.

Although the martensitic nature of the δ to α′ transformation is now well established, we must explain the rate (or time) dependence of the transformation. As shown in Figure A on page 323, the onset and extent of martensitic transformations are typically determined by temperature, independent of cooling rate. The transformation behavior during cooling illustrated in Figure 23 is that observed at a constant cooling rate. However, Orme et al. (1975) found the δ to α′ transformation in Pu-Ga alloys followed a C-curve behavior similar to that shown schematically in Figure A on page 323 for diffusional transformations. In fact, they found the "double C" curves shown in Figure 26. The times and temperatures for the onset of transformation depend strongly on gallium concentration. Hecker et al. (1982) found similar time dependence for Pu-Al alloys. They concluded that the transformation occurs by an 'isothermal' martensitic transformation. As explained in the box on page 322, such transformations proceed by a thermally activated nucleation stage (hence the time dependence) followed by a rapid martensitic growth stage.

Recent work by Deloffre et al. (1998) has shed some light on the double-C-curve nature shown in Figure 26. They claim that the crystallographic mechanisms of the martensitic transformations differ for the upper and lower C-curves and for different gallium concentrations. Low gallium concentrations and higher transformation temperatures (upper C curve) favor the transformation to proceed from δ to γ′ to α′, whereas higher gallium concentrations and lower temperatures (lower C curve) favor transformation directly from the δ- to the α′-phase. They also showed that the morphologies of the martensite products differ accordingly. As in the isostatic pressing case, this two-step transformation (but in this case δ to γ′ to α′ instead of δ to β′ to α′) produces a product phase of thin plates or laths, whereas the direct transformation produces lenticular martensite as shown in Figure 24.

They also found that products for the two different paths transformed very differently when heated, as shown in Figure 27. The two-step transformation products (upper C curve) showed evidence of α′ to δ, as well as α′ to β and β to γ transformations. The one-step product, on the other hand, appeared to

(a)

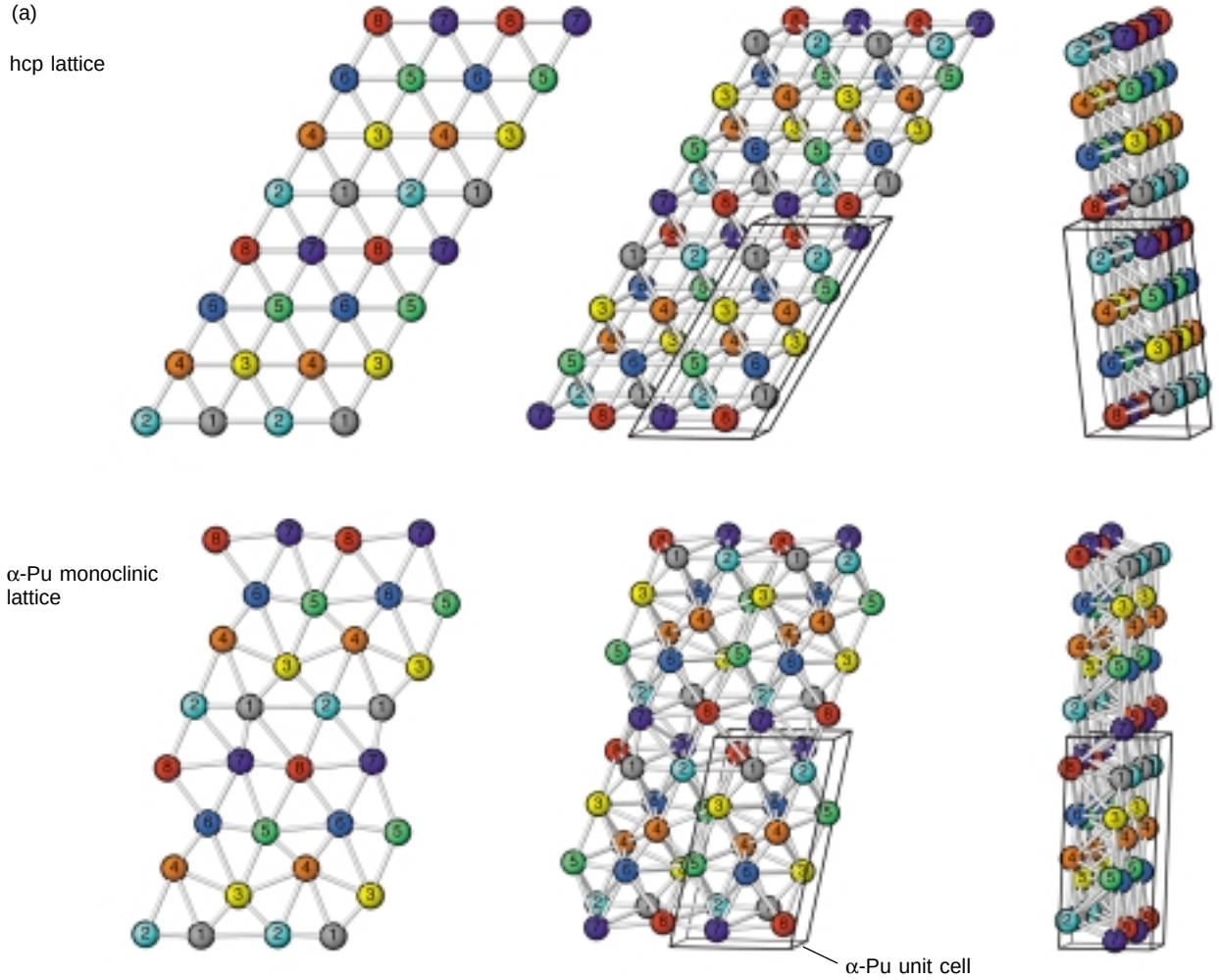

(b)

Table III. Bonds in α-Plutonium

Atom	Number of Short Bonds[a]	Average Length (Å)
1	5	2.57
2–7	4	2.54
8	3	2.77

[a]Short bond 2.57–2.78
Long bond 3.19–3.71

(c)

Table IV. Monoclinic α-Lattices

Structure	a (Å)	b (Å)	c (Å)	β (deg)	Atomic Volume (Å^3)
α	6.183	4.822	10.963	101.79	319.96
α′	6.217	4.859	11.019	101.84	325.79
Change (%)	0.56	0.77	0.51		1.82

Figure 25. α-Plutonium Compared to an hcp Structure and Parameters for α- and α′-Plutonium
(a) The figure contrasts the hcp structure with the monoclinic structure of α-plutonium, demonstrating that the latter resembles a distorted hcp. The bonds shown are between nearest neighbors. Each of the eight numbered sites in α-plutonium is crystallographically unique, and the second plane is a 180° rotation of the first plane. (b) Table III shows that the eight nearest-neighbor bonds fall into two groups. (c) Table IV shows the lattice parameters for the normal α-lattice (unalloyed plutonium) and for the α′-lattice transformed from the δ-phase of the Pu–2 at. % Al alloy shown in Figure 23. The lattice parameters along all three axes are expanded slightly, and the monoclinic angle is increased slightly. Overall, forcing 2 at. % Al into the α′-lattice expands the lattice volume by approximately 2%.

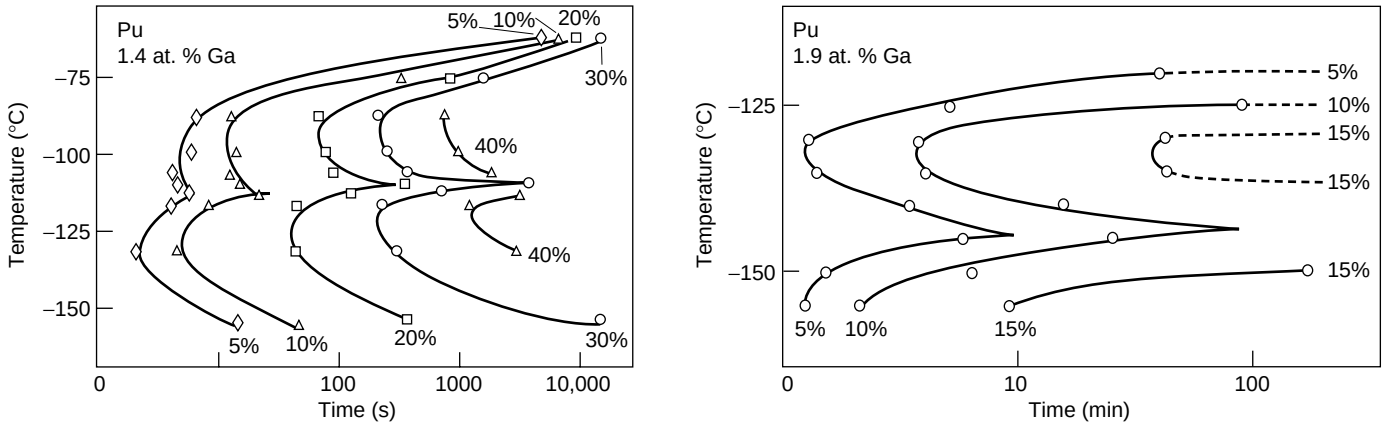

Figure 26. Temperature-Time-Transformation Curves for Two High-Purity Pu-Ga Alloys

High-purity alloys with two gallium concentrations had been homogenized to retain the fcc δ-phase to room temperature before isothermal transformation experiments were conducted at low temperatures. The transformation behavior follows a double-C-curve behavior (Orme et al. 1975). Each curve of the nested set represents a different level of transformation from δ to α′. Note that time in the Pu–1.4 at. % Ga diagram is given in seconds whereas that in the Pu–1.9 at. % Ga diagram is in minutes, indicating how much more unstable and ready to transform the lower gallium alloy is.

revert from α′ directly back to δ in one step. All these results are inferred indirectly from the dilatometry experiments shown in Figure 27. Unfortunately, because no TEM studies were performed, it is not possible to draw definitive conclusions about the exact nature of the transformation mechanisms for either C-curve or the reverse transformations upon heating. Likewise, we do not know the exact transformation mechanism or crystallography of the pressure-transformed alloys. For example, the Pu-Ga alloys do not show the β′–phase as an intermediate step as do the Pu-Al alloys. In addition, we have no insight into the isothermal nature of the martensitic transformations upon cooling—that is, how the nucleation sites are thermally activated for either of the two mechanisms. By comparison with other alloy systems, we can only surmise that the pre-existing nuclei are insufficient to trigger the transformation at these temperatures and that a thermally activated rearrangement of dislocations must occur to successfully nucleate the transformation. Once nucleated, the transformation proceeds rapidly by the combination of lattice deformations and lattice-invariant deformations.

One additional complication, similar to the tempering of martensite products in steels, is worth noting. The α-phase has virtually no solubility for any alloying element except neptunium. Yet, the diffusionless martensitic transformation of δ to α′ is composition invariant—that is, the gallium or aluminum atoms that substitute for plutonium atoms in the δ-phase are now stuck unhappily in the α′-phase. Consequently, these solute atoms expand the monoclinic α-phase as shown by the change in lattice parameters for a Pu-Al alloy in Figure 25. The properties of the α′-phase (supersaturated in aluminum or gallium) can differ substantially from that of the normal monoclinic α-phase. For example, when heated above room temperature, α′ transforms directly to δ just above room temperature—much like the transformation product derived from the lower C-curve in Figure 26(b)—and essentially completes that transformation by 150°C. The α-phase of unalloyed plutonium, by contrast, transforms to β, γ, and δ sequentially at the temperatures shown in Figure 1.

Holding the α′-phase at slightly elevated temperatures (from 50°C to 100°C) will cause the gallium or aluminum atoms to migrate away from those lattice sites that cause expansion of the α′-phase. Unfortunately, we have no microstructural information on where the solute atoms are trapped during the transformation, nor about how they migrate and to what locations they migrate. We suspect that the migration occurs in stages—first to crystallographically different sites in the plutonium lattice, next to defects such as dislocations and lattice vacancies, then to grain boundaries, and eventually, given sufficiently long times and elevated temperatures, out of the α′-platelets altogether.

A Program of Future Studies on Phase Stability and Transformation. To summarize phase stability and phase transformations in plutonium and its alloys, we have a large body of experimental phase diagram information and a limited number of transformation curves such as the TTT curves for a few Pu-Ga alloys. Unfortunately, we have very little fundamental understanding of the transformation mechanisms and essentially no theoretical understanding of the effect of alloying on phase stability or on transformation mechanisms. Consequently, we are not able to

extrapolate phase stability or transformation behavior outside our limited data base. For example, we have little understanding of the effects of multiple alloying elements or impurities on phase stability and transformation behavior. We do not understand the effects of transformation rate—either during cooling or during pressurization. We have insufficient knowledge of the effect of the stress state on transformations. Unlike most other martensitic transformations that depend primarily on the shear stress, those in plutonium are governed primarily by the hydrostatic stress component. We do not understand the role of the electronic transition from the δ- to the α-phase or the reverse transformation.

XAFS measurements provide hints that a local structure may be superposed on the long-range fcc δ-structure. Yet, we do not understand what controls this local structure and what role it plays in phase transformations. We do not know if premartensitic phenomena, such as phonon softening, play a role in the transformation behavior of δ-phase alloys, or if CDWs play a role at low temperatures as they do in uranium—see Lander et al. (1994). We have little information about the role of surfaces. If a free surface is present, it may change the stress state sufficiently to affect transformation mechanisms. Moreover, we do not even know the sign of the effects of self-irradiation on δ-phase stability. In other words, do the defects generated by the radioactive decay stabilize or destabilize the δ-phase during aging? Unfortunately, the list of what we don't know about phase stability and transformations goes on and on.

On the other hand, this seemingly endless list also presents us with exciting scientific challenges. Electron-electron correlations play an important role in determining the structure and properties of the fcc δ-phase, and correlated-electron materials are currently at the forefront of the challenges in condensed-matter physics. For the δ-phase, we have the additional challenge of trying to understand its transformation behavior to α′, both the electronic transition from partially localized to itinerant 5f electrons and the crystallographic transformation from an fcc to a monoclinic lattice. We must now bring to bear not only the tools used routinely in other alloy systems (for example, TEM and in situ x-ray diffraction), but also such powerful tools as XAFS, neutron scattering, and PES that can provide us with additional electronic and structural information. For example, neither the local atomic structure nor the electronic structure of the α′-phase has ever been measured experimentally. PES experiments, such as those conducted by Arko and coworkers (see the article on page 168), are particularly important for the α′-phase to see if this phase sits between the electronic structures of the α- and δ-phase. Likewise, XAFS experiments on α′ may identify where in the α′-lattice the gallium or aluminum atoms are trapped and how they migrate with time and temperature. Neutron diffraction offers the possibility of following the transformation in bulk samples (unlike x-ray diffraction which is limited to the near-surface region) in situ during cooling or pressurization.

Theoretically, we must now extend the band-structure calculations to include alloying effects. Moreover, we must attempt to include the effects of electron correlations in first-principles calculations. Neutron-scattering experiments to determine the phonon dispersion curves will be crucial to help

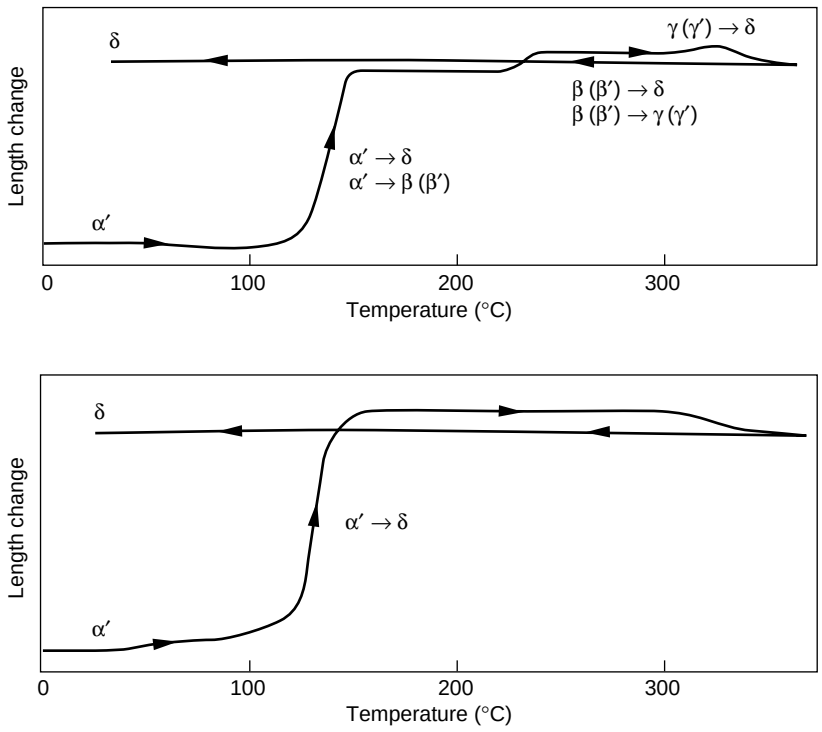

Figure 27. Reverse Transformation Behavior during Heating

Deloffre et al (1998) conducted experiments similar to those of Orme et al. (1975) shown in Figure 26. They transformed a well-homogenized Pu–1.2 at. % Ga alloy to establish the double-C-curve. They subsequently heated samples transformed at low temperature and measured the resulting length changes (indicative of reverse transformations). (a) Shows the results for a sample previously transformed in the upper C-curve and (b) a sample transformed in the lower C-curve. The likely transformation path during the reverse transformation of α′ is indicated in each diagram.

guide theoretical prediction of temperature effects. Likewise, careful ultrasonic measurements of elastic moduli will be important to understand temperature effects and phonons. To understand the role of defects and microstructure, we must develop an accurate interatomic potential that would allow modeling such effects.

Experimentally, we need high-purity, high-quality single crystals and polycrystals of α- and δ-phase plutonium alloys to study fundamental properties. As we have pointed out, knowing the precise nature of the metallurgical processing is paramount to ensuring that we understand the starting material. Moreover, surface preparation is crucial because most processing steps alter the surface crystal structure. In addition, we absolutely need plutonium-242 to conduct neutron scattering experiments.

Summary of Challenges in Plutonium Metallurgy

The properties of plutonium depend on its crystal structure, which depends critically on temperature, pressure, chemistry, and microstructure. Finally, the microstructure depends on all of the previous variables plus the details of thermal and mechanical processing. We demonstrated that plutonium is truly unique because of its position in the periodic table and that its unusual properties are derived from the nature of the 5f electrons. Specifically, it is the narrow band and the high density-of-states of the 5f electrons at the Fermi energy that make plutonium unique. Although these features favor an unusual low-symmetry monoclinic structure at room temperature, it takes only a slight change in temperature or the addition of a few atomic percent of elements such as aluminum or gallium to approach a structure that is closer to that of americium, with a much larger atomic volume than the monoclinic α-phase and a high-symmetry crystal structure. The uniqueness of plutonium can only be appreciated and understood by studying its neighbors in the actinide series, and I am convinced that it will be understood only through the close collaboration between the condensed-matter physics and metallurgical communities.

All the peculiarities of plutonium have a profound effect on its physical and mechanical properties. Many physical properties such as electrical resistivity and magnetic susceptibility are expected to reflect directly the peculiarities of the 5f electrons in plutonium (see the article by Boring and Smith on page 90). The low-temperature behavior of plutonium is highly anomalous—for example, the electrical resistivity for α-plutonium (which is already very high at room temperature) climbs as the temperature is lowered to approximately 100 kelvins before it falls as it is cooled toward absolute zero. Some of the other transport properties such as diffusion depend primarily on the bonding properties of the electrons, hence they scale with the homologous melting point as mentioned earlier. The mechanical properties of plutonium depend to first order on the crystal and defect structure—varying dramatically from those of the soft, ductile δ-phase to that of the strong, brittle α-phase. Other peculiarities of the mechanical behavior of plutonium and its alloys are discussed by Hecker and Stevens (page 336).

Finally, the complexities of plutonium are further exacerbated by the continuous lattice damage inflicted during its self-irradiation as discussed by Wolfer (page 274) and Hecker and Martz (page 238). From a practical point of view, we know that plutonium does not destroy itself over a period of a few decades. All indications are that significant self-annealing heals much of the damage of self-irradiation. Yet, by comparison with other metals and alloys that suffer similar irradiation from external sources, the conditions in plutonium are ripe for substantial property changes to happen as plutonium ages. ■

Further Reading

Adler, P. H., G. B. Olson, and D. S. Margolies. 1986. *Acta Metall.* **34**: 2053.

Adler, P. H., G. B.Olson, M. F. Stevens, and G. F. Gallegos. 1992. *Acta Metall. Mater.* **40**: 1073.

Ardell, A. J. 1963. *Acta Metall.* **11**: 591.

Bain, E. C. 1924. *Trans. AIME.* **70***:* 25.

Brewer, L. 1983. *Systematics and the Properties of the Lanthanides.* Edited by S.P. Sinha, 17. Dordrecht: D. Reidel Publishing Company.

Choudry, M.A. and A. G. Crocker, 1985. *J. Nucl. Mater.* **127**: 119.

Clapp, P. C. 1973. *Phys. Stat. Sol.* **57**: 561.

Deloffre, P., J. L. Truffier, and A. Falanga. 1998. *J. Alloys Compounds* **271-273**: 370.

Ellinger, F. H., W. N. Miner, D. R O'Boyle, and F. W. Schonfeld. 1968. "Constitution of Plutonium Alloys" (Dec.). Los Alamos National Laboratory report LA-3870-MS.

Eriksson, E., J. D. Becker, A. V. Balatsky, and J. M. Wills. 1999. *J. Alloys and Compounds* **287**: 1.

Goldberg, A., and T. B. Massalski. 1970. In *Proc. of 4th Int. Conf. on Plutonium and Other Actinides 1970.* Edited by W. N. Miner, 875. New York: The Metallurgical Society of AIME.

Haasen, P. 1992. *Physical Metallurgy.* Cambridge: Cambridge University Press. Cambridge.

Hammel, E. F. 1998. Plutonium Metallurgy at Los Alamos, 1943-1945. Los Alamos, NM: Los Alamos Historical Society.

Hecker, S. S. 2000 (to be published). Plutonium Aging: From Mystery to Enigma. In *Proceedings of the International Conference on Aging Studies and Lifetime Extension of Materials.* Edited by L. G. Mallinson, 191. Dordrecht: Kluwer Academic Publisher.

Hecker, S. S., J. R. Morgan, and R. A Pereyra. 1982. In *Proc. Int. Conf. Solid-Solid Phase Tranf.* Edited by H. I. Aaronson, 1339. New York: Am. Inst. Min. Engrs.

Heine, V. 1969. *The Physics of Metals: 1. Electrons*. Edited by J. M. Ziman, 1. Cambridge: Cambridge University Press.

Hill, H. H., and E. A. Kmetko. 1976. *J. Phys. F* **6**: 1025.

Johansson, B. 1974. *Phil. Mag.* **30**: 469.

Kaufman, L., and H. Bernstein. 1970. *Computer Calculation of Phase Diagrams.* New York: Academic Press.

Lander, G. H., E. S. Fisher, and S. D. Bader. 1994. *Adv. Phys.* **43**: 1.

Lawson, A. C., J. A. Goldstone, B. Cort, R. J. Martinez, F. A. Vigil, T. G. Zocco, J. W. Richardson, and M. H. Mueller. 1996. *Acta Crystall.* **B52**: 32.

Lawson, A. C., B. Martinez, J. A. Roberts, and B. I. Bennett. 2000. *Phil Mag.* **80**: 53.

Liptai, R. G., and R. J. Friddle. 1967. *J. Nucl. Mater.* **21**: 114.

Lomer, W. M. 1963. *Solid State Commun.* **1**: 63.

Massalski, T. B. 1996. *Physical Metallurgy.* Edited by R. W. Cahn and P. Haasen, 136.

Mitchell, J. N., F. E. Gibbs, T. G. Zocco, and R. A. Pereyra. 2000 (to be published). *Met. Trans.*

Morgan, J. R. 1970. In *Proc. of 4th Int. Conf. on Plutonium and other Actinides 1970.* Edited by W. N. Miner, 669. New York: The Metallurgical Society of AIME.

Nelson, R. D., T. K. Bierlein, and F. E. Bowman. 1965. Battelle, Pacific Northwest National Laboratory report BNWL-32.

Olson, G. B. and M. Cohen. 1981. *Ann. Rev. Mater. Sci.* **11**: 1.

Orme, J. T., M. E. Faiers, and B. J. Ward. 1976. In *Proc. of 5th Int. Conf. on Plutonium and Other Actinides*. Edited by H. Blank and R. Lindner, 761. New York: North Holland Publishing Co.

Peierls, R. E. 1955. *Quantum Theory of Solids.* Oxford: Oxford University Press.

Peterson, D. E., and M. E. Kassner. 1988. *Bull. Alloy Phase Diagr.* **9**: 261.

Porter, D. A., and K. E. Easterling. 1981. *Phase Transformations in Metals and Alloys.* New York: Van Nostrand Reinhold Company.

Sherby, O. D., and M. T. Simnad. 1961. *Trans. ASM* **54**: 227.

Smith, J. L., and E. A. Kmetko. 1983. *J. Less Common Met.* **90**: 83.

Söderlind, P., O. Eriksson, B. Johansson, J. M. Wills, A. M. Boring. 1995. Nature April 6 issue: 6522.

Söderlind, P., J. M. Wills, B. Johansson, O. Eriksson. 1997. *Phys. Rev. B.*: **55**: 1997.

Wallace, D. C. 1998. *Phys. Rev. B* **58**: 15433.

Wayman, C. M. and H. K. Bhadeshia. 1996. In *Physical Metallurgy.* Edited by R. W. Cahn and P. Haasen, 1507. North-Holland: Elsevier.

Wittenberg, L. J., G. A. Vaughn, and R. DeWitt. 1970. In *Proc. of 4th Int. Conf. on Plutonium and other Actinides 1970.* Edited by W. N. Miner, 659. New York: The Metallurgical Society of AIME.

Zocco, T. G., M. F. Stevens, P. H. Adler, R. I. Sheldon, and G. B. Olson. 1990. *Acta Metall. Mater.* **38**: 2275.

Zukas, E. G., S. S. Hecker, J. R. Morgan, and R. A. Pereyra. 1982. In *Proc. Int. Conf. Solid-Solid Phase Tranf.* Edited by H. I. Aaronson, 1333. New York: Am. Inst. Min. Engrs.

Acknowledgments

I acknowledge all those who helped with this article: for technical discussions on electronic structure, Mike Boring, Nikki Cooper, Jim Smith, and John Wills; on metallurgy, Frank Gibbs, Del Harbur, Mike Stevens, and Tom Zocco; on crystallography, Steve Conradson, Angus Lawson, and Luis Morales; on thermodynamics, Marius Stan and Duane Wallace. I thank Jeremy Mitchell and Ramiro Pereyra for allowing me to use their plutonium segregation data and micrographs. The critical reading of the manuscript by Mike Baskes, Bob Field, and Dan Thoma is appreciated. I also thank my scientific collaborators in plutonium metallurgy over the years: Dave Eash, Reed Elliott, Del Harbur, Jim Morgan, and Gene Zukas. The motivation for writing a metallurgical article directed at a broader audience came from many discussions with Mike Boring, Nikki Cooper, and Jim Smith. I also thank the entire *Los Alamos Science* staff for their wonderful and very professional support.

Siegfried S. Hecker received his B.S., M.S., and Ph.D. in metallurgy from Case Western Reserve University. After two years as a postdoctoral appointee at Los Alamos, he became a senior research metallurgist with the General Motors Research Laboratories. He joined the Laboratory as a technical staff member in the Physical Metallurgy Group, and served as Chairman of the Center for Materials Science and Leader of the Materials Science and Technology Division before becoming Director. Sig was Director of Los Alamos National Laboratory from 1986 to 1997. He is currently a Senior Fellow at Los Alamos. Sig is a member of the National Academy of Engineering, Fellow of the TMS (Minerals, Metallurgy and Materials Society), Fellow of the American Society for Metals, and Honorary Member of the American Ceramics Society. In recognition of his achievements, Sig was named Laboratory Director of the Year by the Federal Laboratory Consortium, (1998). In 1998, he also received the honorary Doctor of Science degree (Honoris Causa) from Case Western University. Sig received the Department of Energy's Distinguished Associate Award, (1997), the University of California's President's Medal, (1997), the ASM Distinguished Life Membership Award, (1997), an Honorary Degree of Scientiae Doctoris, Ripon College (1997), the Navy League New York Council Roosevelt Gold Medal for Science (1996), the Aviation Week Group Laurels Award for National Security (1995), the James O. Douglas Gold Medal Award (1990), the ASM International's Distinguished Lectureship in Materials Society (1989), the Kent Van Horn Distinguished Alumnus Award, Case Western Reserve University (1989), an Honorary Degree of Scientiae Doctoris, College of Santa Fe (1988), the Year's Top 100 Innovations Award from Science Digest (1985), and the Department of Energy's E. O. Lawrence Award (1984). In addition to his current research activities, Sig is a member of the Council on Foreign Relations and the Pacific Council on International Policy. He also serves on the National Academy of Engineering Committee on Membership (chairman), Nominating Committee, and Draper Prize Committee, and on the Fellows Awards Committee of The Metallurgical Society.